Universitetet i Stavanger

FACULTY OF SCIENCE AND TECHNOLOGY

MASTER'S THESIS

Study programme/specialisation: Industrial Economics Project Management and Materials Technology	Spring 2019 Confidential
Authors: Olaf Nornes Kvamsøy, Kristoffer Nielsen	*(signatures)* (signature of authors)
Internal Supervisor: Dina Zhenisovna Kairbekova External Supervisor: Frode Flugheim Heggestad	
Title of master's thesis: Feasibility of a wireline punching tool	
Credits: 30	
Keywords: FEA, Material Selection, Material Treatment, P&A, Wireline, PWC, Perforation	Number of pages: ………142………… + supplemental material/other: ……102…… Stavanger, June 12th 2019 date/year

Titlepage for Master's Thesis
Faculty of Science and
Technology

This page is intentionally left blank.

Preface

This thesis is a result of a countless number of hours testing, designing, simulating and producing for E Plug AS.

In addition to working on the thesis, we have been fortunate to be a part of the R&D team at E Plug during the last six months. Subsequently, we have been involved in all projects currently being conducted in the company and to quantify the knowledge and experience gained is an impossible task.

We are both truly grateful for the opportunity to work with the excellent engineers at E Plug and complete our thesis following their working principles and design philosophy. This has been a fantastic journey with great learning and new challenges.

We want to express our utmost gratitude to all employees at E Plug AS and in particular our supervisor Frode F. Heggestad and Lead R&D Engineer Thomas Berge for making this such a fantastic time.

We would also like to thank our faculty supervisor Dina Kairbekova, for the excellent guidance through the writing of this thesis.

Lastly, we would also like to thank our friends and family who have endured with us this whole time and especially Martine and Karoline. We are truly grateful.

Kristoffer and Olaf

This page is intentionally left blank.

Contents

Abstract

This thesis describes the process of the development work completed for E Plug AS. A feasibility study on a downhole punching tool has been conducted. Furthermore, a simulation model has been created and evaluated through testing.

Throughout the project, several tests on different punching geometries have been conducted. These tests have resulted in essential knowledge regarding how different shear geometries behave when punched through a casing. Additionally, these tests have been used to verify hand calculations and highlight any deviations. The results show a promising correlation for simple geometries, while being inaccurate for complex geometries with varying shear areas throughout the punching process.

A material model has been established from specimina obtained from a L80 casing. This material model has been used to generate a FEA model, enabling iterative design evaluations of different punch geometries. Different punch geometries were designed, produced and tested to verify the accuracy of the established FEA model. The correlation between hand calculations, test results and FEA is proven to be satisfactory for further development of the punch head.

Moreover, this thesis includes a study of materials, coatings and treatments of components for tool optimisation. Conclusions are not made, but recommendations for further testing and evaluation are presented. These recommendations involve duplex treatments consisting of nitriding as a base layer with PVD applied nitride compounds for the punch head. Similarly, a nitride base layer with PVD applied transition metal dichalcogenide monolayers as solid lubrication is recommended for sliding surfaces.

In addition to the technical aspect of the thesis, the market needs, economic benefits and risk induced by developing the tool has been researched. Preliminary results obtained through questionnaires and literature, show that it might be a significant risk-reducing contributor in certain aspects of P&A. This is a result of guaranteed perforation of the inner casing only, good topside control and no explosives. However, reasonable estimates on cost reduction or income potential for the tool is hard to establish due to restricted information and variations in well design.

List of Figures

List of Tables

Abbreviations

AISI = American Iron and Steel Institute.

AlCrN = Aluminium Chromium Nitride.

ASTM = American Society for Testing and Materials

CAD = Computer Aided Design.

COF = Coefficient of Friction.

CPS = Combined Punch and Standoff tool.

CVD = Chemical Vapour Deposition.

DLC = Diamond-like Carbon.

DDH = Drilling Data Handbook.

DOF = Degrees of Freedom.

EMT = Electric Manipulation Tool.

FEA = Finite Element Analysis.

FEM = Finite Element Method.

HRC = Hardness in Rockwell C Scale.

LOS = Line of Sight.

MoST = Molybdenum Disulfide Titanium Compound.

NCS = Norwegian Continental Shelf.

PPE = Personal Protective Equipment.

PPF = Pounds Per Feet.

PVD = Physical Vapour Deposition.

PWC = Perf, Wash and Cement.

TiAlN = Titanium Aluminium Nitride.

TiN = Titanium Nitride.

TMD = Transition Metal Dichalcogenides.

TP = TorcPlug.

TPI = Threads per inch.

This page is intentionally left blank.

1 Introduction

1.1 E Plug

E Plug is a technology development company, working primarily with downhole products and increasing the efficiency of both well completion and intervention. E Plug is known for their bridge plug as the only available product on the market which is fully re-settable in the same run through patented technology. Based on previously developed technology, E Plug has seen the opportunity to reuse some of their known concepts and provide solutions to other well operations [7].

1.1.1 TorcMethod

The core concept of E Plug tools revolve around the TorcMethod. This patented way of transferring forces between tools through rotational motion and torque, enable E Plug to produce large axial forces.

1.1.2 Electric Manipulation Tool

At the center of the TorcMethod is the Electric Manipulation Tool. The tool is run using wireline and is supplied with electricity from topside. As a result, this multi-purpose machine outputs either high speed rotational motion or low speed and high torque depending on the tool and application below it. E Plug has been approached by a client to develop a new downhole tool to be precisely controlled at topside using the existing EMT.

1.2 Plug and Abandonment

The oil and gas industry has played a significant role in modern industry. An enormous amount of wells have been drilled both on the NCS and globally. Additionally,

there are still oil and gas wells being drilled for both production and exploration purposes. When all of these wells reach the point in their lifespan where maintenance expenses exceed production income, they move into the phase referred to as plug and abandonment. In some cases, however, leaving the well permanently is not an option. There may be more resources to retrieve from the reservoir. In these cases the desired course of action would be to abandon the lower part of the well and conducting slot recovery [19]. This enables access to fresh areas of the reservoir without drilling an entirely new well.

When doing permanent P&A operations or slot recovery, there are different rules and standards governing the nature of the activities and acceptance criteria. These regulations form the standard procedures for plugging, as well as allowing different approaches to certain aspects of the operation. For abandonment operations, NORSOK D-010 is the governing standard to which any operating oil and gas company must adhere to on the NCS [55]. See appendix C in chapter 8.3.

According to NORSOK D-010, a permanent well abandonment barrier shall seal across the full cross-section of the well including all annuli. In addition, the barrier must hold pressure while being unaffected by the environment. The internal well barrier should be located at approximately the same location as any annulus barrier. The sealability of the annulus barrier must be proven separately from the internal barrier [55].

For this tool, the chosen process for barrier establishment is the perforate, wash and cement (PWC) procedure. When conducting a PWC operation, one must perforate the casing to access the annulus for sealing and barrier verification purposes. These perforations can be done by using either perforating guns or punching tools. Figures 1 and 2 shows the different perforation concepts. Some of these methods require multiple well runs, expensive topside equipment and operations. Some also involve explosives and other risk increasing elements. Because of this, it has become an exciting and hot topic for the industry to solve the P&A challenges in a safe manner with high efficiency and probability for success.
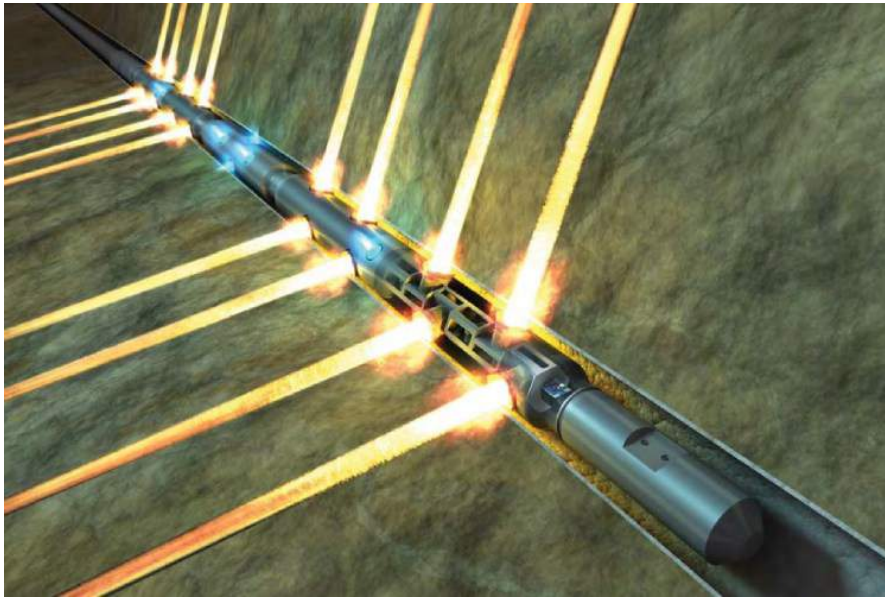
Figure 1: Concept of perforating guns[8].

Figure 2: Concept of punch perforations [34].

1.3 Purpose of equipment

For P&A operations, E Plug shall remove the risk of perforating the outer casing while providing a sufficient tear in the inner casing. These tears should facilitate the flow of fluid used to wash the annulus clear of any debris that ultimately may affect the cementing process. Additionally, the solution should provide sufficient standoffs between the innermost casing and the outer, so that the cement forming the annulus barrier will have a uniform distribution and integrity regardless of the casing being in the horizontal or the vertical. See figure 3 for a illustration of the innermost casing hanging low side in the horizontal. In figure 4 the innermost casing is lifted from the outer casing by the creation of a standoff.
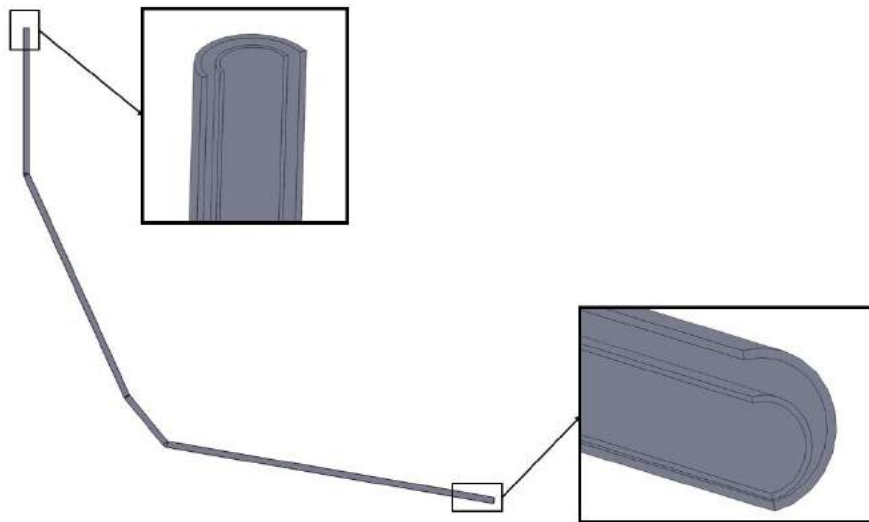
Figure 3: Well layout with low side casing in horizontal zone.
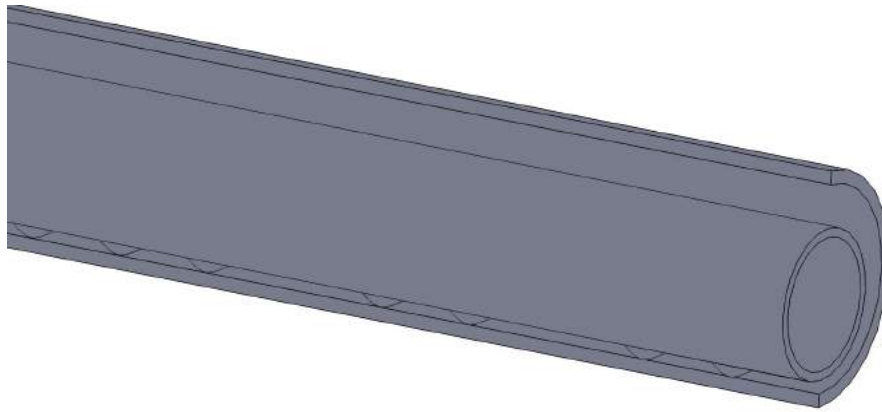
Figure 4: Innermost casing in horizontal lifted due to standoff.

1.4 Physical factors affecting the tool

1.4.1 External and Internal Loads

The purpose of the tool is to mechanically deform and create holes in the casing surrounding it. As a result, it is expected that the components of the tool will need to resist both tensile and compressive forces in the process. Local effects such as the balancing of shear and hoop stress in the casing wall is also a point of interest.

1.4.2 Mechanical Interaction

Interaction between parts is necessary to utilise and correctly transfer the loads applied to them. Sliding under heavy load in both threaded connections and coincident faces is expected. Throughout the thesis work, research will be done to both identify and remedy the effects of these interactions.

1.4.3 Operational Environment

Oil and gas wells stretch thousands of meters into the earth's crust, resulting in them being affected by an environment consisting of both high temperature and high pressure. Additionally, when extracting hydrocarbons, poisonous and corrosive agents are introduced to the wellbore. Material compatibility and resistance to the environment is considered important.

1.5   Scope of work

What

The efforts throughout this thesis will focus on:

- Tool feasibility based on simple concepts, existing technology and resources.

- Research and evaluate different materials, treatments and coatings of the tool components.

- Develop a simulation model based on accurate material data for an iterative design process of the punch head.

Why

The attractiveness of any development project depends on feasibility. The evaluation of whether it is possible to perforate casings with the available forces and known concepts is considered crucial for E Plug's pursuance of this opportunity.

Of equal importance is the research of available materials, treatments and coatings for any tool handling large loads repeatedly in a downhole environment. Durability and reliability are key in this industry as downtime is costly.

A simulation model that outputs results coinciding with physical testing may reduce both time and cost in product development. Different shear geometries can be evaluated prior to production, avoiding resources being spent on inadequate geometries and materials.

How

The approach to solving the problem consists of the following sections:

- Theoretical Background

- Research

- Development

- Testing

- Results

- Discussion

- Conclusion

- Recommendations for further work

1.6   Limitations

Limitations for the thesis have been set due to capacity, complexity and budget. Furthermore, due to the nature of product development, certain aspects cannot be included at the risk of exposing unprotected technology. As a consequence, the work will not include the following:

- Design iterations of punch geometries.

- Design of final tool components.

- Testing of various materials, treatments and coatings.

- Testing of full-scale prototype(s) developed.

2 Theoretical Background

The objective of this study is to identify the mechanisms affecting the behaviour and lifetime of the punch head. Furthermore, the details within FEA will be highlighted in order to create a representative simulation model. Design, material selection and treatment are some of the main ways of controlling undesirable effects on components. What material the punch is made from is vital for its performance and lifespan. A study within both mechanics of material, material behaviour, FEM analysis and coating/treatment of the material is vital to make decisions and educated assumptions.

2.1 Punching Overview

There are multiple similarities between punching as a manufacturing process and a potential punching tool. The concept of punching and blanking parts revolve around forcing a tool component through a work piece, creating a hole or a derived component with a desired geometry.

A typical punching process is as follows [32].

- Punch travelling towards work piece to eliminate any gaps.

- Contact between punch and work piece.

- Elastic and plastic deformation.

- Shearing and crack formation in work piece.

- Work piece failure and penetration.

- Stripping.

These steps are highlighted in figure 5.

contact of the   elastic and plastic   shearing and   breakthrough   stripping
punch   deformation   crack formation
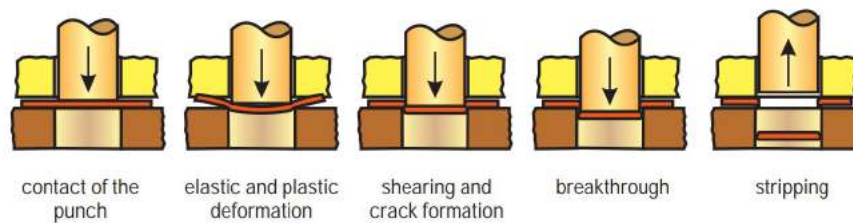
Figure 5: Typical blanking process of a punch and die [32].

2.2 Punch and casing interaction

By analysing the industrial punching process, a preliminary sequence of events is created for the new tool.

- **Punch head expanding to inner diameter of casing.**

- **Initial face contact between the punch head and casing wall.** Any debris has been pushed aside and the tool should be centred in the casing. The optimal number of punches to achieve centralisation and desired end result should be investigated.

- **Compressed forces accumulates and is being stored in the punch head.** Throughout the punching process the punch head will act as a compressed spring. The surface area of the punch head will experience equal stress levels as that of the casing wall. Thus, the importance of material selection becomes evident.

- **Casing loaded into elastic region.** When loading is applied to the punch head, the casing wall absorbs the energy and acts like a spring while in its elastic region. In this region the casing will return to its original geometry upon releasing the forces.

- **Casing loaded into plastic region.** The casing will at some point be exposed to loads exceeding its mechanical strength. At this point the casing wall transitions past its elastic region and into the plastic region. When the plastic region is reached, the wall is unable to return to its original geometry when unloaded.

- **Crack propagation and failure of casing wall.** As the stresses and strains in the wall increases, cracks will form. Whenever the load is sufficient the wall will experience shear failure and tear open.

- **Compressed forces in punch head released at failure.** The built up compressed forces of the punch head will release upon fracture and send a shock-wave through the casing and the punch tool itself.

- **Further expansion of tear.** Following the wall failure due to shear stress, the casing integrity has been compromised. From this point, lower radial force will be required to further expand the tear made in the wall.

- **Punch retraction.** When the tear and stand-off has been made to a satisfactory degree, the tool will retract and remove the punch head from the casing wall.

2.2.1   Punch Wear

Besides failure due to high loads resulting in high stress and strain relations, there are other factors involved in the behaviour and lifetime of a punching tool. This subsection will describe some of the most common wear concepts the punch head will be affected by [56].

Wear is permanent damage to a solid surface resulting in loss or displacement of material. This is caused by two faces sliding against each other. Most often wear can be divided into two main types; abrasive and adhesive [56].

Abrasive wear occurs when a hard surface slides against a softer surface. According to ASTM standards, this type of wear occurs when hard particles move along the sliding surfaces and damages the faces involved [56].

Adhesive wear occurs when small local areas of two sliding surfaces bond together. Whenever the sliding motion is forced to continue, this bonding is broken and may result in material loss for one or both of the sliding parts [56].

Due to the repetitive nature of the punch tool, a third wear type in the form of **fatigue wear** is considered. Fatigue wear occurs due to repetitive cycling where debris is produced. This debris damages both the surface and the involved parts. This wear type is divided into high and low cycle fatigue wear. High cycle fatigue wear occur to parts that can withstand a high number of cycles before debris is produced. Low cycle fatigue is evident when debris accumulates after a low number of load cycles due to the parts being loaded into the plastic region for each cycle [58].

Flank wear

Flank wear is wear damage that happens on the flank of any operated working material. Flank wear is a commonly known wear type within machining for cutting tools, and is often used to define the lifetime of a cutting tool by defining the maximum wear damage which may be present before the tool is broken [45].
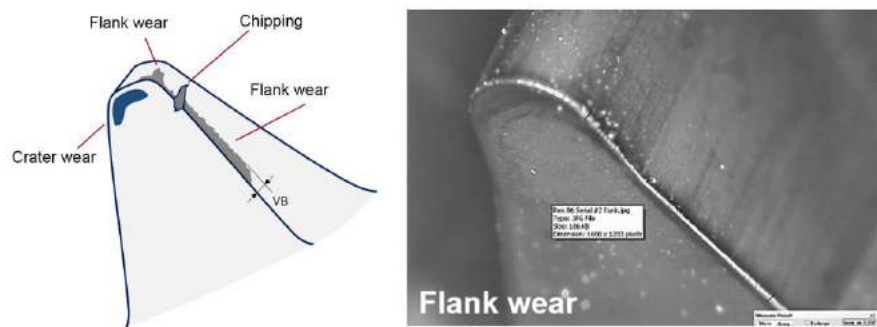
Figure 6: Illustration of typical flank wear [37].

For punching purposes flank wear will occur whenever the sides of the punching tool is sliding along the casing during sharing of the casing. For such purposes flank wear is a combination between adhesive wear, fatigue wear and abrasive wear. For a punching operation, flank wear will cause the internal diameter of the punched geometry to decrease, however this effect is of limited significance when punching a well casing. An increase in flank wear is expected to result in an increase in deformation.

Face wear

This wear mechanism describes wear on the punching face. This wear is a result of mechanical attrition and micro-chipping of the face leading to rounder and less sharp edges on the punch. Such loss in sharpness may along with flank wear increase the deformation of the casing and create a larger standoff than necessary before shearing the casing open [45].
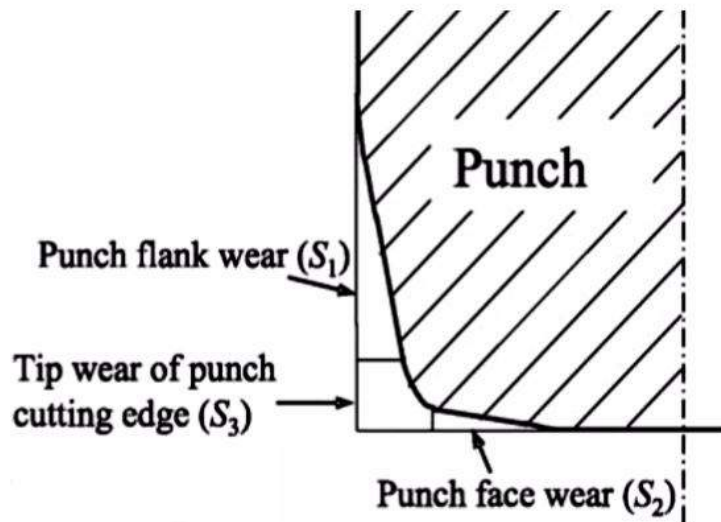
Figure 7: Illustration of where face wear occurs [56].

Chipping occurs when small areas on the edge of a mechanical part experience high stresses exceeding the ultimate strength or fatigue capacity of the material over time. It appears as micro crouches, small fragments or breakage on the side of a punching tool, illustrated in figure 8 [56].
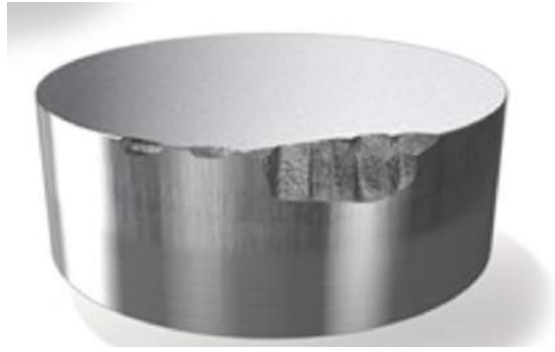
Figure 8: Example of chipping wear [43].

Cracking of a material is often defined as small microscopical cracks which occurs on the edges due to mechanical fatigue, high loads or thermal fatigue during shear loads. Such cracks may propagate further during punching and may result in chipping or macro mechanical chipping which may cause premature failure of the punch. An example of severe cracking is illustrated in figure 9 [56].
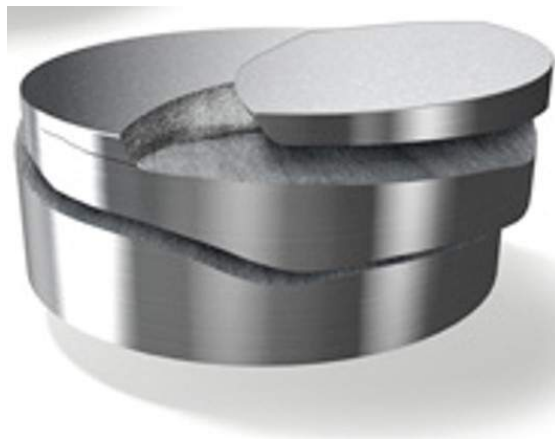
Figure 9: Example of cracking wear [43].

Gross Fracture is a type of wear that is a result of fatigue damage. It is recognisable by its characteristic benchmarks in the fracture zone, see figure 10. Gross fracture often include other wear modes such as chipping or cracking on the surface or edge of the punch [45].
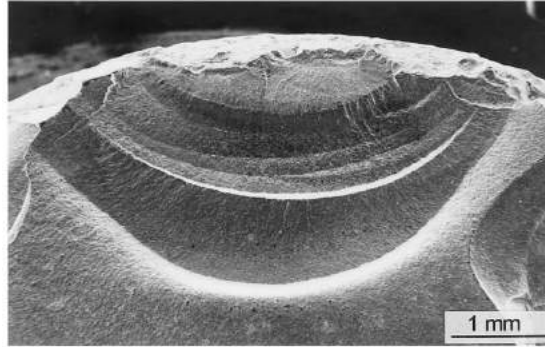
Figure 10: Close up illustration of gross fracture [45].

Galling, also referred to as "pick up", is a wear type occurring due to high frictional forces on sliding surfaces and the possible adhesion between them. Galling is closely related to adhesive wear [59]. An example of galling wear is presented in figure 11.

Figure 11: Example of galling wear [59].

2.2.2   Factors affecting punch wear

To reduce the risk of punch failure, a proper understanding of why and due to what factors the wear failure modes occur is vital.

Contact Pressure is one of the most important factors and may lower the probability of all wear failure modes if controlled. Contact pressure is a result of different mechanisms and depend on punch material, punched material, punch impact area and casing thickness.

Some of these dependencies are preset and impossible to influence, such as casing thickness and material. Other factors that impact the contact pressure may be manipulated and are important for the punch design.

The **surface quality** of a part affect the risk of galling. The punching tool may have multiple parts where sliding under high loads occur. Furthermore, surface quality affects the adhesion of any coatings that are to be applied to the substrate. As a result, an overall good surface finish on affected areas is of importance. However, any increase in surface quality increases the manufacturing cost, requiring a proper balance between the two.

Lubrication, if used correctly, may contribute in reducing the risk of galling and wear. Lubrication may also increase performance where material selection, the treatment or coating is unsuccessful. Due to the nature of the oil and gas industry, any reliance on lubrication is difficult due to uncertainty surrounding the environment of each individual well. Fluids with high solubility and high temperatures are only two of the many factors affecting lubrication selection.

A study into which lubricant to use is considered necessary for any downhole application, but the best approach will always be to not be dependent on any lubrication for the tool to function properly. Details about available lubricants is assessed further later in this chapter.

2.3   Mechanics of Materials

Different materials has different properties based on their chemical composition, production method and subsequent treatment. These properties are important to understand to be able to successfully select a material for any application.

2.3.1   Stress

Stress is one of the fundamental concepts of mechanics of materials and is widely used within mechanical engineering. When punching a casing, the loads created will act both tangentially (F_T) and transversely (F_{TR}) to the casing wall (figure 12). As a result, the shear strength of the casing will be one of the most important factors defining the forces acting upon the punch.
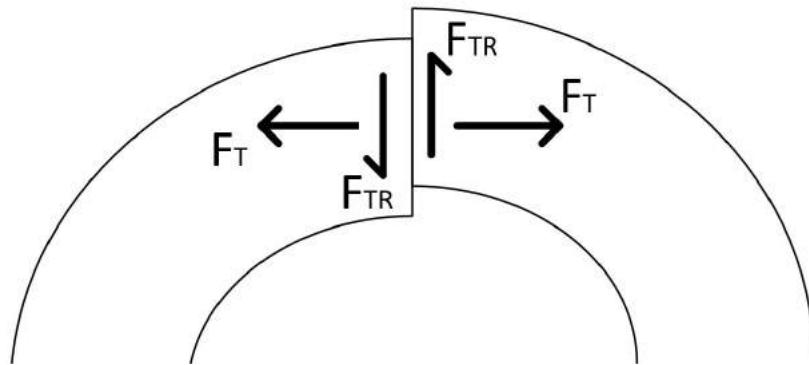
Figure 12: Transverse and tangential loads in a casing.

2.3.2   Strain

Strain is defined as the extension of any material relative to its original length. Together with stress, strain defines the elongation at different points of interest for a material. These points include the yielding point and ultimate tensile strength. The strain values may subsequently be used as comparative numbers for e.q. ductility of a material [53].

Knowledge regarding the relationship between stress and strain in a material is of utmost importance in mechanical design. The relationship is increasingly important when conducting FEA of highly loaded components due to the nonlinear behaviour post yielding.

2.4 Material Properties

2.4.1 Tribology

Tribology is the study of friction and wear. Mechanical interaction between different surfaces is evident in various applications such as brakes, engines, machining processes, polishing and writing with a pencil. Bhushan states that one third of the global energy consumption is lost through friction [11]. Subsequently, an understanding of tribological concepts is important when designing components subjected to large forces and interaction with other components.

Friction is a system property, depending on a multitude of variables. As a result, any specifications obtained through a study of literature should undergo physical testing in the desired application for verification purposes. Friction induces wear and can be controlled to an extent through lubrication and material treatment. The following sections contain a study into various material treatments, processes and coatings.

2.5   Material treatment

2.5.1   Material Hardening

The process of hardening a metal seeks to increase the hardness or strength to a satisfactory degree for a specific application. Different hardening processes include:

- Hall-Petch hardening.

- Strain Hardening.

- Precipitation hardening.

- Solid solution hardening.

- Martensitic transformation.

Hall-Petch hardening, often referred to as grain boundary strengthening, is a method of hardening metals by controlling grain size in the material. Plastic deformation of metals occur due to the travel of defects, called dislocations, through the microstructure of the material. The imperfections stop moving when arriving at grain boundaries. By decreasing the grain size, the number of grain boundaries increase and thus, dislocations are stopped at an earlier stage than in large grain microstructures - resulting in higher mechanical strength [27]. Figure 13 shows the increased amount of grain boundaries following the reduction in grain size.
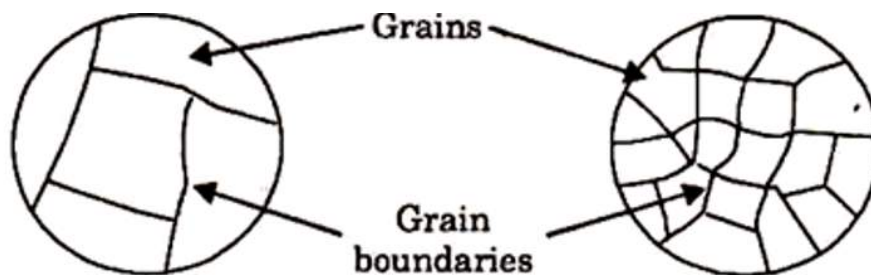
Figure 13: Increase in grain boundaries following grain size reduction [27].

Strain hardening describes the process of using plastic deformation to increase the strength and hardness of a material. During deformation, dislocations collide and accumulate at the grain boundaries, intertwining and creating strong bonds. These dislocation clusters further prevent deformation by increasing the required energy needed to deform the grain. The process is reversible through annealing which resets the crystalline structure through a high temperature exposure [29]. Low carbon steels are typically hardened through strain hardening as an alternative to heat treatment. Figure 14 shows the characteristic behaviour of strain hardening compared to perfectly elastic-plastic, strain-softening and brittle behaving materials.
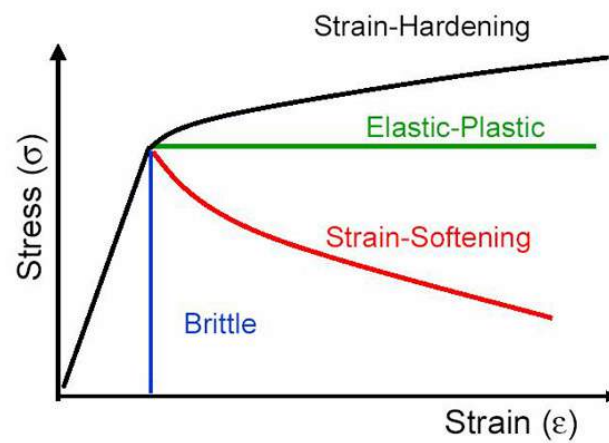
Figure 14: Strengthening curve of metals subject to precipitation hardening [63].

Precipitation hardening is the process of improving the strength of materials through facilitating the growth of precipitates in the crystal lattice. The precipitates inhibit the movement of dislocations and results in higher yield and tensile strength. The method is typically used on ductile materials such as alloys with aluminium, nickel, magnesium or titanium. The alloy has to be kept at an elevated temperature for an extended period of time for the precipitates to form [30]. Figure 15 displays the effect of ageing time on the strength and hardness of a material.
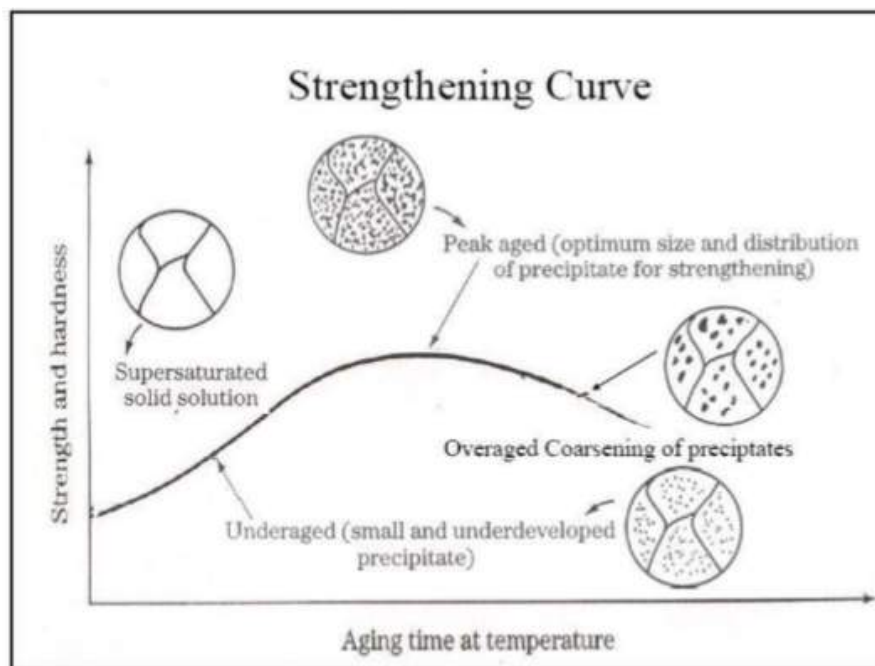
Figure 15: Strengthening curve of metals subject to precipitation hardening [44].

Solid solution hardening is done by dissolving a metal in a different metal. The amount of solvent may be increased until the solubility limit of the base material is reached. The introduced solvent enters the crystalline matrix of the solute material and crystallises. The dissolved atoms either replaces the existing atoms, substitutional solution, or if there is a large enough difference in size, they may locate themselves between the existing atoms. The latter is known as interstitial solution. The upgraded matrix results in a less manoeuvrable path for dislocations, requiring higher stresses and temperature to initiate plastic deformation [28]. Figure 16 high-

lights the differences between substitutional and interstitial solution.
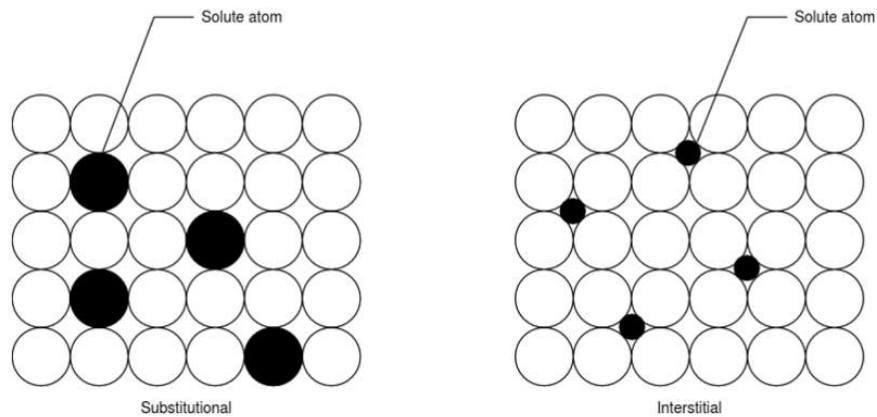
Figure 16: Substitutional and interstitial solution of atoms [13].

Martensitic transformation is a steel specific hardening mechanism. The process involves heating the specimen above a temperature threshold to facilitate phase transformation of the iron, resulting in a change in crystal structure. Steel is capable of dissolving larger quantities of carbon in this austenitic phase, rather than in the original ferritic phase. Upon the dissolution of carbon, the material is rapidly cooled, a process referred to as quenching, which renders the carbon atoms unable to rearrange themselves [20]. The process leads to the carbon atoms being locked interstitially in a distorted crystal lattice, forming a structure referred to as martensite. Carbon content in the steel is a governing variable and is to an extent proportional to the strength and hardness potential. The strengthening mechanism can be simplified by imagining the increase in force needed to further elongate an already extended spring [61]. Figure 17 show the relationship between carbon content and the maximum reachable hardness measured in Rockwell C.
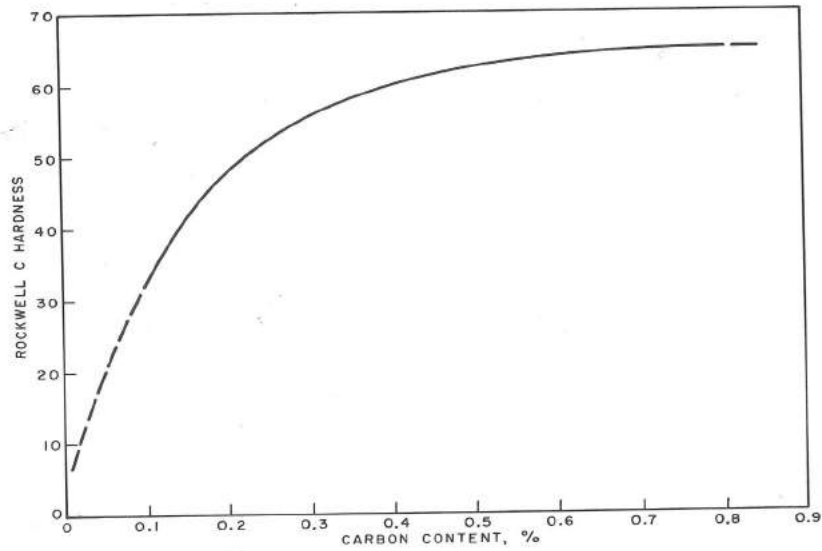
Figure 17: Relation between carbon content and hardenability [25].

In cases where martensite is formed to an excessive extent and the material exert unwanted brittle and hard characteristics, a reversing process called tempering may be required. Tempering involves heating the material to a temperature well below critical temperature. By addition of thermal energy, carbon atoms are allowed to diffuse out of the micro structure, relieving the internal stresses which in turn results in increased ductility and lower strength.

2.5.2 Surface treatment

Case-hardening describes a process using controlled quenching or the addition of nitrogen and/or carbon atoms to the substrate material through diffusion. This results in a material with high surface strength and hardness whilst maintaining the ductility of the core. Traditional surface treatments are generally divided into three categories - **thermochemical**, **thermal** and **coating/plating**[18].

Thermochemical treatments can further be divided into three subcategories:

- Carburizing

- Nitriding

- Carbonitriding

Carburizing, the addition of carbon to the surface region of the substrate, is usually done at temperatures between 815-1095°C to increase the carbon solubility of the steel [38]. However, high process temperatures increases the probability for undesired side-effects to the substrate such as geometric changes or changes in the microstructure resulting in unwanted properties. The process may be performed with a gas, liquid or solid as the medium. Table 1 shows a comparison of the different carburizing processes as stated by Campbell [13].

Table 1: Characteristics of different carburizing processes [13].

Process	Process temperature		Typical case depth		Case hardness,	Typical base metals	Process characteristics
	°C	°F	μm	mils	HRC		
Pack	815–1095	1500–2000	125–1525	5–60	50–63	Low-carbon steels, low-carbon alloy steels	Low equipment costs; difficult to control case depth accurately
Gas	815–980	1500–1800	75–1525	3–60	50–63	Low-carbon steels, low-carbon alloy steels	Good control of case depth; suitable for continuous operation; good gas controls required; can be dangerous
Liquid	815–980	1500–1800	50–1525	2–60	50–65	Low-carbon steels, low-carbon alloy steels	Faster than pack and gas processes; can pose salt disposal problem; salt baths require frequent maintenance
Vacuum	815–1095	1500–2000	75–1525	3–60	50–63	Low-carbon steels, low-carbon alloy steels	Excellent process control; bright parts; faster than gas carburizing; high equipment costs

Nitriding is the process of the diffusing nitrogen into the surface of a material where it combines with iron, creating iron nitride [13]. The process is done at a temperature range of 345 and 595°C [13]. At low processing temperatures, nitriding proves to be superior in cases where dimensional control is of importance.

Reasons for using nitriding include[18].

- The need for high surface hardness.

- Increasing wear and galling resistance.

- Improving corrosion resistance.

- Low processing temperatures, minimise the chances of distorting the substrate.

Table 2 highlights the nitriding process characteristics [13].

Table 2: Characteristics of different nitriding processes [13].

Process	Process temperature		Typical case depth		Case hardness, HRC	Typical base metals	Process characteristics
	°C	°F	μm	mils			
Gas	480–595	900–1100	125–760	5–30	50–70	Alloy steels, nitriding steels, stainless steels	Hardest cases from nitriding steels; quenching not required; low distortion; process is slow; is usually a batch process
Salt	510–565	950–1050	2.5–760	0.1–30	50–70	Most ferrous metals, including cast irons	Usually used for thin, hard cases <25 μm (1 mil); no white layer; most are proprietary processes
Ion	345–565	650–1050	75–760	3–30	50–70	Alloy steels, nitriding steels, stainless steels	Faster than gas nitriding; no white layer; high equipment costs; close case control

Carbonitriding is a process combining the diffusion of both carbon and nitrogen atoms onto the substrate through a modified gas carburizing process [13]. The process takes place at a temperature range between those of nitriding and carburizing and offers a harder case than carburizing. Furthermore, risk of distortion is reduced due to lower process temperatures.

Figure 18: Characteristics of different carbonitriding processes [13].

Process	Process temperature		Typical case depth		Case hardness, HRC	Typical base metals	Process characteristics
	°C	°F	μm	mils			
Gas	760–870	1400–1600	75–760	3–30	50–65	Low-carbon steels, low-carbon alloy steels, stainless steel	Lower temperature than carburizing (less distortion); slightly harder case than carburizing; gas control critical
Liquid (cyaniding)	760–870	1400–1600	2.5–125	0.1–5	50–65	Low-carbon steels	Good for thin cases on noncritical parts; batch process; salt disposal problems
Ferritic nitrocarburizing	565–675	1050–1250	2.5–25	0.1–1	40–60	Low-carbon steels	Low distortion process for thin case on low-carbon steel; most processes are proprietary

2.6 Thermal Treatments

Thermal treatments is further divided into;

- Flame hardening

- Induction hardening

Flame hardening involves heating the substrate to austenizing temperature before quenching it to form martensite at the surface. It can be performed manually by the use of a torch or be automated through a production line with torches and quench showers [13]. Due to the nature of the process, poor case depth control is evident. The method is commonly used on large parts where local regions require hardening or on parts exceeding available space in treatment facilities. Figure 19 illustrates the concept of flame hardening.
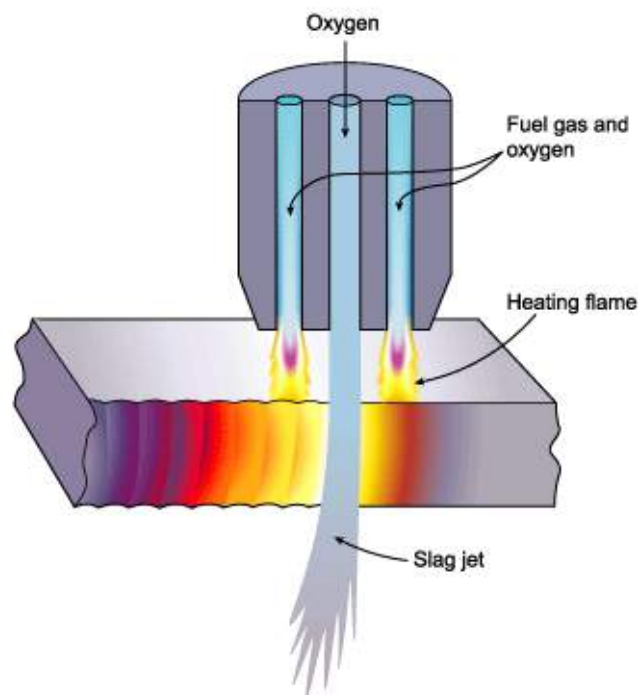
Figure 19: The concept of flame hardening [57].

Induction hardening has similar characteristics as that of flame hardening with the key difference being that the thermal energy is supplied and controlled through an inductor coil. This in turn leads to increased control of case depth through adjustment of the frequency, current and exposure time [13]. Figure 20 shows the concept of induction hardening.
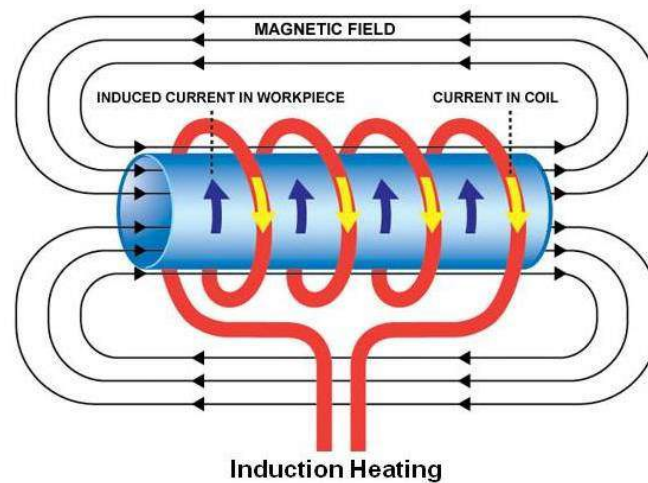
Figure 20: The concept of induction hardening [3].

2.7 Coating and Plating Treatment

The use of protective coatings is widespread within metal forming tools that are subjected to heavy wear, high temperature and high local stresses. Appropriate coatings manipulate the coefficient of friction, reducing several of the wear mechanisms previously mentioned. This project involves both tribological interactions between sliding surfaces as well as the typical wear mechanisms seen in punching. Common types of metal coating techniques involve:

- Electrodeposition

- Thermal spraying

- Vapour deposition

2.7.1 Electrodeposition

Electrodeposition, the process behind electroplating, has been considered the industry standard for metal plating for a long time. Through an electro-chemical setup, similarly to figure 21, with an anode and a cathode submerged in an electrolyte - cations flow to the anode, forming a thin metal coating on its surface. This is done by applying electric current to the setup, leading to the oxidation of the cathodic material. The process is a result of the difference in nobility of the metals, where the lesser material will become the cathode of the cell.
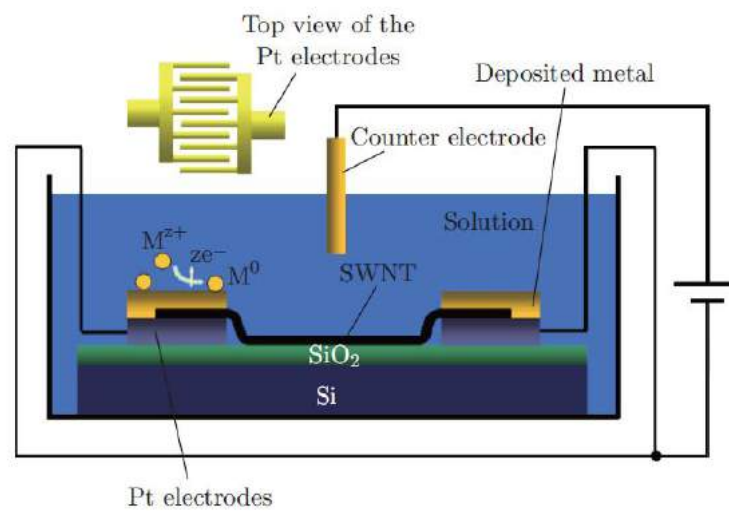
Figure 21: Illustration of electrodeposition process [64].

Advantages of Electroplating

- Low cost.

- Low complexity.

- Able to apply thicker coats than other processes.

- Easier to isolate areas for no coating.

- Does not depend on LOS.

29

Disadvantages of Electroplating

- Poor adhesion due to low energy input.

- Toxic chemical by-products.

- Low surface hardness.

- Requires a conductive substrate material.

2.7.2 Thermal Spray

Thermal spraying as a coating technique involves a coating material, typically a powder or wire, being heated into the liquid phase. The molten material is then sprayed onto the substrate with great velocity using a pressurised gas or other medium, as illustrated in figure 22. According to Sulzer Metco, a company specialising in thermal spraying, substrate materials with hardness below 55 HRC and sufficient strength to withstand the process preparation are suitable materials [46].
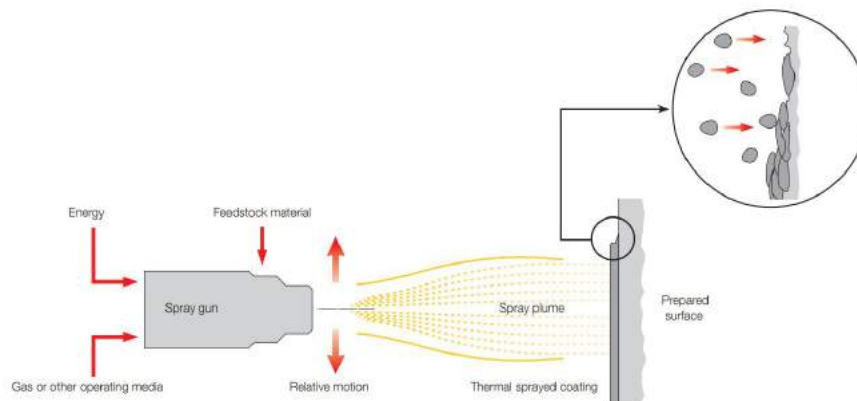
Figure 22: Illustration of thermal spray process [46].

Thermal spraying can be done through a wide temperature range and offer coating thickness up to that of welding. Any coating material that does not deteriorate when heated into liquid may be used for the process. Drawbacks of the process include

high minimum thickness and LOS dependability. The technique is often used in repair of worn components.

Advantages of Thermal Spray [18]

- Almost all substrate and coating materials may be used.

- Wide temperature and thickness range.

- Limited substrate heating.

- Removal of coating possible without damaging or affecting substrate.

- Possibility of localised treatment .

Disadvantages of Thermal Spray

- LOS technique.

- High thickness.

- Porosity of finished layer, prone to corrosion.

- Poor adhesion compared to other processes.

2.7.3 Vapour Deposition

Vapour deposition is used as a collective term for the processes in which layers are deposited on an atomic or molecular level to a solid surface. The involved processes are divided into physical and chemical vapour deposition, depending on the state of the source material. In physical vapour deposition the source is either a liquid or solid material while it in chemical vapour deposition is a chemical precursor [50]. An example of a coating applied using vapour deposition is showed in figure 23.

Figure 23: Example of vapour deposition coating.

Physical vapour deposition, PVD, is a coating technique revolving around material deposition through a vapourisation and condensation process. This is done through evaporation of the coating material using either a heat source or ion bombardment. The typical process temperature is 200-550°C [41].

In the evaporation deposition process, the source material is vapourised before it is led to the substrate. After having reached the substrate, the material condenses on the surface and creates the desired layer. Additionally, reactive gases may be used to form desired nitride, oxide or carbide coatings. The process is dependant on a protected environment in closed process chambers due to sensitivity towards contamination.

The ion bombardment or sputtering process works through sending high energy ions to the coating material. During the collisions on the surface of the coating material atoms are ripped out and form a vapour stream which travels to and condenses on the substrate.

A wide range of methods exist to energise the coating materials and complete the PVD process. The selection of method depends on the involved materials, financial

aspect and desired quality of the finished layer. The interaction between high energy atoms from the source material onto the substrate results in great adhesion between the materials. However, the process relies on the substrate surfaces being within line of sight, rendering it sub-optimal for complex geometries. A remedial step is to revolve the substrate around its axes to ensure condensation on all surfaces.

Advantages of PVD [18]

- Versatility and wide selection of both coating and work piece materials.

- Low temperature process.

- Environmentally friendly.

- Good adhesion to substrate.

- High surface hardness.

- Does not require a conductive substrate material.

Disadvantages of PVD [18]

- LOS technique, not optimal for complex geometries.

- High costs, up to 10x electroplating [21].

- Time consuming due to low coating rates .

- Limitations on component size due to vacuum chamber.

Chemical vapour deposition is similar to PVD in concept. However, this process forms coatings through chemical reactions between introduced chemical precursors and the heated surface of the substrate. This leads to the process being able to uniformly coat complex geometries as well as surfaces outside the line of sight.

The CVD process involve temperatures of up to 1000°C. As a consequence it is not recommended for components with tight tolerances and thin-walled geometric features. This is due to the risk of deflection and warping of the substrate. Additionally, several harmful by-products may be produced in the process.

Advantages of CVD[18].

- Multi-directional deposition, good coating conformance, does not rely on LOS.

- Less time consuming than PVD.

- Proven to be superior in applications where sliding friction and galling is problematic.

- Does not require a conductive substrate material.

- Excellent adhesion to substrate.

- High hardness

Disadvantages of CVD[18].

- High cost.

- High process temperatures.

- Harmful by-products.

- Material limitations

2.8 Coating Types

The number of available coatings is almost as large as the number of metals, each specifically tailored to their respective environments and load cases. Vettel et. al. discovered an increase in tool life of 3 to 100 times in coated tools within metal forming. Furthermore, they uncovered a reduction of up to 85% in required lubricant during production [62]. Throughout this chapter a few of the available coatings for similar applications to the puncher head as well as the sliding surfaces are researched and compared.

Titanium-nitride, TiN, is a well established and widely used coating within the metal forming industry. Figure 24 shows an example of TiN coated tools. Its strength of > 20GPa results in it being a beneficial coating for machining and heavy wear applications. According to A.J. Gant et. al. [26], one of the major drawbacks of TiN is limited oxidation resistance at working temperatures above 500°-550°C. The coating may be alloyed with aluminium, yielding Titanium aluminium nitride to remedy this. TiAlN delivers a strength of > 30 GPa and excellent oxidation resistance due to the rapid formation of aluminium oxide on the surface [26].

Figure 24: Drill bits coated with titanium nitride[1].

A.J. Gant et. al. discovered through their efforts that TiAlN has a low initial COF during load [26]. The coefficient rises under constant load to a steady-state of about 0.65. This is suspected to being due to the oxide layer being worn away, before a constant coefficient of friction at the pure base layer is established. Additionally, TiAlN is not intended to be used as a low-friction coating primarily, but rather as a protective layer preventing overheating of the substrate material. TiN and TiAln is commonly applied to substrates through both PVD or CVD techniques.

Diamond-like Carbon, DLC, are a series of coatings with superior hardness and low friction when compared to traditional nitride compounds. According Gant et. al, traditional DLC coatings are often used on lightly loaded components due to high brittleness and poor adhesion to the substrate.

High internal stresses contribute to the brittleness of the coating. By adding metallic elements, the internal stresses may be reduced. **Metal:C** is a range within DLC coatings that exhibit less brittleness and hardness, excellent adhesion and good wear properties. This results in low COF, usually around 0.15 according to Gant et. al. [26]. Diamond-like carbon coatings are usually deposited onto substrates using PVD or CVD techniques. Parts coated with DLC is shown in figure 25.

Figure 25: DLC coated parts[52].

Chromium Nitride, CrN, is a commonly used coating in several industrial applications. Unlike DLC coatings, CrN possesses low internal stresses. This results in excellent adhesion to the substrate as well as ductility in the coating. Additionally, the coating provides lubrication and corrosion resistance while having a low COF. According to Jagielski et. al., a 1.5 times decrease in COF was observed when comparing a CrN-coated AISI 304 piece to an uncoated one in self interaction [42].

Figure 26: Bolt carrier coated with chromium nitride [6].

One of the drawbacks of the widely used CrN is the low hardness and abrasive wear resistance which leads to early failure of coated tools [47]. Efforts into improving the CrN properties have been done by alloying various metals with the chromium nitride. One of the most promising compounds is aluminium chromium nitride[47]. According to Chandiran et. al., AlCrN coated carbide tools has a performance increase of close to 70% compared to TiN coated carbide tools [14].

2.9 Lubrication

Further friction reduction is made possible by the use of lubricants in the tribological interactions. By selecting an appropriate lubricant, a thin film will place itself between the interacting components, separating them. This results in an active COF between the component and the lubricant, rather than between the components. Throughout this chapter, a few lubricants will be discussed. Oils are considered non-viable as the tool will be open to the environment. As a result, solid lubricants are researched.

2.9.1 Solid Lubricants

Similar to the coatings discussed previous in this chapter, there exists solid coatings that offer active lubrication during wear by depositing thin films from itself. Due to the nature of their lubricating mechanism and predetermined thickness, the solid lubricants are typically applied using the following methods[48]:

- Vacuum deposition or thermal spraying of proprietary compounds.

- Rubbed onto the substrate as a powder, creating a burnished film.

- Dispersed with resin and sprayed onto the substrate where it cures and bonds.

- Dispersed in non-volatile fluids and applied to the substrate as a liquid lubricating medium.

Molybdenum disulfide, MoS_2, is one of the most widely used compounds applied to substrates as a solid lubricant. The compound is part of a family of materials referred to as transition metal dichalcogenides (TMDs). The unique feature of these materials is the difference in material properties within. This is due to their anisotropic crystal structure which results in strong binding forces in the x- and y-directions, but weak bonds in the z-direction. This gives the material high compressive strength perpendicular to the sliding motion and low shear strength along with the sliding motion.

This causes the compound to delaminate during tribological interaction, resulting in minimal friction between the sliding surfaces [33]. One of the drawbacks of MoS_2 is deterioration in environments with high humidity. According to T. Gradt and T. Schneider, a COF of between 0.15 and 0.30 is observed together with high wear in normal humid air, inducing premature failure of the coating [33].

Multiple research efforts into the improvement of MoS_2 mechanical properties have been done. One of the well-known concepts is the co-deposition of titanium in the coating, a method developed and patented by Teer Coatings Ltd. [26]. According to Teer Coatings Ltd., their compound $MoST$™exceeds typical MoS_2 coatings with a superior load carrying capacity, increased hardness, increased wear resistance, good adhesion to the substrate and improved performance in humid conditions [16].

Tungsten disulfide, WS_2, is a lamellar solid lubricant within the same material family and that has similar properties as MoS_2. According to Lowerfriction Lubricants, WS_2 is superior to MoS_2 in several aspects. It is stated that WS_2 is more stable due to its higher density, has a broader working temperature range, up to 60% higher load bearing ability as well as being more resistant to oxidation than MoS_2. Appendix B in chapter 8.2 highlights the differences. The compound is commercialised by Lubrication Sciences International under the name Dicronite™.

Graphite resides in the same material family as MoS_2 and WS_2, and abides the same working principle. However, unlike MoS_2 and WS_2, graphite relies on the presence of water molecules to function properly as a solid lubricant. The water molecules are absorbed into the structure where they weaken the bonding energy between the planes, giving the compound the easy shear characteristic of TMDs.

Research shows that most of the used coatings exhibit one or more compromises with regards to high temperature, loading, wear, environment, durability or application method. Within literature, the compound of **graphene** is mentioned as a possible solution and above-all coating. According to Berman et. al. graphene exhibits extreme mechanical strength, liquid and gas impermeability as well as low surface energy and COF[9].

Graphene is still in a early stage in terms of development and subsequently also in

literature. As a result of this, the price of the compound is significantly higher than its counterparts. This is largely due to high production costs.

2.10 Finite Element Analysis

2.10.1 Linearity and non-linearity

Materials behave differently throughout the process of undergoing loads to failure. The process involves elastic deformation into plastic deformation before one or more failure modes occur. To accurately predict materialistic behaviour in simulation software is a complex endeavour. Finite element analysis can be divided into two groups, linear FEA and non-linear FEA.

Linear FEA is the simplest and most widely used method of analysing loading effects in components. However, one of the greatest drawbacks of this method is the linear approach which is based on these assumptions:

- Displacement in the model is minimal and not of importance.

- The material is infinitely linearly elastic.

- The boundary conditions of the model does not change throughout loading.

- The system is steady-state and not time dependent.

When an analysis is based on a material model that is infinitely linearly elastic, any given increase in the applied load will result in an increase of the strain by the same factor [4]. Yielding of the material will never occur, and the analysis will output an incorrect component behaviour with unrealistically high stresses and strains. It is expected that the punch project will involve components subject to heavy loading, resulting in plastic deformation. Additionally, the aim of the tool is to deform and inflict failure upon the casing. Due to this an effort into the theory behind non-linear analysis is completed.

The non-linear approach accounts for the pitfalls found in the linear approach and may, if used correctly, yield a more accurate result. Non-linear analyses can be divided into material non-linear analysis, geometric non-linear analysis and a combination of the two [4].

The **material non-linear analysis** is used in cases where there are small strains and the change in stiffness is due to the changes in material properties. Here, the traditional engineering stress and strain measuring approaches may be used to develop the material model[4]. Such material model is often approximated into a bi-linear model, where the material stiffness before yielding is given by young's modulus and after is given by tangential modulus. An example of a Bi-linear graph is shown in figure 27
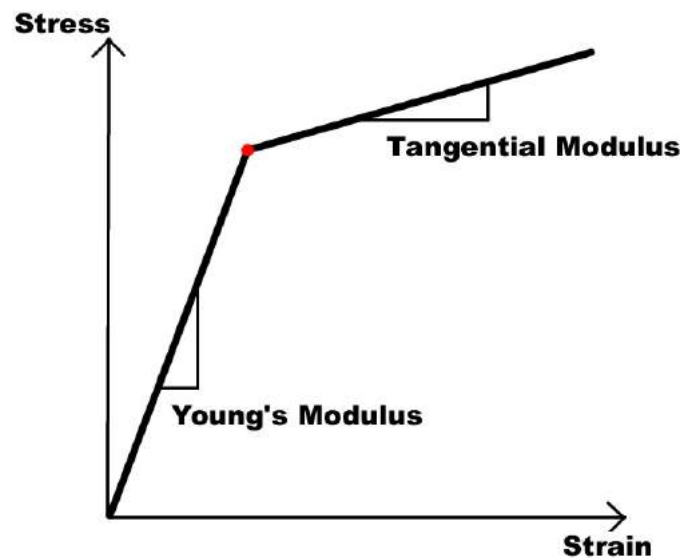
Figure 27: Example of a bilinear material model[39].

The **geometric non-linear analysis** is used where large strains and rigid body displacement are expected. Some problems involve non-linear strain-displacement relations and require consideration of actual strain-displacement relations as opposed to the linear relationship [10]. An example of this is the point loading of a simply pin-pin supported beam. Initially, the bending stiffness of the beam holds the load. However, with increased loading the beam will undergo transverse deflection. After

reaching a certain point, the axial stiffness of the beam will contribute to the overall stiffness, increasing its load bearing capacity. This situation is referred to as membrane locking [51]. Figure 28 illustrates this concept.
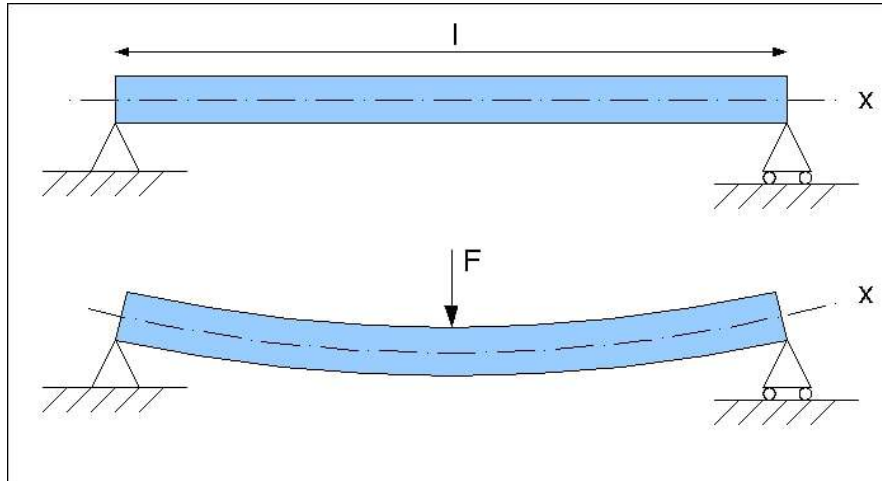
Figure 28: Simply supported beam with length l, both loaded with load F and unloaded.

According to Dassault Systèmes, a general rule of thumb is to conduct a geometric non-linear analysis if the deformations are above 1/20 of the largest dimension of the part [54].

Some problems requires the study of both material and geometrical non-linear effects due to large deflection or strain. In such problems, the stiffness may change throughout the loading process as a result of displaced geometry and change in material properties [10].

2.10.2 Non-linear Analysis

Time dependency is one of the major factors to consider when conducting nonlinear analysis. For dynamic events such as the impact of a bullet onto a metal plate, the inertia and acceleration effects have to be accounted for in the solution of the problem. These events occur during such a short period of time, that the solver have

to take time into account.

However, in many cases load is applied slowly. This enables the solver to neglect the dynamic effects of the interaction and simplify the problem into a static or quasi-static scenario that essentially is independent of time.

Generally there are three approaches to solving non-linear problems[10].

- Incremental approach.

- Iterative approach.

- Combination of incremental and iterative approach.

The **incremental approach** to solving non-linear problems revolves around dividing the applied load into a set number of increments and solving the set of equations for each increment. The accuracy of the solution depends on the number of increments, at the cost of computing power. The stiffness equation is created and solved for each increment [10].

The **iterative approach** takes the incremental approach one step further. From a solver perspective, the iterative approach can either be solved implicitly or explicitly. The implicit process pursues equilibrium between external and internal forces in the component, with a predefined tolerance span that is deemed acceptable by the user. The solver moves through several iterations until the residual is within the accepted tolerance, before it moves onto the next increment.

The explicit analysis does not take equilibrium into account and has as a consequence a larger margin of error than its counterpart. To remedy this, a larger number of increments is carried out to retrieve results closer to the exact solution. As explicit solvers do not consider the fulfilment of equilibrium in each increment, the process is overall less time consuming than the implicit approach. Generally, the implicit approach is used for slow events with minimal strain rate effects while the explicit method proves beneficial in extreme events such as high velocity impact scenarios [36].

2.10.3   Mesh Creation

The finite element method revolves around converting a continuous model into a finite number of elements to reduce complexity. The system of equations is solved for each element based on degrees of freedom, properties and external factors. The local solutions are subsequently combined to form a global solution for the entire geometry being analysed[60]. In FEA, such element division is referred to as mesh creation.

Element types

The individual elements are structured according to the geometry they are made to mimic. The element structures are grouped into:

- 0D Elements - utilised on rigid bodies, i.e. elements where the displacement is equal for all nodes.

  - Examples are any components that are insignificantly affected by the interaction or deemed not of interest for the analysis being done. Nuts, bolts, and welds are typical examples [15].

- 1D Elements - utilised on geometry where $x » y, z$.

  - Examples are shafts, beams and rods [60].

- 2D Elements - utilised on geometry where $x, y » z$.

  - Examples are sheet metal parts and plates [60].

- 3D Elements - utilised on geometry where $x \approx y \approx z$.

  - Examples are transmission casings, engine blocks or crank shafts [60].

In FEA it is possible to utilise all element types for a model. However, through careful and educated selection one may reduce the DOF of a component by a factor of several thousand [60]. This will in turn lower the demand for computation power and thus, the time.

Element shape

For 2D and 3D elements, triangular or square based elements are used. According to Christensen, J. et. al, good general engineering practice is to maximise the number of square elements in the model due to generally increased accuracy as opposed to triangular elements [15]. However, the use of square elements is not always practical and may lead to distortion of the elements. Figure 29 illustrates this concept through applying square and triangular element to a circular plate.
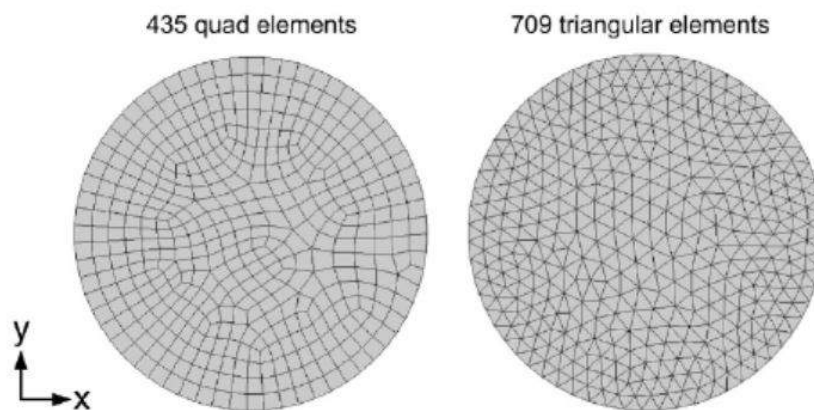
Figure 29: Shows difference between two circular bodies meshed with either quad elements or triangular elements[15].

Element size

Depending on the desired accuracy of the results, the element size should be considered. A preliminary understanding of the optimal element size may be found through evaluating the expected extent of deformation. With large displacements, a smaller element size is recommended to capture "all modes of deformation" [15]. It is recommended to tweak the mesh density, i.e. the number of elements created as a function of element size, at points of interest. A mesh convergence study may be done, where the mesh density is increased until the relative change in results diminishes when compared to computation time.

2.11 Failure of Materials

Due to the nature of the punching tool, this chapter includes a study into the literature of mechanical failure. Collins defines mechanical failure as any change in the geometry or the material properties of a component that results in it no longer performing its function to a satisfactory degree [17].

2.11.1 Mechanical Failure Modes

In mechanical design, failure criteria may be grouped into four categories [17].

- Elastic deformation

- Plastic deformation

- Rupture or fracture

- Material changes

These criteria are a result of a combination of force, time, temperature and environment. These occur either in the body or at the surface of the material [17]. By combination of these failure pillars, all commonly observed mechanical failure modes may be defined.

A few failure modes were considered critical for the punch head development. These include:

- Yielding of the puncher head and the casing.

- Ductile rupture failure of the casing wall.

- Brittle fracture failure of the puncher head.

- Various wear mechanisms.

- Galling failure of sliding surfaces.

Yielding failure is of concern when the plastic deformation of a part interferes with its ability to function properly [17].

Ductile rupture failure becomes evident when plastic deformation is carried out to an extent where the member separates into two entities. This is the failure mode the punching tool will inflict on the casing and thus, of interest.

Brittle fracture failure is the consequence of extensive elastic deformation in brittle components leading to breaking of the primary interatomic bonds [17]. Brittle fracture failure is considered to be probable as a consequence of utilising hardened or coated parts in the punch head.

Wear mechanisms is deemed highly relevant due to tribological interactions within the punching tool.

Galling failure is included due to it being an extension of wear failure.

2.11.2 Stress Concentration

Mechanical failure of components often originate at points with local stress concentrations due to discontinuities in the geometry or atomic structure[17]. Local stress concentrations may reach greater values than what is indicated through calculated design stress over the cross section of the part. Figure 30 visualises the introduction of a stress concentration by displaying the force flow through a loaded component with a notch. The applied loads has to be accounted for and there is effectively less area to distribute them. This leads to higher stresses in the areas of non-uniformity.
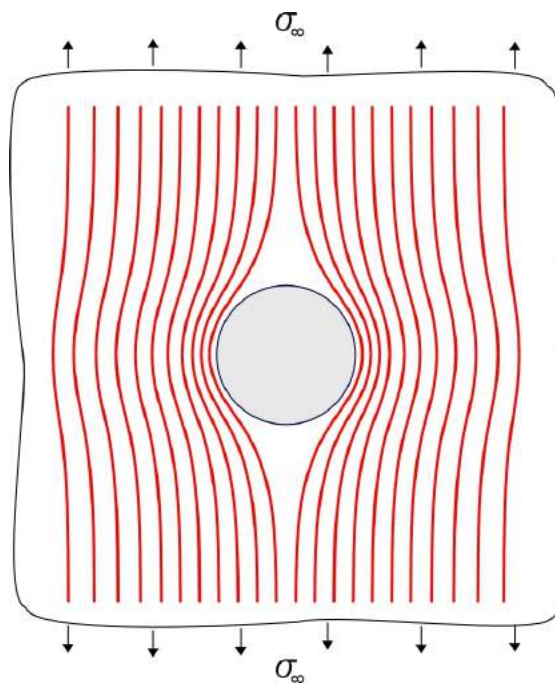
Figure 30: Illustration of stress concentration principle [12].

Local stress concentrations can be classified as either highly local or widely distributed when investigating stress concentration effects [17]. For highly local cases the total volume affected by the stress concentration is significantly smaller than the surrounding volume. Consequently, such cases are often considered acceptable as the material usually yields and redistributes the forces locally without affecting overall component performance. Widely distributed concentrations affect a larger fraction

of the overall volume of the component. This may lead to distorted geometry and affect the function of the stressed component [17].

2.12 Casing study

A preliminary questionnaire identified the target casing being a 4,5" casing for the tool development. Tables 3 and 4 below outline the specifications and properties for this casing.

Table 3: Typical casing materials with respective mechanical properties [31].

Properties Grade	H40	J55	K55	M65	N80	L80	C90	C95	T95	P10	Q125
Minimum Yield Strength (MPa)	276	379	379	448	552	552	621	655	655	758	862
Maximum Yield Strength (MPa)	552	552	552	586	758	655	724	758	758	965	1034
Minimum Ultimate Tensile Strengt (MPa)	414	517	655	586	689	655	689	724	724	862	931
Minimum Elongation (%)	29,5	24,0	19,5	X	18,5	19,5	18,5	18,5	18,0	15,0	18,0

Table 4: Typical casing sizes [31].

Size		Weight	ID		Drift	
Inches	mm	lbs/ft	Inches	mm	Inches	mm
		9,50	4,090	103,89	3,965	100,71
		10,50	4,052	102,92	3,927	99,75
		11,60	4,000	101,60	3,875	98,43
		12,60	3,958	100,53	3,833	97,36
		13,50	3,920	99,57	3,795	96,39
		15,10	3,826	97,18	3,701	94,01
4 1/2	114,30	16,60	3,754	95,35	3,629	92,18
		16,90	3,740	95,00	3,615	91,82
		17,70	3,696	93,88	3,571	90,70
		18,80	3,640	92,46	3,515	89,28
		21,60	3,500	88,90	3,375	85,73
		24,60	3,380	85,85	3,255	82,68
		26,50	3,240	82,30	3,115	79,12

The casing designation is 4.5" 12.6ppf L80. Here 4,5" gives the outer diameter of the casing, ppf defines the internal diameter and wall thickness, and L80 defines the casing material. The L80 material has a minimum yield strength and hardness requirement. Casings in this material is often used in sour environments containing hydrogen sulphide.[5]

3 Method

3.1 Basic Calculations

To determine the forces needed to punch any casing with a given material, hand calculations are a quick and easy way to start. This has been done to see what is possible and what limitations there are given the available forces from the EMT. This subsection will define the equations needed to do these calculations and present the key figures for what to expect from punching simple geometry through a given casing with a given material.

3.1.1 Available forces

Having the target casing defined, available forces must be identified to verify if punching is feasible. The E Plug EMT is capable of supplying 5600Nm of torque to its connected tool(s). Through the power thread interface in the top connection of the tool, this torque is converted to axial force. The following formulas apply.

Necessary inputs are;

- Coefficient of friction - μ_s

- Collar mean diameter - d_c

- Thread pitch diameter - d_m

- Number of thread starts - n

- Threads per inch - TPI

Given the constants above, the metric pitch of the thread is given by

$$p = \frac{in}{TPI} \tag{1}$$

For further calculations the pitch circumference is needed

$$C = \pi \cdot d_m \tag{2}$$

Lead as a factor of thread starts is given by the following equation

$$L = p \cdot n \tag{3}$$

Thread lead angle is given by

$$\alpha = atan\frac{L}{C} \tag{4}$$

To include any friction accounting for trapezoidal threads the following friction factor can be found

$$\mu = \frac{\mu_s}{cos(\phi)} \tag{5}$$

Given all the above definitions and equations the torque required to raise any thread given the axial load is

$$T_r = F_n \cdot \frac{d_m}{2}\left(\frac{(\mu + tan(\alpha))}{(1 - (\mu \cdot tan(\alpha)))} + \frac{d_c}{d_m} \cdot \mu_c\right) \tag{6}$$

Also the torque required to lower the thread given any axial load is

$$T_l = F_n \cdot \frac{d_m}{2}\left(\frac{(-\mu + tan(\alpha))}{(1 + (\mu \cdot tan(\alpha)))} - \frac{d_c}{d_m} \cdot \mu_c\right) \tag{7}$$

3.1.2 Axial forces vs radial forces

The punching tool will have to redirect the axial forces into radial forces. One way of doing this is by using components sliding on incline planes relative to each other. Force redirection through incline planes depend on the angle between the components as well as the coefficient of friction between slider and slidee. The angle between the interacting components must result in sufficient force efficiency as well as offer the required radial expansion without demanding excessive axial travel. The following formulas allows for evaluation and retrieval of punching forces on potential prototypes. Figure 31 illustrates the load case.
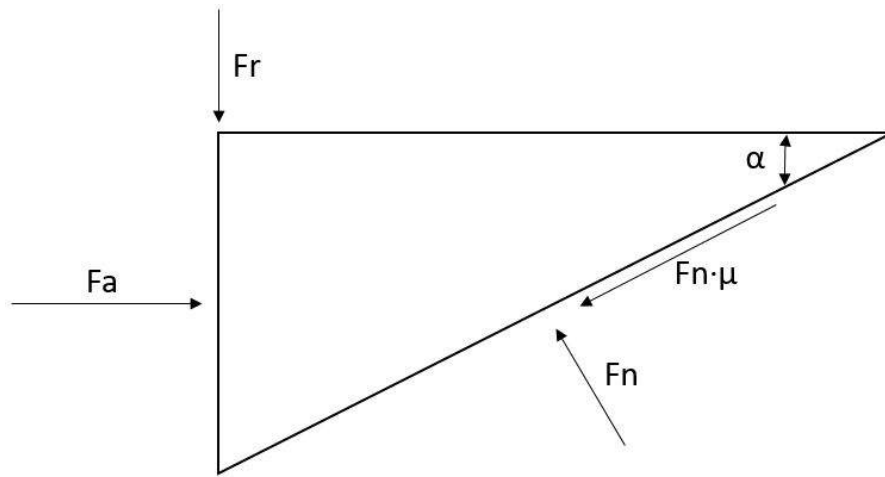
Figure 31: Shows different forces acting on a angled sliding surface.

Axial force as a function of radial force, angle and coefficient of friction

$$F_a = \frac{F_r \cdot ((cos(\alpha) \cdot \mu) + sin(\alpha))}{cos(\alpha) - (sin(\alpha) \cdot \mu)} \tag{8}$$

Radial force as a function of axial force, angle and coefficient of friction

$$F_r = \frac{F_a \cdot ((cos(\alpha) - (sin(\alpha) \cdot \mu))}{(cos(\alpha) \cdot \mu) + sin(\alpha)} \tag{9}$$

3.1.3   Shear forces for simple geometry

Having identified available forces and how to transfer them, the required forces for punching a casing is the next objective. A simplified approach to the shearing interaction between a plate and a punch is used. This interaction depend on the following factors:

- The circumference of the punch and the thickness of the plate. These give the total shear area.

- The plate's tensile strength combined with the Von Mises yield criterion gives the shear strength of the material.

Circumference of a circular punch is given by:

$$C_p = D_p \cdot \pi \tag{10}$$

Shear area based on plate thickness, t_p, and circumference of the punch, C_p then yields:

$$A_s = C_p \cdot t_p \tag{11}$$

The shear strength of a material is found through the tensile strength, σ_t, and the Von Mises yield criterion.

$$\sigma_S = \frac{\sigma_T}{\sqrt{3}} \tag{12}$$

The theoretical radial shear force required is subsequently found through the following equation:

$$F_s = \sigma_S \cdot A_s \tag{13}$$

54

3.1.4 Force Distribution

To model the force propagation throughout the cross-section of the pipe, a simple polygonal approach can be used, see figure 32. Modelling the punch heads as a polygon with radial forces applied to the nodes outwards gives an estimation to the hoop stress involved in the process, see figure 33. This enables evaluation of the optimal number of punches, and indicates whether the casing will shear before yielding between the punches and creating a standoff.
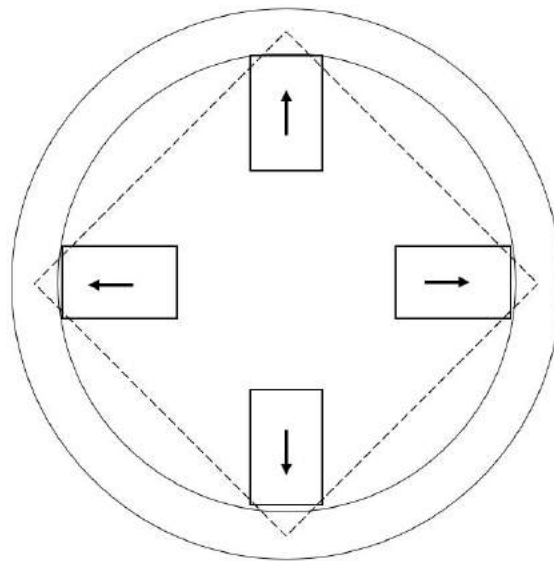
Figure 32: Illustration of polygon distributed punches.
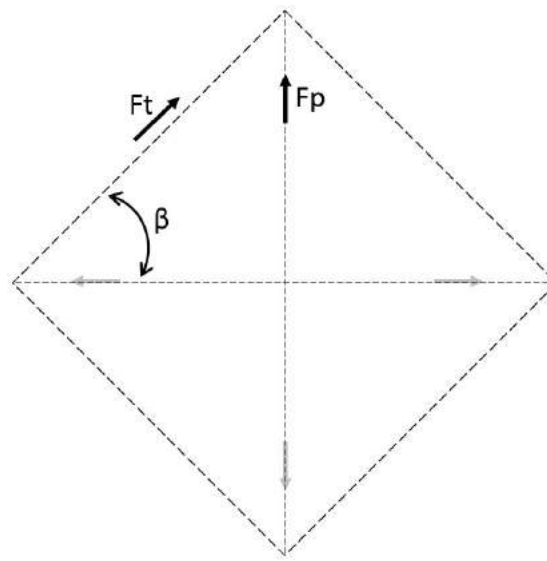
Figure 33: Illustration of decomposition of polygon distribution.

The relationship between the hoop force and the applied radial force opposing it can be found through the following formulae.

Acting hoop force angle as a function of polygon.

$$\beta = \frac{360°}{2 \cdot N}$$

(14)

Where N is the number of edges in the polygon.

Hoop force decomposition as a function of radial force and the hoop force angle. This gives the portion carried by the casing wall between the punch in question and the subsequent one.

$$F_t = \frac{F_p}{2 \cdot sin(\beta)}$$

(15)

3.2   Initial punch testing

Hand calculations have their limitations and may be inaccurate compared to testing. To evaluate the established theory, initial punch tests were performed.

This subsection will give a look into the initial testing that was completed to verify the forces needed to punch a casing. This subsection will also explain how different punching geometries were tested to learn more about punch and casing behaviour, as well as provide useful data for simulation comparison later.

3.2.1   Test equipment

The following list illustrates the the test equipment needed to complete all testing for this thesis.

- Hydraulic Press.

- Lathe.

- Manual milling machine.

- Rotary table.

- Tensile testing machine.

- Angle grinder.

- Angle grinder jig.

- Kingsland standard punch.

- 4,5" 12,6ppf L80 casing.

- AISI 4145 bolt.

- Axial load cell.

- Logging computer.

- Linear potentiometer.

- Pressure transducer.

- HBM logging unit.

- CAD computer with SW and Autodesk Fusion installed.

- PPE.

3.2.2   Simple cylindrical punching

The first tests completed involved a 5,5" Q125 casing and multiple promising punch objects. This is a different casing and material that is defined as the main casing to punch, but the whole purpose of these tests was to define a relation between the hand calculations and the test results.

The first test was completed using a M12 12.9 grade machine bolt. The bolt was placed inside a guidance disc to centralise the bolt over the casing. When load was applied, the M12 bolt failed in bending, due to poor centralisation. See figure 34 under for illustration of the failed bolt and the marks it left on the casing.

Figure 34: M12 bolt deflected after punch attempt.

After the M12 bolt had failed, a parallel pin made from hardened carbon steel was found. The tip of the parallel ping was sharpened using a grinder to give it a small initial area. Similarly to the bolt, the pin was placed in an aluminium block to give it support. See figure 35 below.

Figure 35: parallel pin placed inside aluminium bolt for guidance.

Unfortunately, the pin penetrated the aluminium block without punching the Q-125 casing, leaving only a dent in the surface.

The failure of the previous test was mitigated though using a guidance block in steel. This time the pin was left with a blunt end to see what impact such geometry would have on the indentation on the casing. See figure 36 below.

Figure 36: Parallel pin placed in steel bolt for guidance.

Due to alignment issues, the parallel pin experienced bending and subsequent brittle fracture rather than penetrating the casing. See figure 37 below.

Figure 37: Shows broken parallel pin after punching.

The indentation made by the parallel pin showed promising characteristics and opted for another attempt with an identical setup. However, a combination of poor central-isation and no rotational constraint on the casing resulted in the casing sliding and the pin bouncing off. Figure 38 below show the indentation in the casing.

Figure 38: Indentation in casing from parallel pin punching.

Despite multiple failures due to insufficient support of both punch and casing, the punch geometry yielded promising results. An improved setup was established through purchasing a standard punch, as shown in figure 39) below. Additionally, the casing was rotationally constrained using a chain vise. This standard 12mm punch was then punched through the casing.

Figure 39: 12mm standard punch.

3.3   TB-punch development

Punch design and production

After initial testing was completed, a more systematical test approach was initiated using rectangular or square punch head geometries. Here the objective was to see what impact different geometries would have whenever the shear area from the punch was kept constant. Another point of interest was to observe what impact different angles had on the hole geometry.

These test punches, hereby referred to as TB-punches, were also intended to be used for comparison purposes towards simulations. The test results from the punches can be used to adjust variables in the simulation model to generate more accurate results.

In figure 40 there is a CAD illustration of the TB-punches with the different variables for the punching geometry shown in blue. The target was to keep the shear area constant, i.e. maintaining the relationship between length (B) and (A), yielding the circumferential distance (pink square/rectangle) constant.
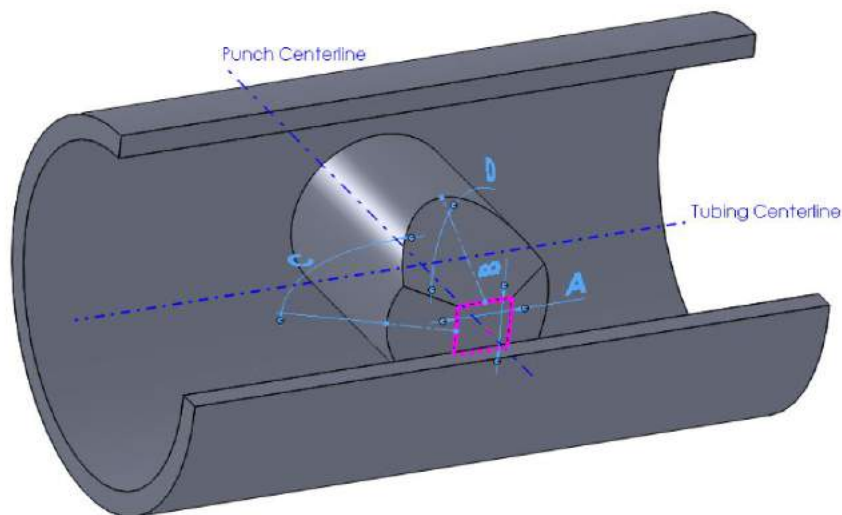
Figure 40: Illustration of punch model with variables illustrated.

Four different punches were made in AISI 4145 using an angle grinder held in a support jig, see figure 41) below.

Figure 41: Punch in production, fastened at an given angle in an angle grinder jig.

Table 5 shows the different punches manufactured with dimensions according to figure 40.

Table 5: Different punches with respective variable values.

Description	Dimensions ref. illustration figure				Shear Area [mm^2]
	A [mm]	B [mm]	C	D	370
TB-1	17	17	30°	30°	370
TB-2	17	17	60°	30°	370
TB-3	24	10	30°	30°	370
TB-4	29	5	30°	30°	370

Once all punches were produced, they were ready for testing. Figure 42 below shows the transformation from bolt to finished punch.
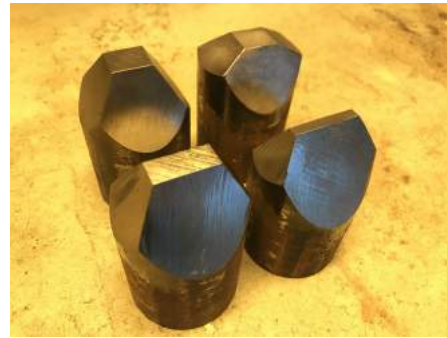
(a) 4145bolt before production and finished punch after.

(b) All punches after production ready for testing.

Figure 42: Transformation of bolt to punch.

TB-punch testing

A 4,5" L80 casing was used by cutting out a square hole on the side of the casing. This was done to ensure the casing had sufficient support when the punch was pressed through from the inside. The prepared casing was placed on steady rests in the hydraulic press as shown in figure 43.

Figure 43: Casing placed in the hydraulic press.

The first punch (TB-1) was placed in the hydraulic press and load was applied as the reaction force and travel was measured and logged. Load was applied until the casing reached its ultimate strength, and a significant indication of casing failure was observed. After the press was raised, log data was retrieved and the casing was inspected on both the inside and outside.

The same test procedure was completed for all of the four TB-punches previously listed in figure 5

To see what impact the different TB-punches had on the final hole geometry, all punches had to be pressed through the casing. Additionally, any wear or damage of the punches would be magnified due to more interaction with the casing. To test this, new casing specimina were made and full extension tests were done on all punches.

3.4   Material test specimina

To further aid development of the punch geometry, it was necessary to construct a material model for the evaluation of more complex geometries. It is possible to find information about the L80 casing material through literature, but this information only supply an envelope where the different material values are given with a tolerance. Each individual material batch and casing will vary within these tolerances, and to build a solid and valid simulation model which can be compared with calculations and test results, it is needed to get accurate test data from the casing.

To construct the material model, tensile tests were produced directly from the test casing. Since the casing has a given wall thickness, the tensile test specimina were limited in geometry. Using SolidWorks, the casing was modelled and the test specimina were maximised in size. See figure 44 below, where a cross-section of the casing is shown together with the cross-section of the test specimina.
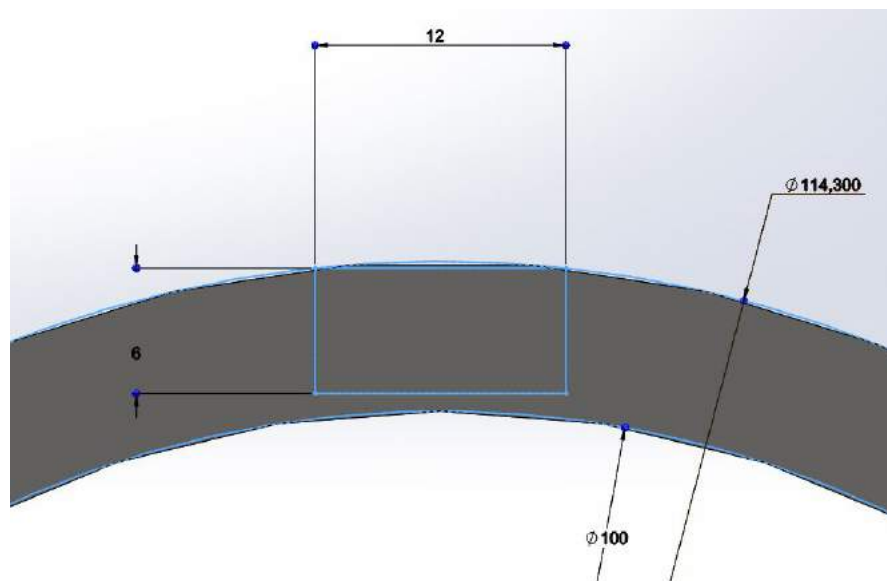
Figure 44: cross-section of casing with maximum area of tensile sample sketched.

Once the maximum cross-section area of the test specimina was established, their length and geometry was defined from ISO-0689 (see appendix A in chapter 8.1). Us-

ing the standard, the final CAD model of the material test specimina is shown in figure 45.
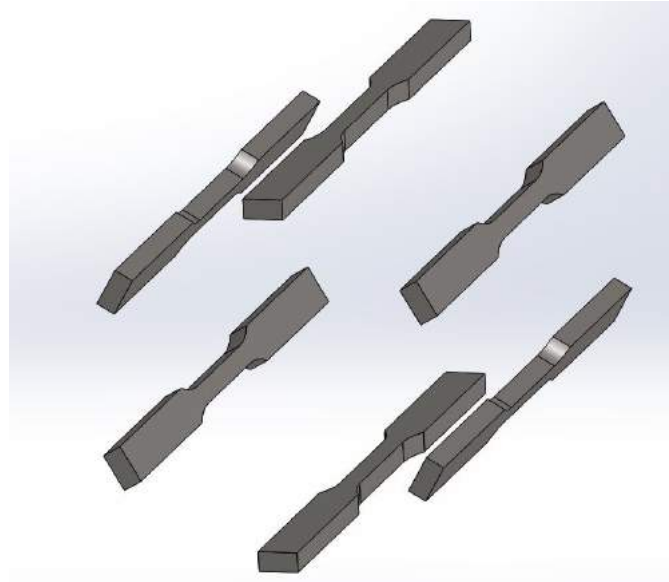
Figure 45: CAD model of tensile test specimina.

Following the design of the test specimina, the casing was secured to a rotary table in the milling machine and six individual test specimina were machined. See figure 46 below for an illustration of how the casing was rotated to produce several specimina using the rotary table.

Figure 46: Casing secured to rotary table during machining.

After the test specimina were milled from the casing they had three flat surfaces, where the last face was milled using a face mill and a vise in the milling machine. To get the specimen failure area as shown in figure 46, the specimina were placed in a CNC milling machine in the University workshop. Here, the parallel area of the test specimina were milled according to ISO-0689.

Once the specimina were completed, as shown in figure 47, they were placed in an Instron tensile test machine where the testing was performed.
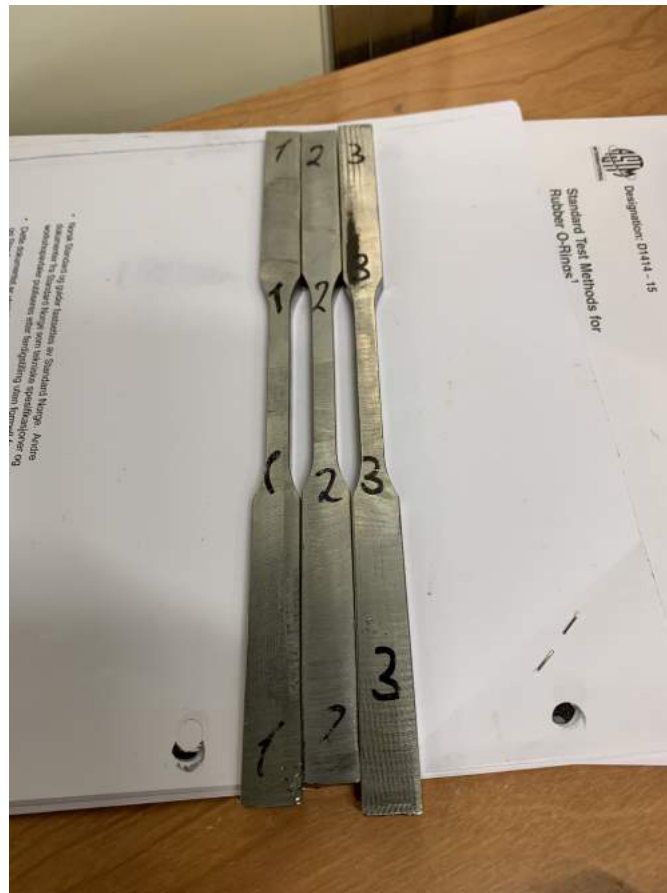
Figure 47: Three tensile test specimina ready for testing.

3.5 TB-punch simulation

Simulation Objective

Having established a material model from the casing and conducted tests with different punch geometries, a simulation model was generated. The purpose of the model was to be able to iterate and evaluate various geometries without incurring capital costs related to the production of these. Through this approach, time and effort may be put into promising geometries while discarding sub-optimal solutions at an early stage.

The objective of the simulations was to compare and investigate the effects of the following parameters:

- Reaction force on the punch at casing failure.

- Elastic deformation of casing.

- Coefficient of friction in punch and casing interaction.

Puncher geometries

The results from testing the TB-punches were used to validate the simulation model.

Numerical model approximation

The punch geometries were, together with a quarter section of the casing, run on an axisymmetric modelling assumption to reduce the required computational power and run time. The punches were given a prescribed displacement of 15mm in the y-direction to sufficiently penetrate the casing wall. Additionally, the punches were fixed in the remaining degrees of freedom. The casing was fixed at three of four edges using frictionless constraints, disabling relative motion normal to the edge faces. The fourth edge was kept unconstrained to enable the flow of material during deformation. The casing was modelled using mechanical properties from the material study.

The stress levels in the punch heads were considered to not be of importance at this stage, as a wide range of materials are available to remedy any unwanted effects. As a result, the punch geometries were modelled as rigid bodies to reduce computational power and time. A contact set was defined using the faces of the punch head as the master and the inside face of the casing as the slave. The COF was defined in the contact set and iterated to evaluate the tribological effects on the radial force required to penetrate the casing.

Mesh Setup

The casing was partitioned into two different zones, where the zone closest to the punch was given smaller elements and the remainder of the casing elements were automatically scaled relative to its total size to reduce computational power and time. Figure 48 below, shows the partitioning of the casing.
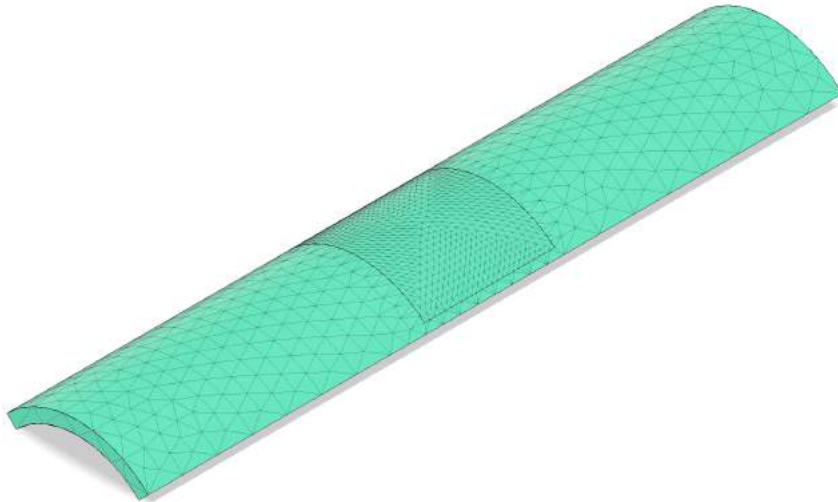
Figure 48: Casing mesh - 75x75mm.

It was observed through a simple convergence study on one of the punch geometries that an element size of 3 mm provided satisfactory results while keeping computation time at a minimum. Due to software limitations, parabolic tetrahedron elements were chosen and the software was allowed to create curved mesh elements for better approximation of curved and rounded faces.

Solution Method Employed

The simulation of the rupture failure of a casing due to shear forces is assumed to be a quasi-static problem. According to literature, the iterative implicit solution should prove beneficial in this case. However, due to software limitations, an iterative explicit solution was used in the model. The event duration in the simulation was 0.001

second and element deletion was activated corresponding to the material elonga-
tion at break of 21.21%. This module deletes elements that reach strains above the
predefined threshold to emulate real life failure.

3.6 Prototype Development

Following the testing and simulation of the TB-punches, the development of a more
complex geometry was desired. The test data and findings from punched hole ge-
ometry gave indications of which geometries to pursue. This subsection explains the
work done to further explore the puncher geometry with simulations, production of
a simplified test model and testing of said model.

3.6.1 Simulations

The TB geometries gave useful indications as to what geometric features results in
the desired perforation shape. The cutting edge of a sharp axial vertex, combined
with angled geometry in the opposite end result in a satisfactory tear and flap char-
acteristic. In TB-2, the shearing and flap lifting process occurred simultaneously. To
remedy this, concepts where the shearing process is completed prior to the flap being
lifted were explored. Furthermore, minimising the initial shear area was prioritised.
Figure 49 below shows one of the promising designs.
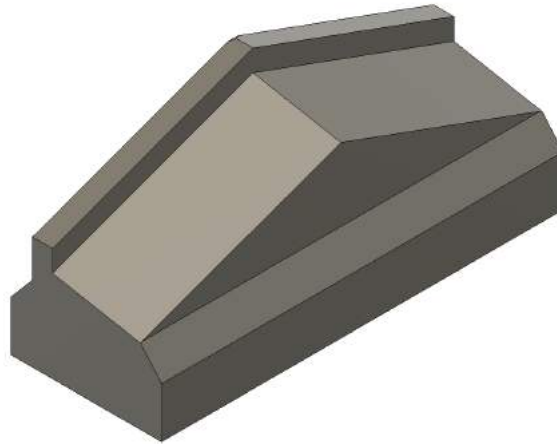
Figure 49: Prototype 3 model.

Due to budget limitations, the punch geometry was designed with simple features to enable production in a manual milling machine. The angle scale on both the milling machine and the vise is divided into 360° at 1° increments. As a result the angles on the test punch had to be of whole integers to enable manual production. See figure 50 below for an illustration of how the different tools on the milling machine can be oriented by two axes. Furthermore, the prototype was modelled using the same material (AISI 4145) as the TB-punches.
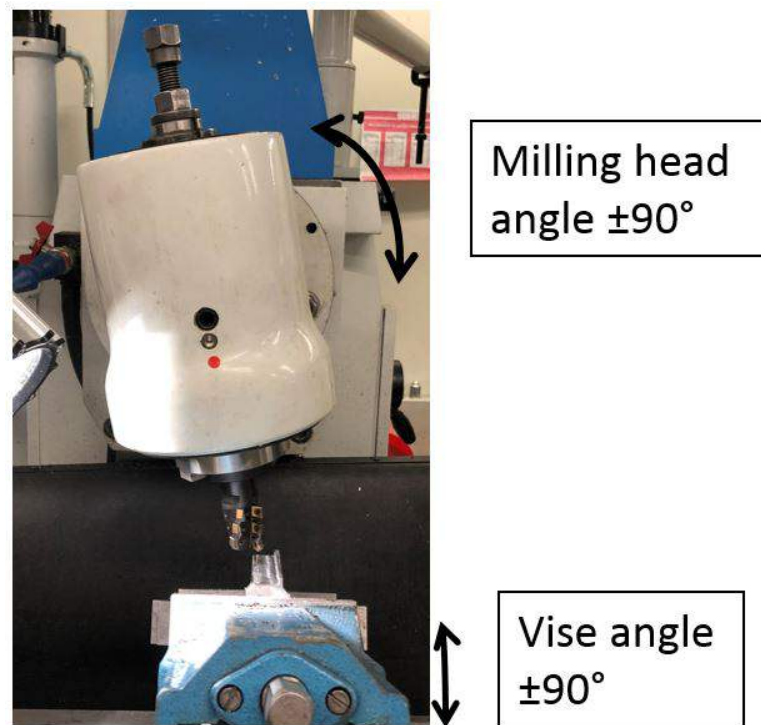
Figure 50: Adjustment capabilities in two axes on the milling machine.

3.6.2 Production

Based on the simulation results, it was desired to verify if the simulations were giving correct output and thereby useful conclusions. To test this, a punch prototype was produced.

The puncher was first milled square from the AISI 4145 bolt, then the angles were milled using a face mill. After this, an end mill was used to make the cutting edge, which was made through milling one section lower than the top of the cutting edge, see figure 49 for an illustration from the CAD model.

Once the angles were milled on both sides of the head, the milling machine was tilted to create the last angles relative to the angled face from the previous operation. See figure 51 below for an illustration of the milling. After one side was milled, the puncher was turned around in the vise and the last angled side was milled. See

figure 52 where the finished puncher head is illustrated.

Figure 51: Punch machining in process.

Figure 52: Punch head completed.

To secure the puncher to the hydraulic press, different mounting tools were created based on the original mounts in the press. The puncher was drilled and threaded in the bottom side to fit these mounting tools. See figure 53 for an illustration of the finished test puncher fastened to the mounting tool.

Figure 53: Completed punch mounted.

3.6.3   Testing

After the test punch was completed, it was mounted to the hydraulic press using the mounting tools produced for the purpose. See photo in figure 54 for illustration of the punch mounted to the hydraulic press.

Figure 54: Puncher mounted in the hydraulic press.

Once the press, casing and puncher were ready, two tests were performed with the resultant force and distance logged using the logging devices on the hydraulic press. The first test was completed by punching the casing to failure and then return the puncher to inspect the casing. After the first test, another test casing was punched. In this test, the punch was pressed to maximum extension of the press to get an impression of the reaction force behaviour and how the punched hole evolved.

4 Results

4.1 Basic Calculations

4.1.1 Available Forces

From equation 7 in chapter 3 there are significant variations in the output from the thread, depending on the environment and the thread characteristics. Table6 shows the different axial force outputs from different thread characteristics, given a constant torque of 5600Nm and a constant COF.

Table 6: Thread output given constant friction factor and applied moment.

Available torque (T) [Nm]	5600,00	5600,00	5600,00	5600,00	5600,00	5600,00	5600,00	5600,00	5600,00	5600,00	5600,00	5600,00
Number of thread starts (n)	4,00	4,00	4,00	4,00	4,00	4,00	4,00	4,00	4,00	4,00	4,00	4,00
Thread per inch (TPI)	8,00	8,00	8,00	8,00	8,00	8,00	8,00	8,00	8,00	8,00	8,00	8,00
Axial force (F) [kN]	2715,61	1816,84	1364,15	1091,46	909,22	778,83	680,91	604,68	543,65	493,68	452,02	386,51
Total time [min]	0,66	0,65	0,65	0,65	0,65	0,65	0,64	0,64	0,64	0,64	0,64	0,63
Axial Force/Time	4138,58831	2778,094727	2092,8227	1680,0246	1404,1326	1206,7198	1058,4649	943,03574	850,61355	774,94053	711,83966	610,63742

The available axial force given by the thread is highly friction dependent. As shown in figure 55 the available force, given a constant torque, varies from 2500kN to below 500kN through varying COF. The descending force output describes the efficiency of the thread. The reduction in efficiency is indicative of the power loss in the system due to tribological interaction. The thermal energy generated increases the temperature of the environment and worsen the working conditions of the thread in localised areas. The applied coating or lubrication should as a result be able to withstand extreme temperatures.

81
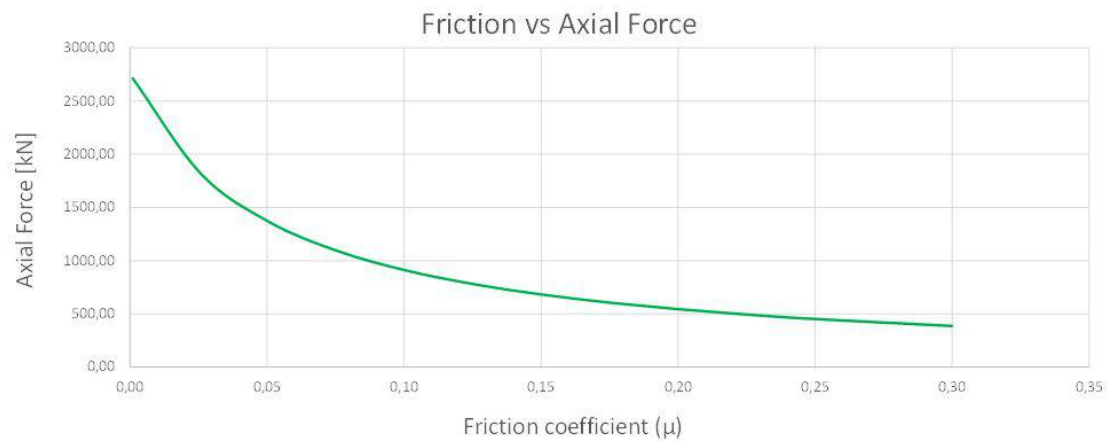
Figure 55: Available axial force as a function of friction factor.

4.1.2 Axial forces vs radial forces

Through equation 9 in chapter 3, different radial forces were obtained through manipulating the sliding angle. The COF and axial force was kept constant at 0,1 and 1000kN, respectively. In table 7 below, these forces found are listed.

Table 7: Radial forces as a result of incline plane interaction.

Angle (α)	Friction factor (μ)	Fa	Fr
10	0,1	1000	3555,1
15	0,1	1000	2644,9
20	0,1	1000	2076,9
25	0,1	1000	1683,5
30	0,1	1000	1391,1
35	0,1	1000	1162,2
40	0,1	1000	975,5
45	0,1	1000	818,2
50	0,1	1000	681,9
55	0,1	1000	560,9
60	0,1	1000	451,3
65	0,1	1000	350,0
70	0,1	1000	254,7

Figure 56 show the efficiency score of each plane angle relative to axial travel. The results were computed through COF increments of 0.1 between 0.1 and 1. The angles were iterated in increments of 5° between 10° and 70°.
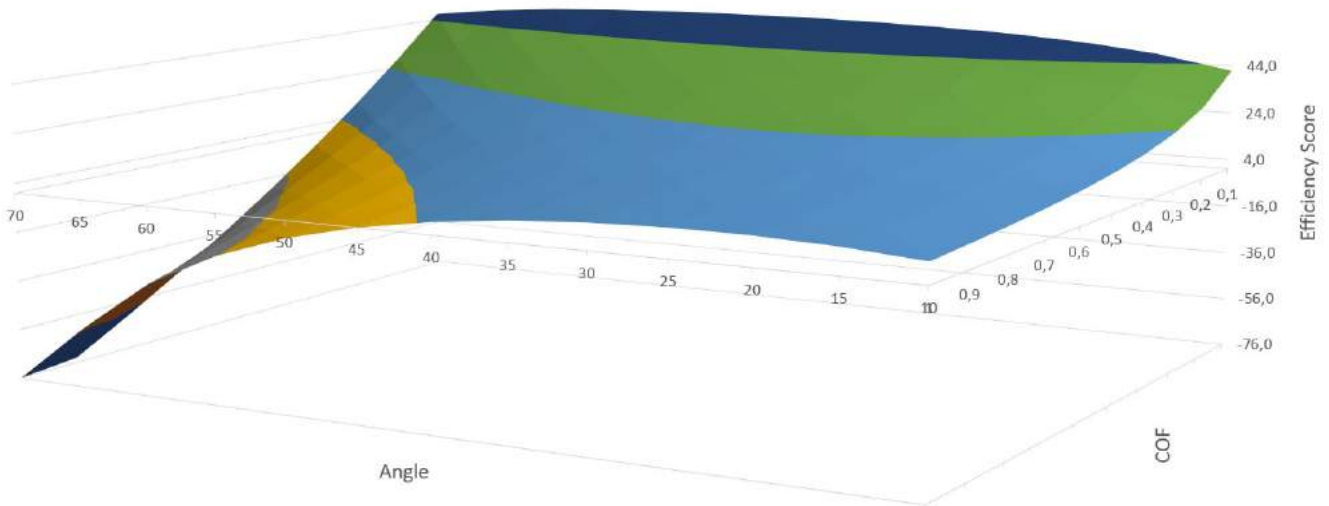
Figure 56: 3D plot with COF, angle and efficiency score.

4.1.3   Force distribution

Through utilisation of the polygon model developed in chapter 3, an indication of the optimal number of punches could be found by considering the desired end result. Table 8 shows the force distribution from radial to tangential hoop force as a function of number of punches.

Table 8: Tangential reaction force as a function of number of punches.

Polygon	Force Angle (rad)	Radial Force (kN)	Tangential Force
3	1,05	100	57,7 %
4	0,79	100	70,7 %
5	0,63	100	85,1 %
6	0,52	100	100,0 %
7	0,45	100	115,2 %
8	0,39	100	130,7 %
9	0,35	100	146,2 %
10	0,31	100	161,8 %

4.2 Initial punch testing

4.2.1 Calculation Results

Through equation 13 in chapter 3, the calculated theoretical reaction force from punching standard punches is shown in table 9 below.

Table 9: Shear force for circular geometry.

Diameter [mm]	Tensile strength [Mpa]	casing wall thickness [mm]	Shear Force [kN]	Tested shear Force [kN]
10	739	8,21	110,05	-
12	739	8,21	132,06	145
14	739	8,21	154,07	-
16	739	8,21	176,07	-

4.2.2 Test Results

The standard punch was punched through the 5,5" Q-125 casing successfully, providing data for calculation comparison. See figure 57 below for illustration of the reaction force from the test.
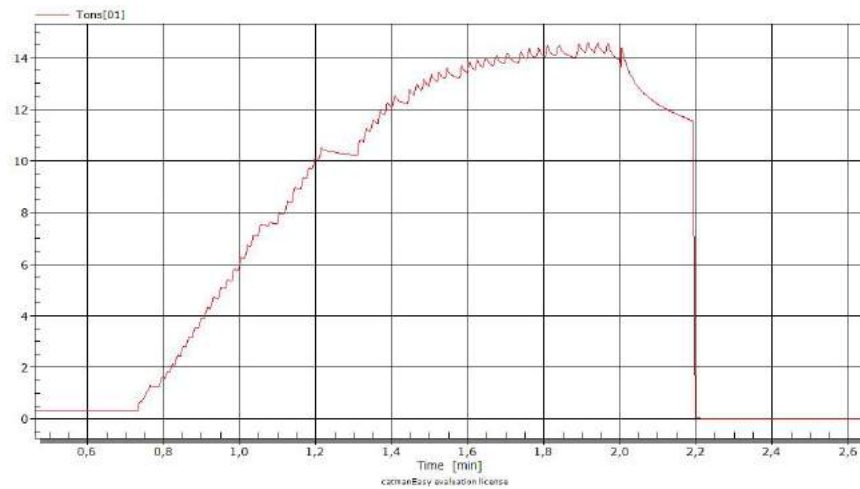
Figure 57: Measured reaction force from 12mm punch.

After initial punching, there was a significant permanent deflection of the casing and some local deformation around the punched hole. See figure 58 below.

Figure 58: Casing after punching, note the deflection in the casing.

4.3 TB-punch testing

4.3.1 Calculation Results

In table 10 below, the calculated results from the TB-punches are illustrated.

Table 10: Punching force based on the pure shear assumption.

Description	Measured Dimensions	Shear Area (mm^2)	Pure Shear Force (kN)
TB-1	17.35x15.75x30°x30°	463,4	197,6
TB-2	16.3x14.8x60°x30°	435,4	185,7
TB-3	23.75x10.9x30°x30°	485,1	206,8
TB-4	28.8x4.6x30°x30°	467,6	199,4

4.3.2 Test Results

In figure 59 the casing indentation for all of the different punch tests performed are illustrated.
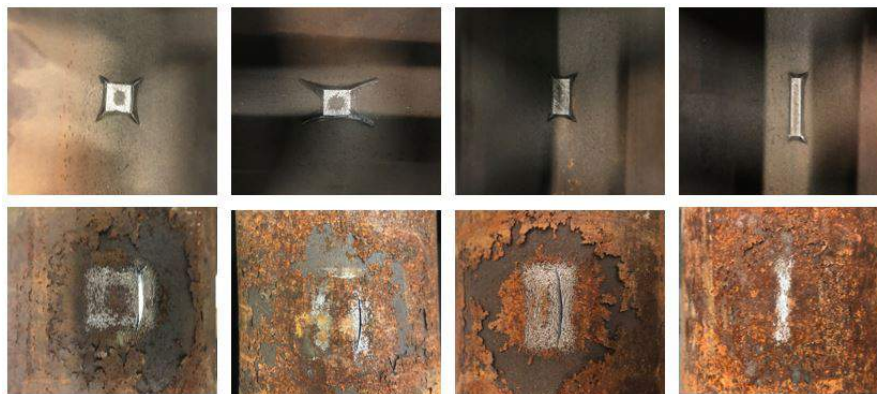
Figure 59: Indentations for all the punches, inside on top and respective outside mark on bottom row.

Through extending the punch geometry to the maximum extension of the press, the following deformed casing geometry was observed. Figure 60 show the characteristic of the hole created by the TB-3 punch.

Figure 60: Punch pressed all through a casing.

Similar tests were completed for each of the different punch specimina. Figure 61 show all of the casings with their respective punches.

Figure 61: All punches with punched casings.

After all tests were completed, the data sets were imported into an excel sheet for evaluation. See the figure 62 below for the different reaction forces compared to distance travelled.
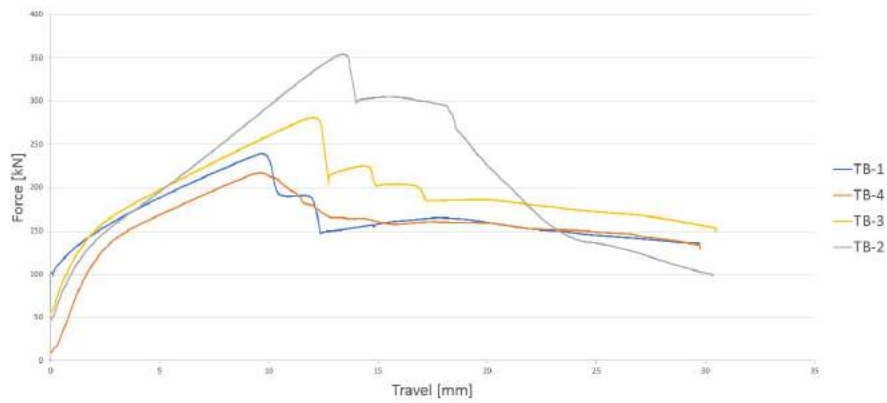
Figure 62: Resultant force from all punches.

4.4   Material Test Specimina

In figure 63 below, the test specimina are illustrated after tensile testing was completed.

Figure 63: All test specimina after tensile testing.

The tensile test data was collected, and stress-strain curves were generated based on output from the Instron machine. These results were imported into the same coordinate system for comparison, see figure 64 for illustration of the tensile graphs.
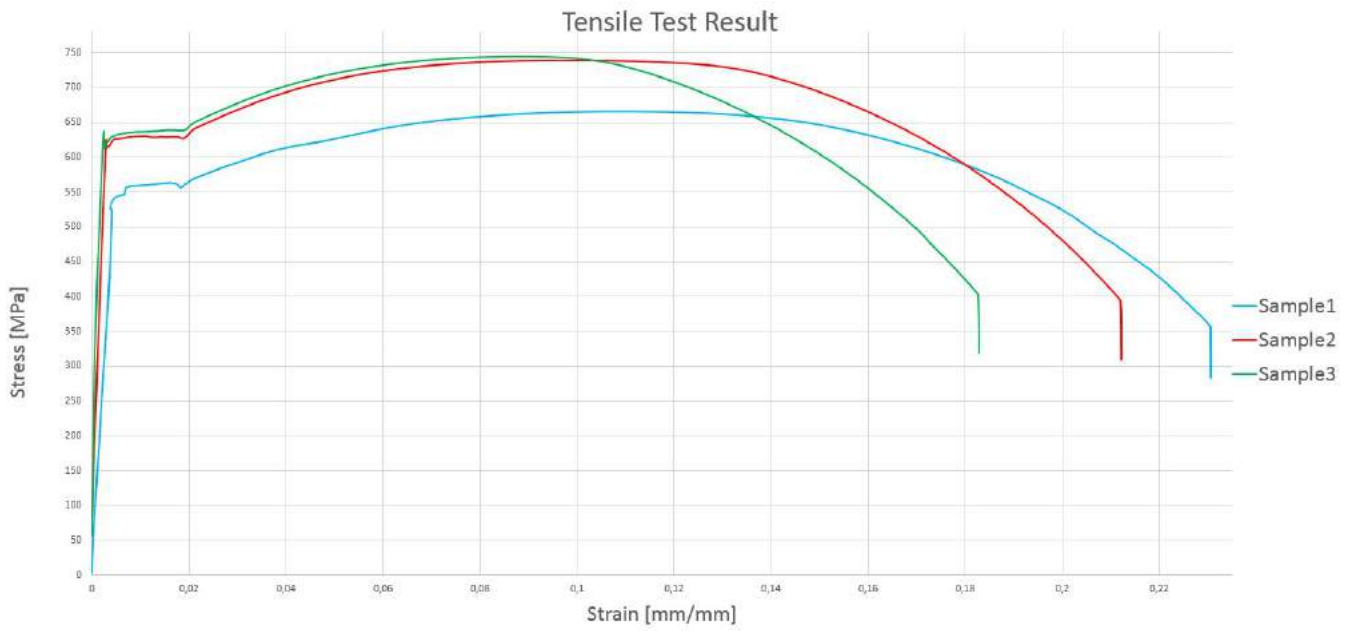
Figure 64: Material model after tensile tests.

In table 11 the key values extracted from the tensile testing are listed together with the minimum requirements for the L80 material.

Table 11: Specimina values compared with required values.

Description	Specimen 1	Specimen 2	Specimen 3	requirement
Yield Strength [Mpa]	565	634	644	552
Tensile Strength [Mpa]	665	739	744	655
Elongation at Break [%]	23	21,21	18,3	19,5

4.5 TB-punch simulation

This section presents the results of the simulation of the TB-punch geometries.

TB-1 Punch Geometry
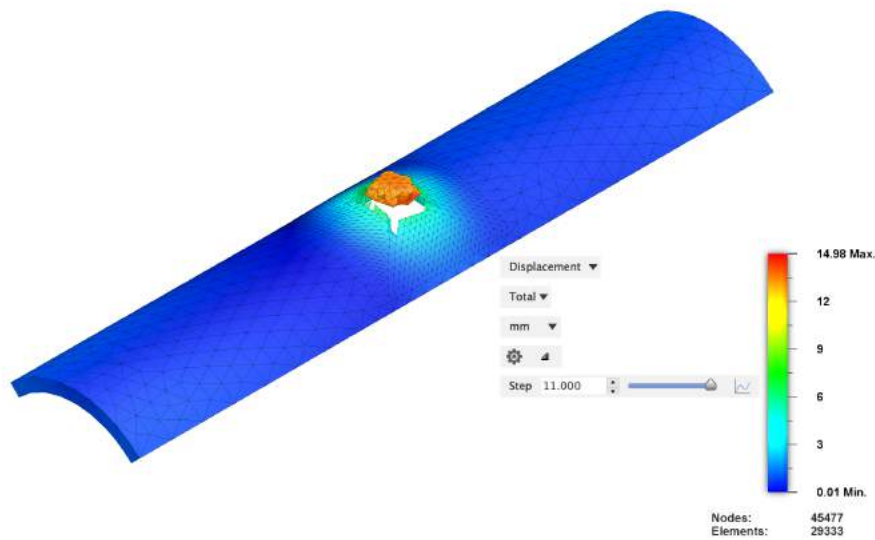
Figure 65: TB-1 Casing deformation.

Figure 65 shows the deformed result from the TB-1 punch geometry. A clean shear is observed, resulting in a perforation corresponding to the geometry of the punch. Figures 66, 67 and 68 show the course of perforation.

91
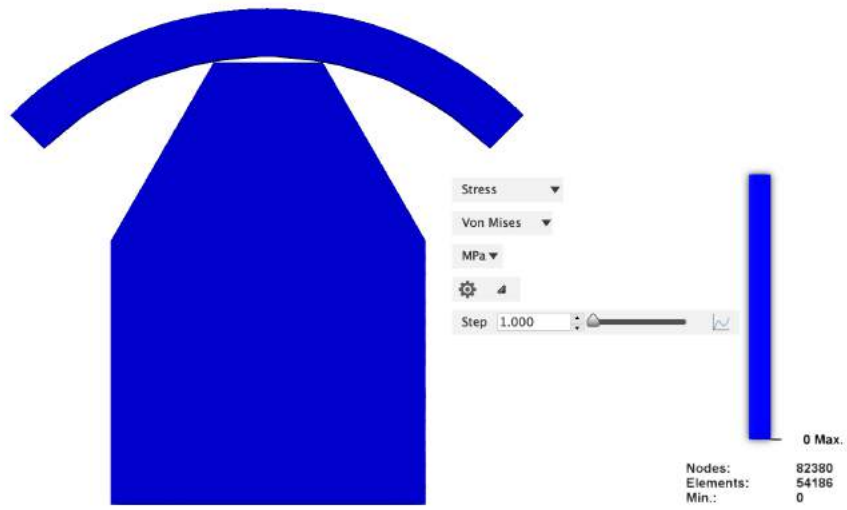
Figure 66: TB-1 Split view initially.
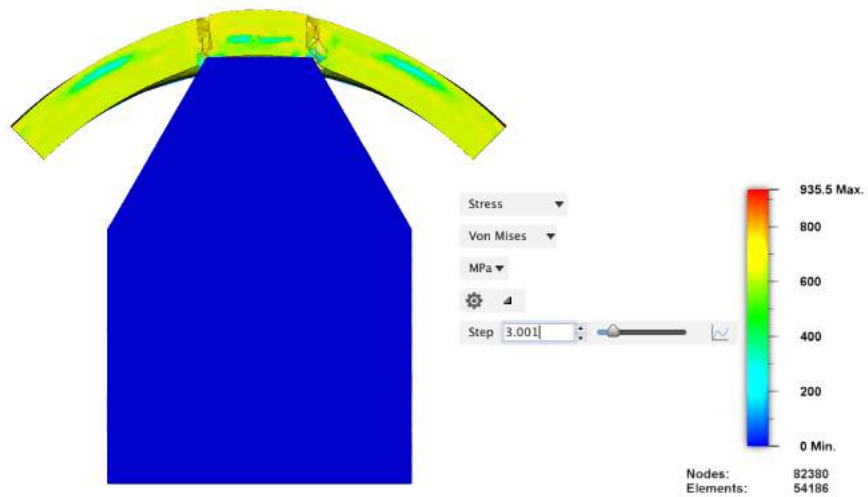
Figure 67: TB-1 Split view at fracture.
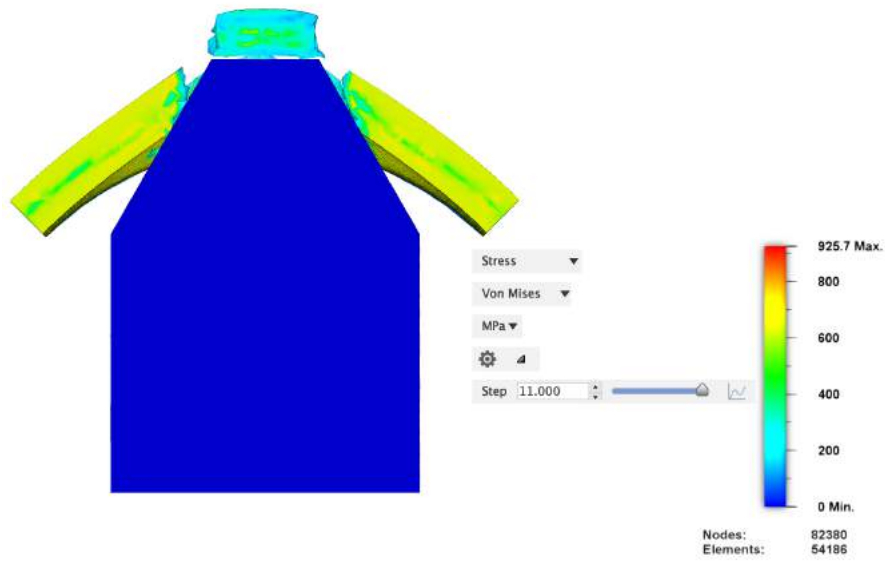
Figure 68: TB-1 Split view at end position.

Stress concentrations are observed around the circumference of the punch face until failure. A coin similar to the face area of the punch head is seen separated from the casing. Figure 69 compares the deformed result from the simulation and the physical testing. The physical test shows the creation of a flap being bent away as opposed to the simulation and its purely sheared coin. This is considered to be due to irregularities in the material, alignment inaccuracy as well as the rigid body assumption used in the simulation. The sources of error will be discussed in chapter 6.
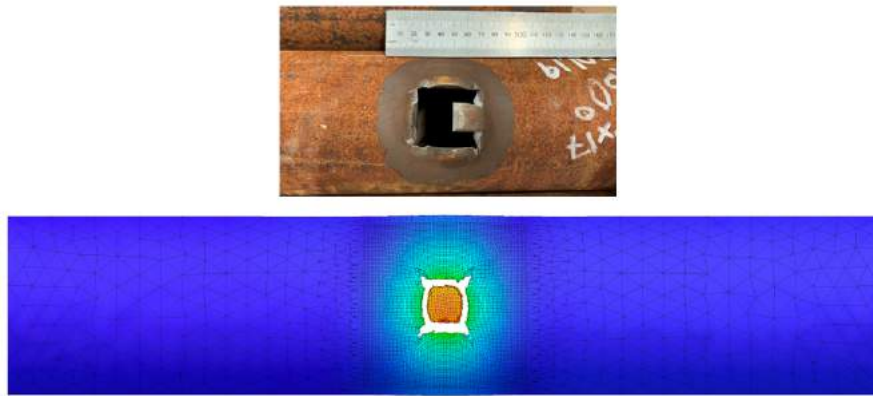
Figure 69: TB-1 Comparison of physical test result and FEA result.

Further evaluation was done in terms of comparing the area of the casing containing elements with strain exceeding 0.2%, i.e. above the yield strength of the material. Figure 70 show the ISO-clipped plot and a closeup of the deformed casing with a linear measurement axially. It is also observed that the area of the casing where the corrosion has flaked off is of similar visual and physical geometry.

Figure 70: TB-1 Comparison of area above yield threshold in test result and FEA result.

The punch forces obtained from FEA, testing and the pure shear assumption are gathered in table 12 below. Here, all external factors were kept constant except the COF which varies from 0,05 to 0,3. Additionally, the TB-punch was modelled after physical measurements of the produced part, taking tolerance errors into account.

Table 12: TB-1 - FEA, test and pure shear comparison.

Description	Shear Area (mm²)	COF	FEA Reaction Force (kN)	Test Force (kN)	Pure Shear Force (kN)	Measured Dimensions	FEA vs. Test	Pure Shear vs. Test
TB-1	463,4	0,05	233,7	240	197,6	17.35x15.75x30°x30°	-3 %	-18 %
TB-1	463,4	0,1	236,6	240	197,6	17.35x15.75x30°x30°	-1 %	-18 %
TB-1	463,4	0,2	241	240	197,6	17.35x15.75x30°x30°	0 %	-18 %
TB-1	463,4	0,3	242,8	240	197,6	17.35x15.75x30°x30°	1 %	-18 %

TB-2 Punch Geometry
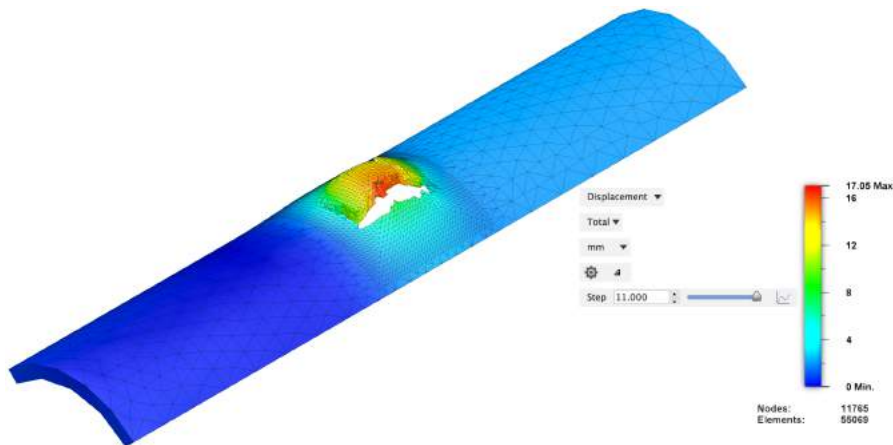
Figure 71: TB-2 casing deformation.

Figure 71 displays the result from the TB-2 punch geometry. A single tear is observed along the axial direction of the casing. The shear occurred along the entire 30° edge, resulting in a tear that subsequently was lifted up and away from the perforation. Figures 72, 73 and 74 show the deformation process from initiation, through fracture to the end of the prescribed displacement.
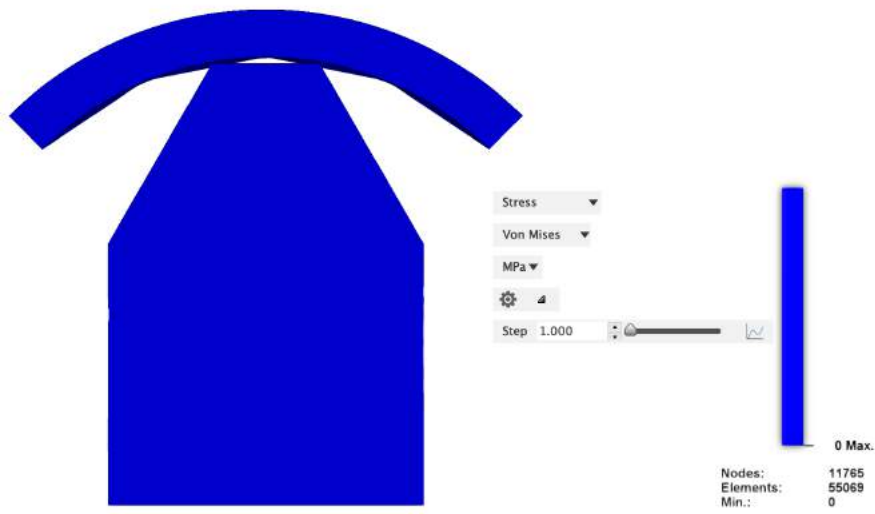
Figure 72: TB-2 split view initially.
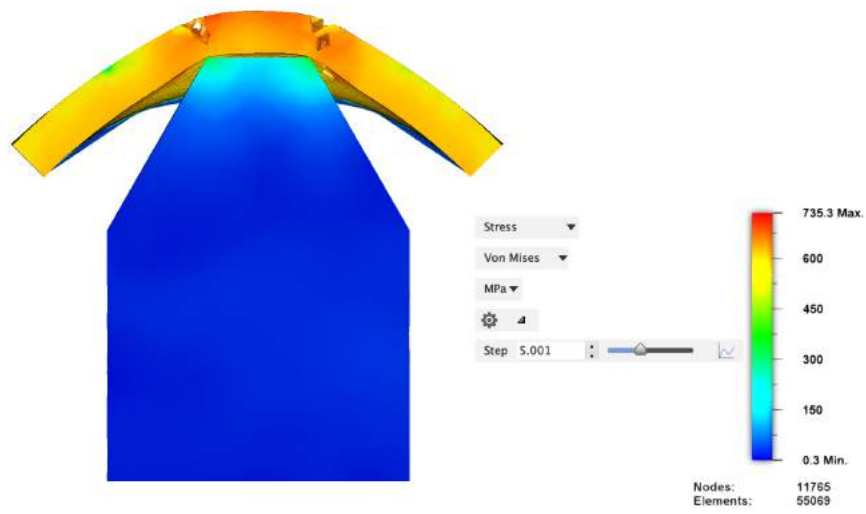
Figure 73: TB-2 split view at fracture.
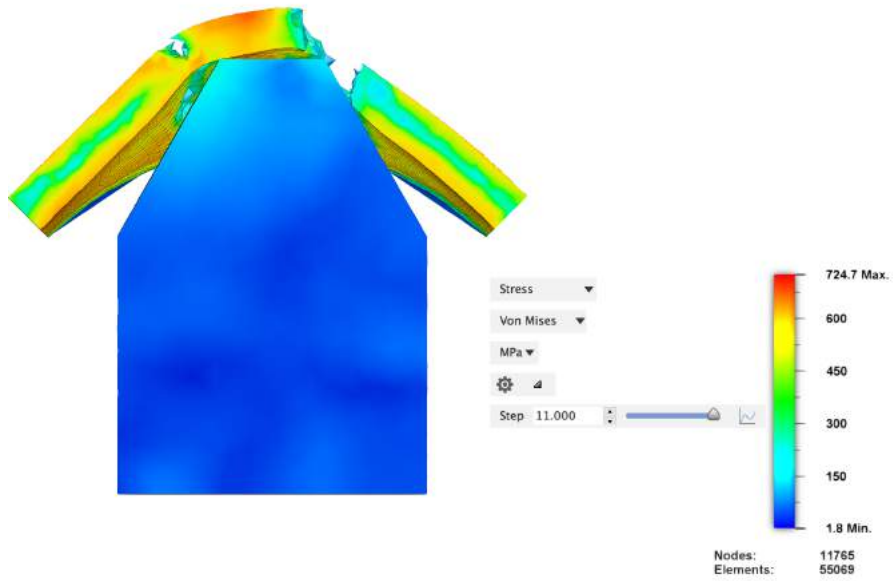
Figure 74: TB-2 split view at end.

Similarly to the TB-1 punch, stress concentrations are observed at the vertices of the punch circumference. As the punch displacement increases, the strain levels in the surrounding elements reach the threshold for element deletion and are removed. Figure 75 compares the simulated result with the test result, showing similarities in plastic deformation. The geometry shows promising characteristics when considering the scope of the product, creating swirl flow in the annulus.
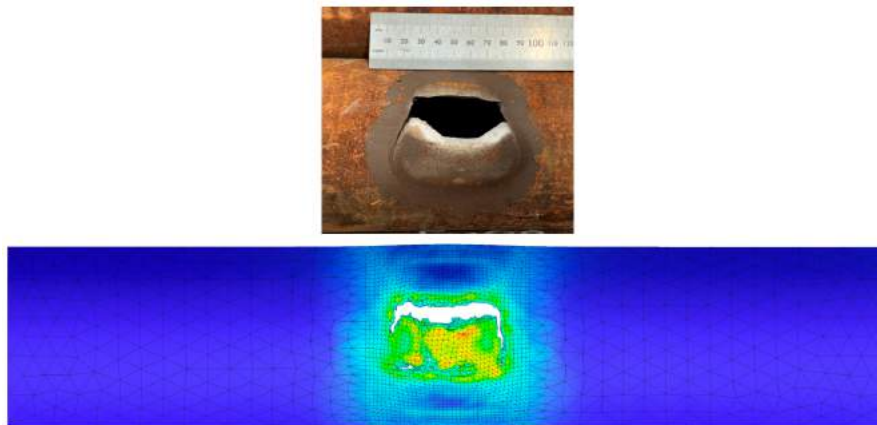
Figure 75: TB-2 comparison of physical test result and FEA result.

The TB-2 punch geometry produced an area of visible plastic deformation corresponding to the simulated ISO-clipped plot highlighting areas above the yield threshold, illustrated in figure 76 below.
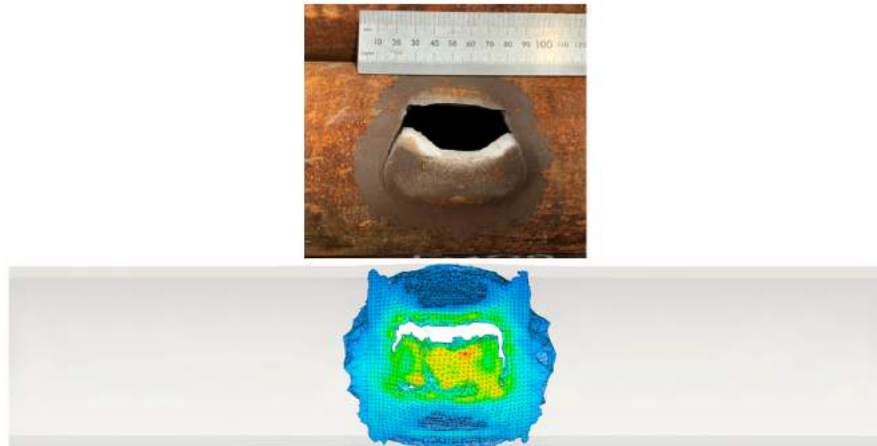
Figure 76: TB-2 comparison of area above yield threshold in test result and FEA result.

The punch forces obtained from FEA, testing and the pure shear assumption are gathered in table 13 below. These results are generated through the same setup as TB-1.

Table 13: TB-2 - FEA, test and pure shear comparison.

Description	Shear Area (mm²)	COF	FEA Reaction Force (kN)	Test Force (kN)	Pure Shear Force (kN)	Measured Dimensions	FEA vs. Test	Pure Shear vs. Test
TB-2	435,4	0,05	323,2	365,5	185,7	16.3x14.8x60°x30°	-12 %	-49 %
TB-2	435,4	0,1	324,2	365,5	185,7	16.3x14.8x60°x30°	-11 %	-49 %
TB-2	435,4	0,2	326,5	365,5	185,7	16.3x14.8x60°x30°	-11 %	-49 %
TB-2	435,4	0,3	328,9	365,5	185,7	16.3x14.8x60°x30°	-10 %	-49 %

TB-3 Punch Geometry
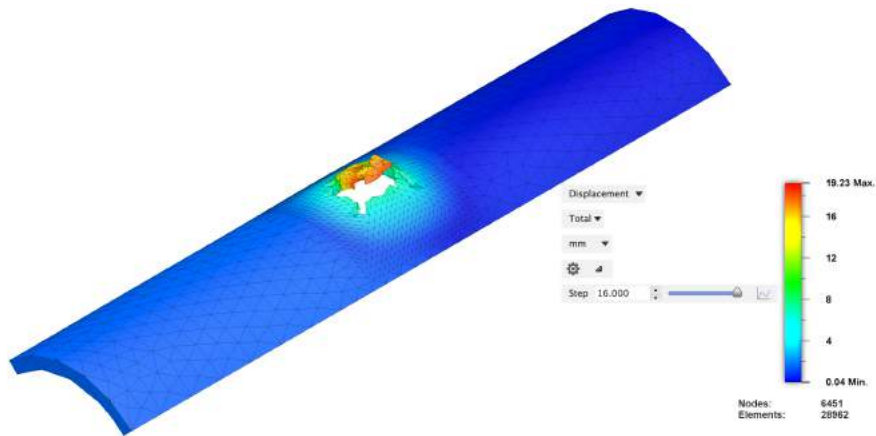
Figure 77: TB-3 casing deformation

Figure 77 display the casing after being punched by the TB-3 punch geometry. This result combine elements from the TB-1 and TB-2 deformations, showing a perforation corresponding to the punch geometry as well as tear characteristics along the axial direction of the casing on the 24mm edge. Figures 78, 79 and 80 display the punching sequence.
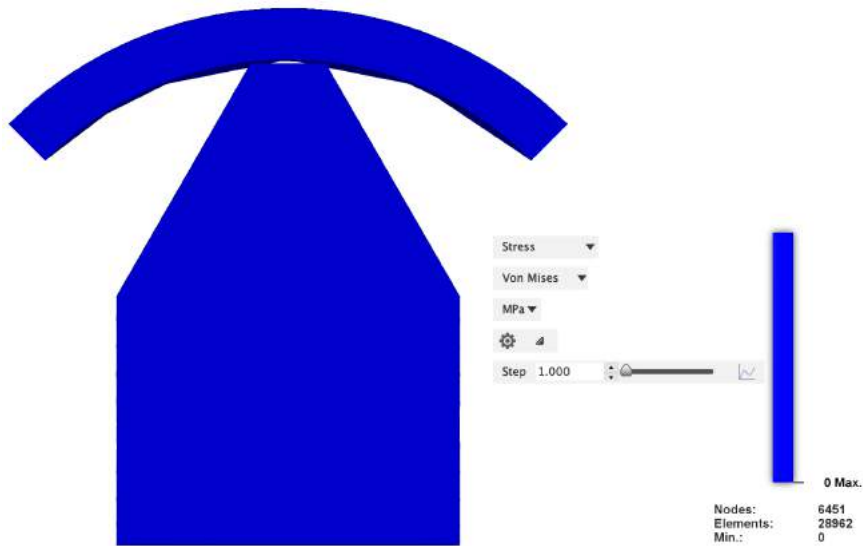
Figure 78: TB-3 split view initially.
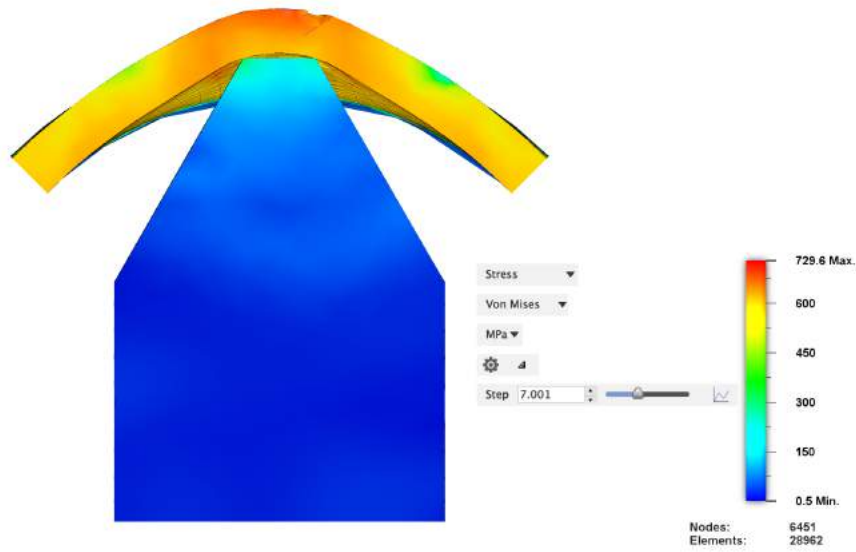
Figure 79: TB-3 split view at fracture.
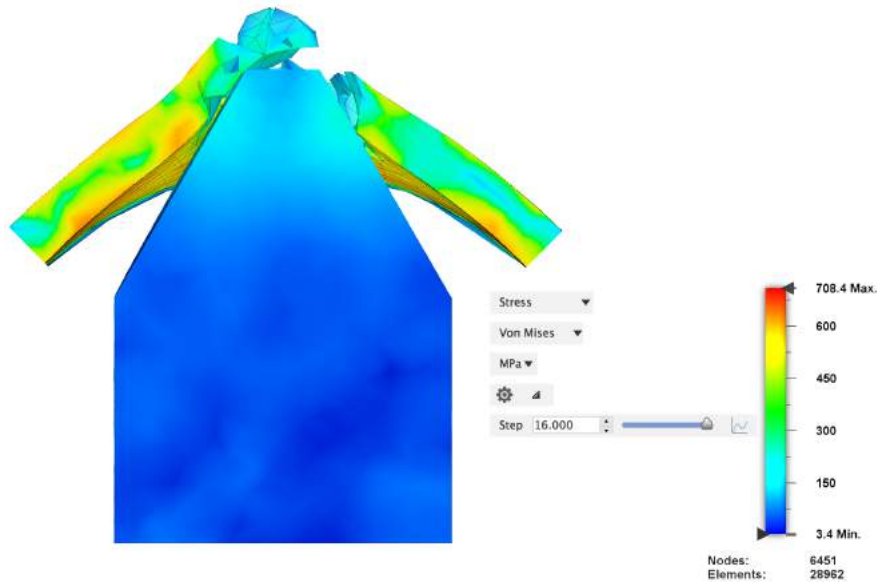
Figure 80: TB-3 split view at end.

The stress concentrations originate at the vertices of the punch face. The crack propagates through 3 of the vertices, creating an overhang that is lifted away. Compared to the TB-2 geometry, the result show similar tendencies with a lower swirl potential.

Figure 81 compares the simulation result with the test result.
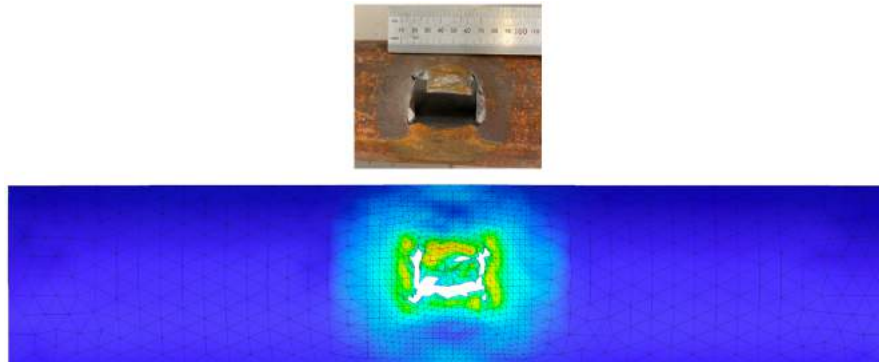
Figure 81: TB-3 comparison of physical test result and FEA result.

Figure 82 below shows the yield area comparison of the simulation and physical test-ing where the corrosion has flaked off.

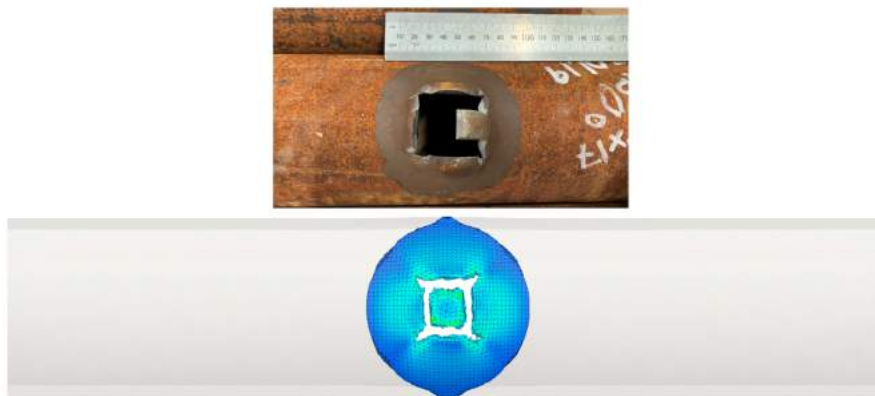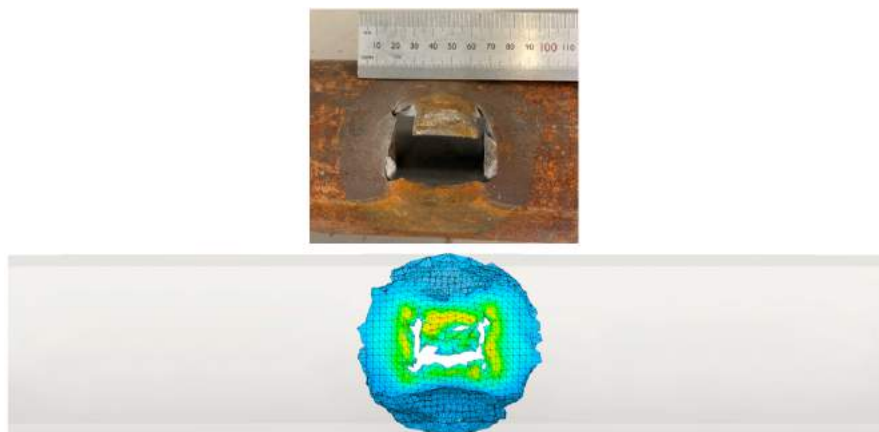Figure 82: TB-3 comparison of area above yield threshold in test result and FEA result.

The punch forces obtained from FEA, testing and the pure shear assumption are gathered in table 14 below. These results are generated through the same setup as TB-1.

Table 14: TB-3 - FEA, test and pure shear comparison.

Description	Shear Area (mm²)	COF	FEA Reaction Force (kN)	Test Force (kN)	Pure Shear Force (kN)	Measured Dimensions	FEA vs. Test	Pure Shear vs. Test
TB-3	485,1	0,05	291,3	281,5	206,8	23.75x10.9x30°x30°	3 %	-27 %
TB-3	485,1	0,1	291,1	281,5	206,8	23.75x10.9x30°x30°	3 %	-27 %
TB-3	485,1	0,2	289,6	281,5	206,8	23.75x10.9x30°x30°	3 %	-27 %
TB-3	485,1	0,3	289,6	281,5	206,8	23.75x10.9x30°x30°	3 %	-27 %

TB-4 Punch Geometry
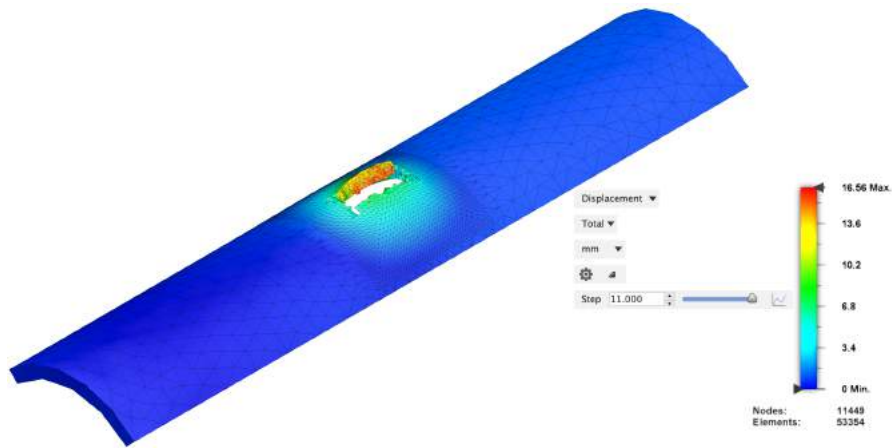
Figure 83: TB-4 casing deformation.

The simulated result of the TB-4 punch geometry is shown in figure 83 above. A rupture corresponding to the geometry of the punch is observed. Figures 84, 85 and 86 show the punch perforating the casing.
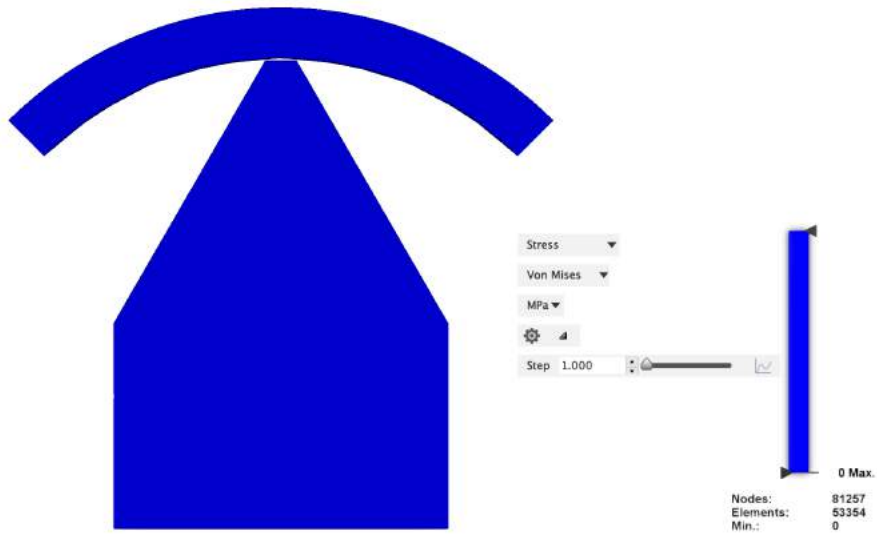
Figure 84: TB-4 split view initially.
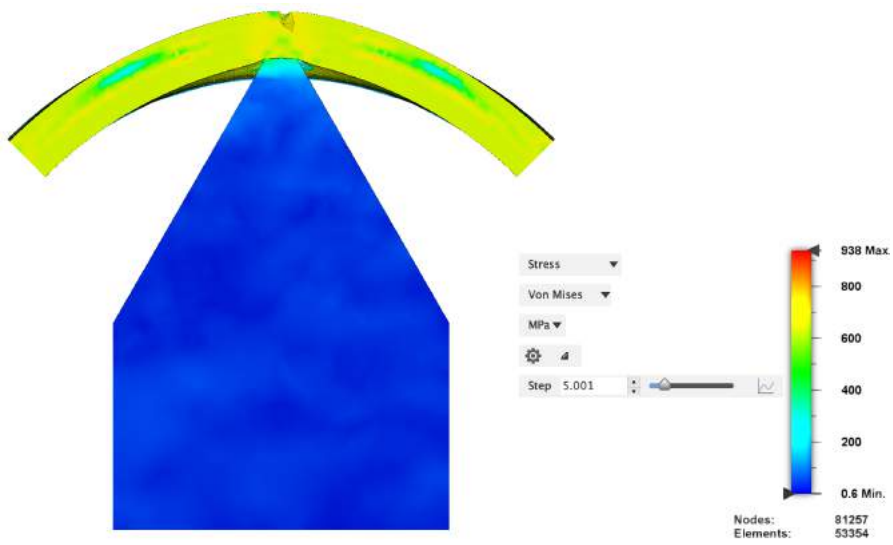
Figure 85: TB-4 split view at fracture.
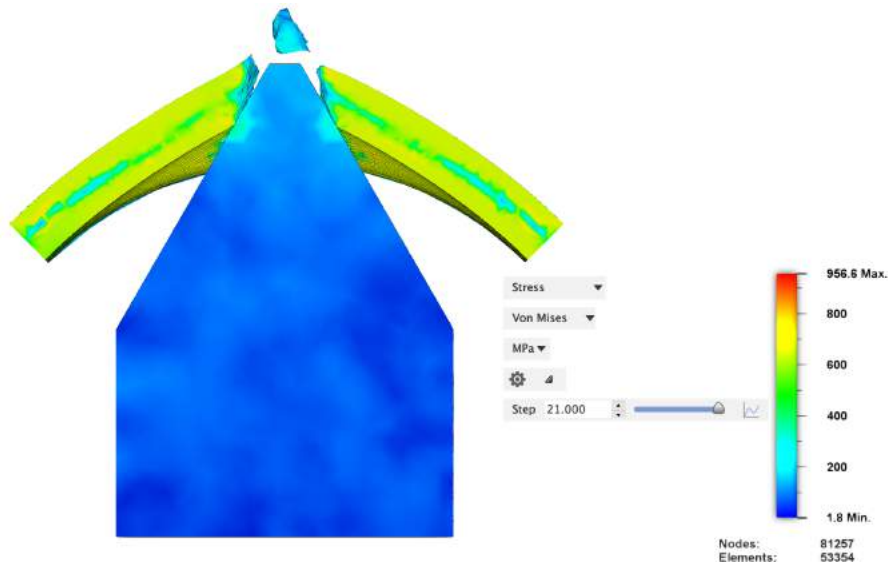
Figure 86: TB-4 split view at end.

Stress concentrations are observed throughout the entire cross section interacting with the punch head. A small coin is dislodged while the material is mainly moved in the tangential direction and produces a substantial perforation. The characteristics are comparable to that of the TB-3 geometry without the flap creation. Figure 87 below shows how the simulated result compares to the physical testing.
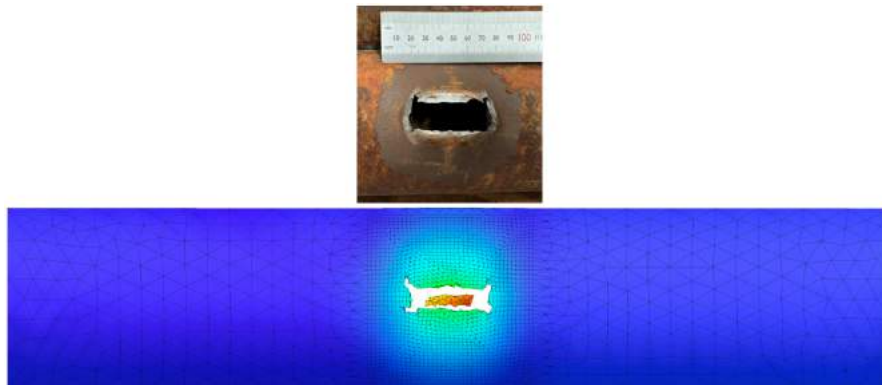
Figure 87: TB-4 comparison of physical test result and FEA result.

The area above the yield strength threshold is highlighted in figure 88 below. Again,

similarities between the simulation and physical test result are observed.

Figure 88: TB-4 comparison of area above yield threshold in test result and FEA result.

The punch forces obtained from FEA, testing and the pure shear assumption are gathered in table 15 below. These results are generated through the same setup as TB-1.

Table 15: TB-4 - FEA, test and pure shear comparison.

Description	Shear Area (mm²)	COF	FEA Reaction Force (kN)	Test Force (kN)	Pure Shear Force (kN)	Measured Dimensions	FEA vs. Test	Pure Shear vs. Test
TB-4	467,6	0,05	208	217,4	199,4	28.8x4.6x30°x30°	-4 %	-8 %
TB-4	467,6	0,1	207,7	217,4	199,4	28.8x4.6x30°x30°	-4 %	-8 %
TB-4	467,6	0,2	208,5	217,4	199,4	28.8x4.6x30°x30°	-4 %	-8 %
TB-4	467,6	0,3	209,3	217,4	199,4	28.8x4.6x30°x30°	-4 %	-8 %

4.6 Prototype Development

4.6.1 Prototype simulation results

The design was evaluated in the FEA model prior to production. The model was run through the same setup as the TB-punches. Figure 89 shows the perforated casing.
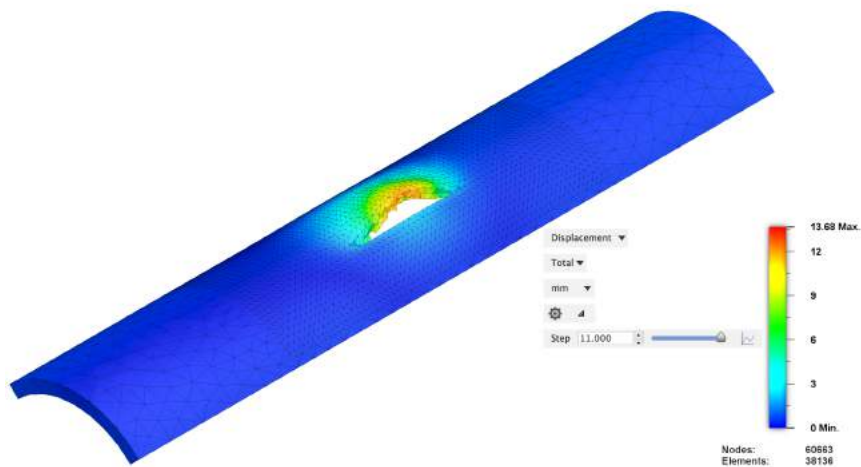
Figure 89: Prototype 3 deformed casing.

The prototype produced promising perforation geometry in FEA. Figures 90, 91 and 92 illustrates the perforation process.
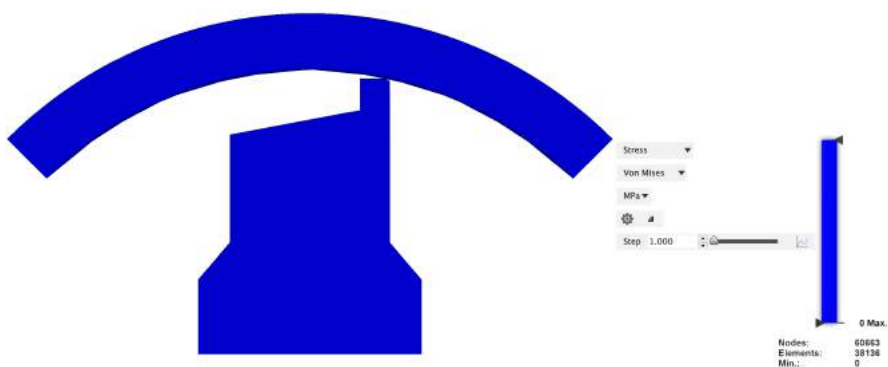
Figure 90: P3 split view initially.

106
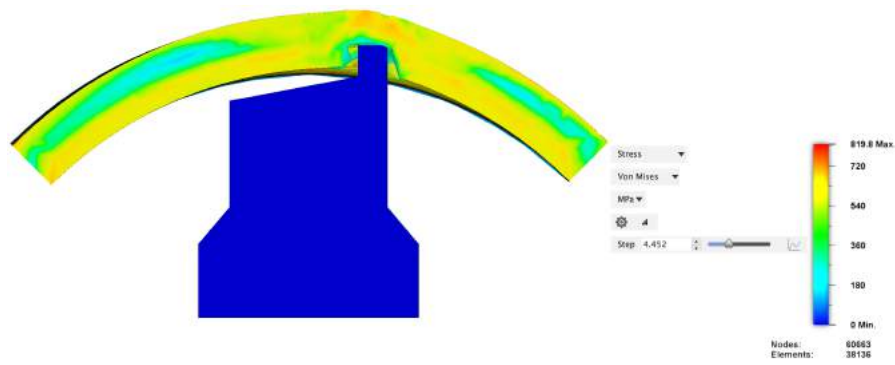
Figure 91: P3 split view at fracture.
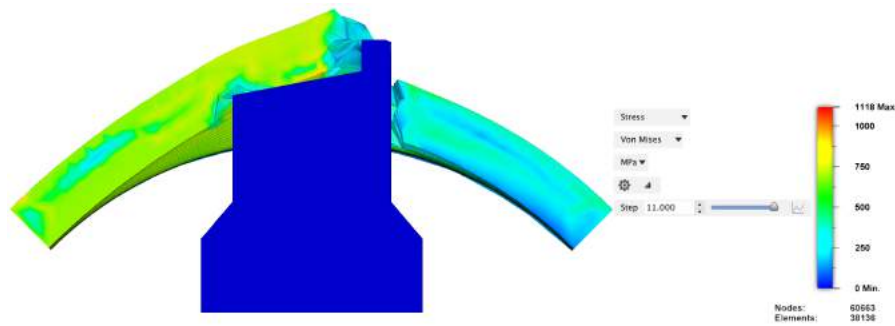
Figure 92: P3 split view at end.

The fracture is initiated at the shear edge. Following the creation of a sufficient tear, flap creation is facilitated by the inclined face. One concern regarding the geometry was sufficient toughness of the shear edge.

4.6.2 Prototype Test Results

Figure 93 below shows the casing after punching to fracture only.
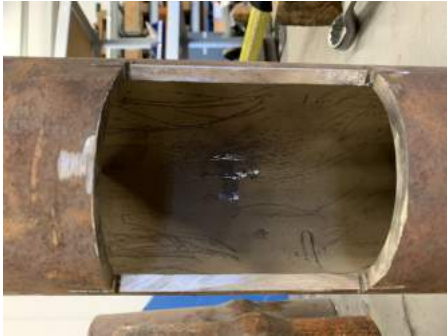
(a) Inside casing after punch pressing.

(b) Outside casing after punch pressing.

Figure 93: First failure pressing.

Figure 94 illustrates the casing after the full extension test.

(a) Inside casing full extent pressing.

(b) Outside casing full extent pressing.

Figure 94: Full extent pressing.

The plastic deformation given from FEA was compared with the physical test result, see figure 95.
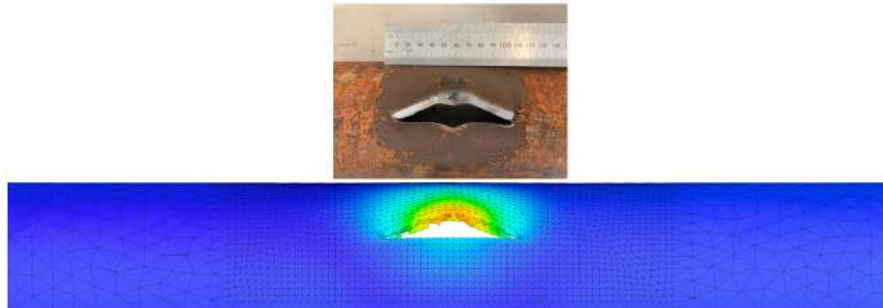
Figure 95: Prototype 3 - test result compared to FEA result.

The punch forces obtained from FEA and testing are gathered in table 16 below. These results are generated through the same setup as TB-1.

Table 16: Prototype 3 - force comparison between FEA and test.

Description	COF	FEA Reaction Force (kN)	Test Force (kN)	FEA vs. Test
Prototype	0,05	133	140	-5 %
Prototype	0,1	123,3	140	-12 %
Prototype	0,2	125,3	140	-11 %
Prototype	0,3	106,4	140	-24 %

This page is intentionally left blank.

5   The Economical Perspective

Statistics show a decline in oil production from existing wells on the NCS. See figure 96 below for historical data provided by the Ministry of Petroleum & Energy and the Norwegian Petroleum Directorate. The decline is due to the deterioration of mature fields combined with low compensation from new fields [24]. Declining production from mature fields is considered one of the industry's biggest challenges, see Appendix D in chapter 8.4.
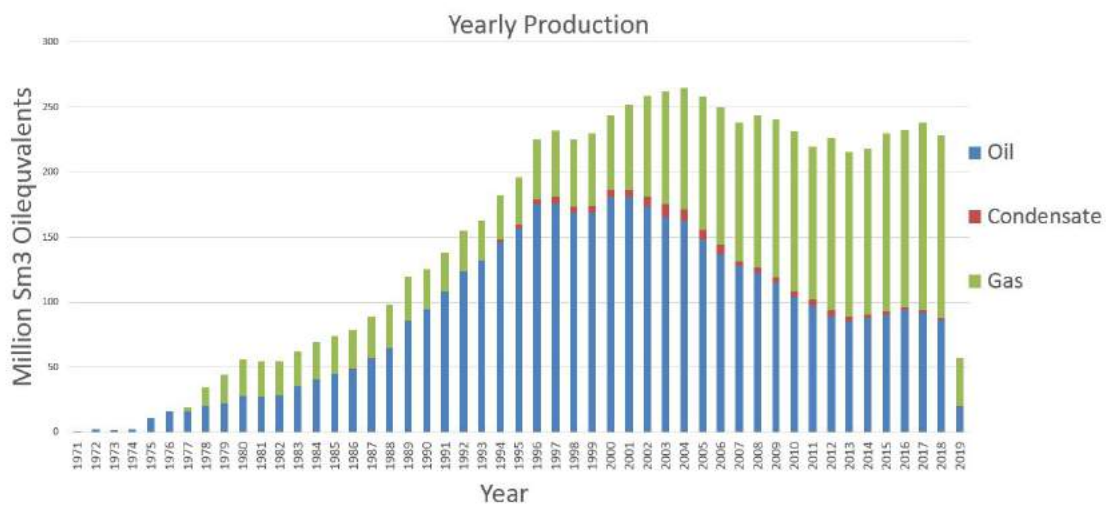
Figure 96: Decline in oil production on the NCS [23].

Furthermore, the trend in exploration is showing less major discoveries. See figure 97 for an illustration based on data from the Norwegian Petroleum Directorate. This in turn elevates the importance of increasing production from existing fields. Only 47% of the estimated recoverable resources have been produced per 2019 [24]. Thus, slot recovery and the exploration of new areas of the reservoir is of interest. However, to successfully conduct a slot recovery operation, plugging of the section of the well below the redirection is required. As discussed in chapter 1, there are several ways of doing this.

111
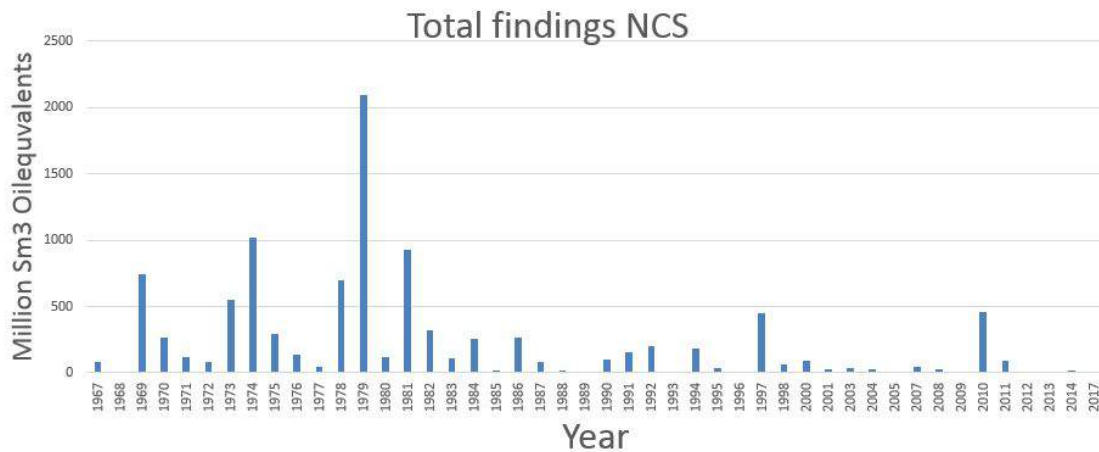
Figure 97: Decline in discoveries on the NCS [22].

Old wells often have the disadvantage of not having standoffs between the inner and outer casing. This leads to the majority of the casings to lay low side when the well diverts into the horizontal direction. Cement integrity depends on the concentricity of the casings. Subsequently, the creation of perforations as well as geometry providing standoff between the casings is highly desirable. Perforating guns have been the go-to solution for these purposes for a long time. One drawback of using guns is the possibility of perforating the outer casing(s). Additionally, perforating guns are often disconnected and left in the well after being used, inducing unnecessary capital costs of acquiring new equipment [49].

With limited control of the conditions outside the outermost casing, it is desirable to avoid perforating it, rendering perforating guns sub-optimal. Current technologies that offers controlled perforation without damaging the outer casing are only available on coiled tubing or drill pipe. However, great benefits arise with the possibility of conducting these operations on wireline.

From the questionnaire in Appendix D in chapter 8.4 it is stated that the rigging time of coiled tubing is substantially longer than for wireline. Any standard production rig on the NCS is usually equipped with a wireline setup at all times. To install a coiled tubing setup, 14 days is usually required before any work may commence.

Another advantage of wireline is that the equipment can be prepared and used separately from the rest of the rig equipment. For coiled tubing, the operation on the rig has to be stopped for installation. Together with the price difference of 500 000 NOK/day vs 250 000 NOK/day for coiled tubing and wireline respectively, this makes any coiled tubing operation a much more expensive operation compared with wireline (see Appendix D in chapter 8.4).

Besides the time and cost difference between coil tubing and wireline, are there also several technical advantages of running on wireline. Wireline is capable of delivering high speed real time data on any downhole tool, which furthermore allows for more complicated tools and work tasks. Wireline also gives a better depth control of the tool string by enabling the use of electrical logging equipment. Besides these technological advantages, wireline is also a much lighter setup and has a more flexible cable with a longer expected lifetime than coiled tubing.

However, despite all the advantages of wireline compared to coiled tubing, wireline does not oppose any solution when pumping cement or running down hole washing. Therefore, a good combination between the two, with wireline operations running before coiled tubing might yield the most efficient and profitable result for operations like those the CPS is planned to complete.

For the CPS tool, slot recovery operations are very interesting and exciting applications to be a part of. As previously discussed, the scope of these operations is to increase the profitability and production rate of a field. Such scopes are naturally something any company is willing to invest in, where the invested capital is returned.

Furthermore, it is also possible to use the CPS tool for permanent P&A applications as a extension of the lifetime of the technology. When compared to slot recovery, the scope for the operation is drastically changed. Any P&A operation where the goal is to leave the well or field permanently, is standing exclusively as an expense for the company. Such operations are not necessarily less attractive for E Plug as a supplier, but in a development phase it might be easier to raise funding if there is a return on investment for the operator.

Whenever the tool is completed, there will be little difference for E Plug whether the

application is slot recovery or permanent P&A as part of a decommissioning campaign. Handal estimates the decommissioning time for the NCS to around 57 years, there are good indications that the technology can provide cash flow for a long period of time [35]. Despite the available applications in today's P&A market, the CPS project will provide E Plug with several different opportunities. This is because the technology behind the CPS allows for similar, yet unique products solving various challenges.

One of these "spin off" development projects is a resin placement tool. Here the purpose will be to punch through the inner casing, and then seal the casing hole using the the desired punch. Once a sufficient seal is verified, a resin mixture can be pumped from topside through coiled tubing, down to the placement tool and through the casing into the annulus. When the resin is successfully pumped into annulus, it will react with the environment, cure and create a resin plug around the circumference of the innermost casing.

Another concept where the CPS technology can be used more directly is for a restriction opener tool. Here the main objective will be to utilise similar punching technology as for the CPS to expand any casing or restriction which may have collapsed or been narrowed for some reason. If a well casing gets weakened or the geological setting in the reservoir changes, the casing may collapse or buckle and possibly entrap equipment located below the collapsed section.

Another spin-off tool from the CPS is a casing cutting tool. Here the tool may work as a cutter in the bottom of a casing prior to removing the casing from the wellbore.

Any commercial engineering project is aiming for either to earn money, reduce cost, reduce risk or a combination of the three. The development of the punch and stand-off tool is no different.

6 Discussion

6.1 Basic Calculations

Time, as a major cost driver, is vital during punching of the casing. Therefore the chosen thread is a 8 TPI Stub Acme thread with 4 thread starts. This is not necessarily the thread with the most efficient force translation, but rather the one with the highest axial displacement per revolution.

From figure 55 in chapter 4 it clear that the efficiency of the chosen thread is highly dependant on the COF. As a result, the operating environment of the thread should be protected and consist of only known lubricants for a predictable output.

Figure 7 in chapter 4 shows that through using incline planes and the available axial force of the tool, the punch head(s) should have no problem penetrating the casing of the specified quality and geometry. The efficiency of the plane interaction, with regards to radial force gained, decreases with the increase in angle. In a frictionless system, the angle of which the gearing change is 45°.

Figure 56 in chapter 4 highlights the efficiency of the angles based on radial force output compared to axial travel and varying COF. Great dependency on friction is observed above 40°.

As observed in figure 8 in chapter 4, an increase in the number of circumferentially distributed punches results in higher tangential forces. Higher tangential forces is believed to increase the level of deformation of the areas between the punches and ultimately, result in a casing with more standoff than pure shear characteristics. The model is simplified and does not consider punch geometry or support from surrounding geometry in the casing.

Depending on punch geometry, casing thickness and material, the radial force may or may not be sufficient in shearing the casing. If the force is sufficient, the casing will be sheared and the tangential force will not act to the extent displayed. If the force is insufficient however, the tangential forces displayed will act and induce circumfer-

115

ential plastic deformation upon the casing. Ultimately, the strain hardening effects of plastic deformation would lead to casing fracture. It is observed that more than 6 punches results in a tangential component (in a single wall) above 100%.

6.2 Initial Punch testing

In figure 9 in chapter 4 a small deviation between the pure shear assumption and physical testing is observed. Due to the insignificant magnitude of this deviation, it is suspected to be a result of several sources of error:

- Material irregularities.

- Misalignment of test setup.

- Inaccurate manual measurements.

- Accuracy of logging sensors.

Material irregularities may affect the result through local material property differences.
Misalignment of test setup can lead to unwanted loading of unwanted components, such as bending in the punch yielding a larger shear area.
Inaccurate manual measurements will cause the calculations to be based on a false assumptions.
Accuracy of logging sensors is important for confidence in the test results.

6.3 Material Model

Figure 11 in chapter 4 shows that the supplied casing fulfils the material requirements as given by DDH [31]. By building the FEA material model based on these results, increased confidence in the simulation output is achieved. Figure 64 shows the stress-strain curves of the specimina. Specimen 1 experienced slippage in the

test setup which resulted in large deviations when compared to the other specimina. Specimen 2 had characteristics exceeding all requirements. The curve of specimen 3 exerted similar characteristics as that of specimen 2. However, the elongation at break value was found to be below the requirement and the curve was discarded as a result. Specimen 2 was ultimately chosen as the basis for the material model due to the irregularities found in 1 and 3.

Sources of Error in Material Model Establishment

Potential sources of error were identified throughout the process of establishing the material model. These include and are not limited to:

- Hardening effects on the test specimen surface due to the machining process.

- Geometric tolerances of test specimina.

- Inconsistencies in test setup.

- Calibration of strain gauges and force transducers in tensile machine.

- Human error in verifying geometric dimensions of test specimina.

Hardening effects in the test specimina may have affected the results through changes in the microstructure on the surface. High temperature induced by the machining process may provoke such changes.

Geometric tolerances of test specimina affect the end result by providing the tensile machine with an incorrect initial cross-sectional area. This results in the test outputting inaccurate stress levels.

Inconsistencies in test setup include slippage of test specimina, misalignment in their fastening and errors in manual setup of strain calipers.

Calibration of strain gauges and force transducers is critical for outputting accurate results.

Human error is present in the verification of geometric dimensions prior to providing input for the tensile machine. This may cause large deviations between test specimina if done inconsistently.

6.4 TB-punch Evaluation

One of the primary objectives of the FEA efforts was to create and validate a simulation model that coincided with results from physical testing. Reaction forces from the constrained faces of the casing were gathered at the point of fracture and compared to the physical test results and pure shear calculations. Figure 98 show this comparison. The shear force from FEA is plotted as the average due to uncertainties regarding the acting COF.
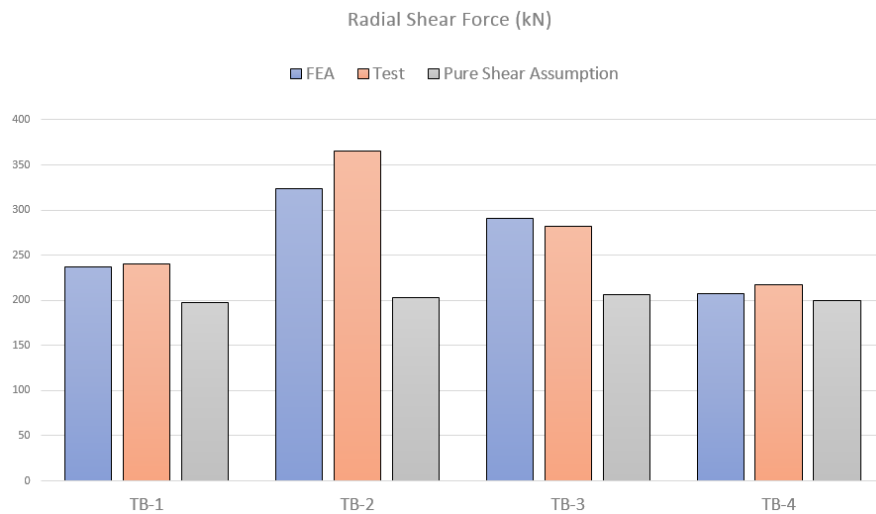
Figure 98: Comparison of radial shear forces obtained through testing, FEA and hand calculations.

From the graphic it is seen that the results from FEA and testing are closely correlated for the different geometries. The pure shear assumption proves accurate for geometries with steep angles and small changes in surface area through the punching process. However, the assumption proves inaccurate for complex geometries. As a result, the established FEA model was considered feasible for further development of the punch head geometry.

As shown in the above figures, all of the punch specimina obtained deformations and wear damages to an extent. The TB-2 and TB-3 geometries produced promising deformations for annular swirl flow due to flap creation.

118

Sources of error in FEA and testing

Similarly to all fields of engineering, the approximation of real world mechanics are subjected to different sources of error - both from a FEA and physical testing point of view. The deviations in the results from the different punch geometries is believed to be a result of and not limited to the following sources of error:

- Geometric tolerances of machined punch geometries.

- Calibration of force transducer in the hydraulic press.

- Plastic deformation of punch and misalignment in test setup.

- Mesh refinement and constraint setup in FEA.

- Bilinear approximation of the mechanical stress-strain relationship.

- Physical material inconsistencies.

- Lower stiffness of punched casings due to being cut open.

6.5   TB-punch wear

Through the completed tests it is clear that AISI 4145 is capable of punching the casing without any major deformations as long as the punching geometry does not get too complex or introduce weak spots. Meanwhile, the TB-punches had signs of different types of wear damage. In figure 99a of the TB-1 geometry, there are indications of both face and flank wear at the contact faces. In figure 99b it is observed deformation at the edge of the punch. These effects are reminiscent of adhesive wear resulting in chipping of the punch edge.
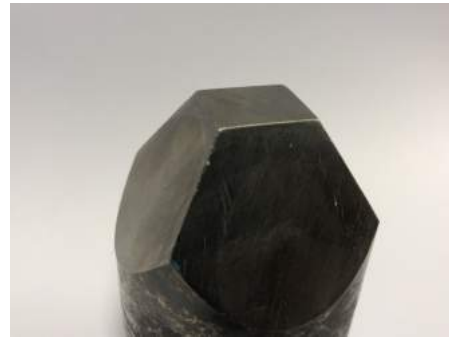
(a) Face and flank wear.   (b) Adhesive wear.

Figure 99: TB-1 wear.

The same type of flank and face wear can be seen on the TB-2 punch. Figure 100a shows the punch after testing. As observed, the wear affected area is larger than in the other punches due to the variation in side angles. Figure 100b shows the plastic deformations on the edges on the punch due to high stress concentrations.

(a) Face and flank wear.   (b) Plastic deformations.

Figure 100: TB-2 wear.

Similarly to TB-1, both TB-3 and TB-4 showed signs of flank and face wear as illustrated in figures 101a and 102a. Overall, the wear damage seen in the TB-geometries is deemed acceptable. The adhesive wear and cracking seen on the TB-3 punch may be a sign of insufficient material properties. Figure 101b illustrate this.

(a) Face and flank wear.
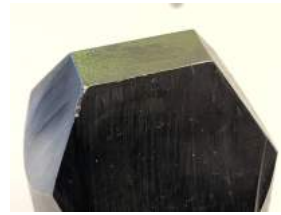
(b) Adhesive wear and chipping.

Figure 101: TB-3 wear.

(a) Face and flank wear.

(b) Minor chipping.

Figure 102: TB-4 wear.

121

6.6 Prototype Development

The punch prototype resulted in a tear with desired characteristics. Figure 103 displays the resultant forces obtained through FEA and testing. Due to geometric complexity, calculations based on the pure shear assumption were not conducted. A 5% deviation was observed in the FEA compared to the test. This is likely due to plastic deformation of the punch head as a consequence of insufficient material strength. The plastic deformation in turn resulted in an increase in shear area and subsequent radial force required.
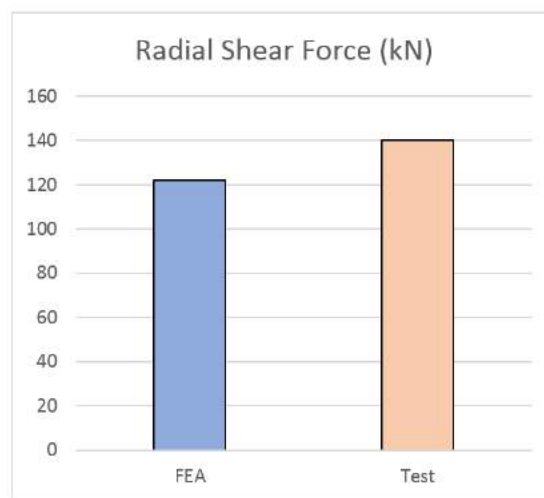
Figure 103: Prototype 3 FEA results compared to test results.

Upon inspection of the prototype following the full extension test, several mechanical failure modes were observed.

Gross fracture is observed at the shearing vertex as seen in figure 104 below. The failure mode is recognised due to benchmarks in the fractured region. High hardness and insufficient material strength is considered the main factors behind the brittle fracture failure.

Figure 104: Gross fracture of prototype.

Plastic deformation is seen on the vertex and on the face of the lifting flank. Figures 105 and 106 illustrate this. Stress concentrations and insufficient material strength is considered the main factors behind the failure modes.

Figure 105: Plastic deformation of face and vertex of lifting flank.
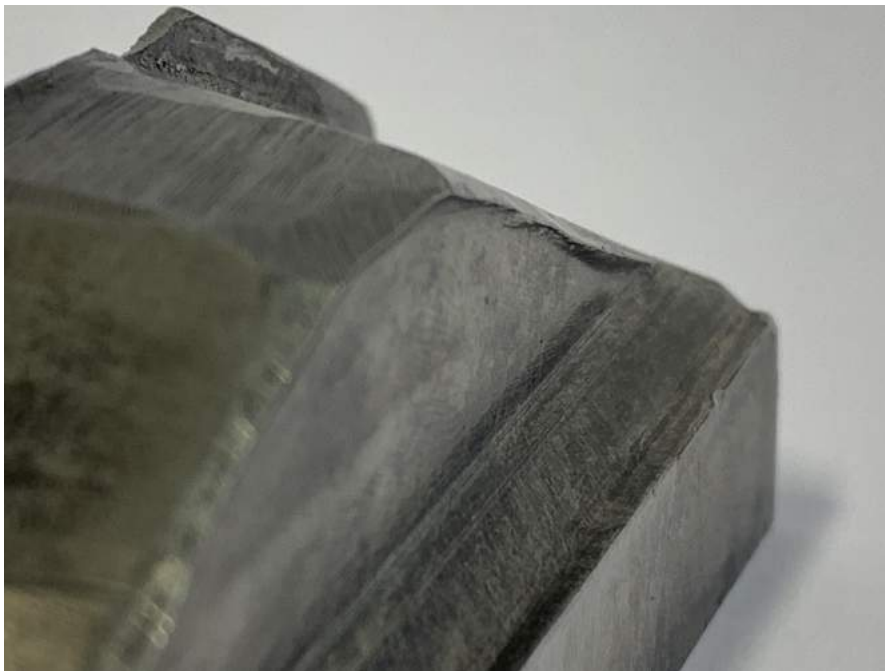
Figure 106: Plastic deformation of vertex on lifting flank.

6.7   Material suggestion

From both FEA and testing it is clear that the resultant force and contact stresses are high. At the same time, the punching mechanism is designed such that the local stresses in the tool parts require a high strength steel to perform its function. Together with the wear signs on the test punches, it is clear that a more suitable material for the punching application should be found.

There exists many different suppliers of strong and durable materials with excellent wear resistance. When choosing or recommending a material, there are different factors which must be taken into consideration. These factors will change as the application of the tool or the working conditions change. For the initial punching application, the following characteristics have been part of the decision making.

- Yield Strength

- Ultimate Tensile Strength

- Ductility / Elongation at break

- Chipping resistance

- Cracking resistance

- Adhesive wear resistance

- Toughness

- Hardenability

- Hardness

- Availability

- Price

Only some of the characteristics above are possible to quantify and compare using data or numbers. However, all of them play an important role in the evaluation of materials. For this application, the important features of the material is high strength combined with high hardness and good ductility. This is due to the fact that the material needs to be able to plastically deflect and deform without cracking or fracturing. Through evaluating different materials it becomes evident that this combination rare. Typically, the ductility of a material tends to drop as the hardness and strength increases.

However, there are some exceptions. Through dialogue with representatives from Sverdrup Steel and Voestalpine Uddeholm, the materials recommended for this application are shown in table 17.

Table 17: Characteristics of different suitable materials.

	AISI 4145	AISI 4330mod	Uddeholm Vidar Superior	Uddeholm Unimax	Uddeholm Elmax
Yield Strength [MPa]	758	1034	1410	1720	2150
Tensile Strength [MPa]	965	1138	1680	2050	2700
Elongation at break (ductility) [%]	14,5	15	12	9	5
Hardness / Hardenability [HRC]	28	36-41	48,5	54	55
Price [NOK/kg]	25	35	90	112	311

Based on the information in table 17, both AISI 4145 and Uddeholm Unimax prove good candidates for punching applications. The cost of Uddeholm Elmax is considered too high for this application. For Uddeholm Vidar and AISI 4330 mod., the availability of correct material sizes is poor.

6.8 Coating and treatment

The theoretical background, presented in chapter 2, provided insight into what coatings, processes and treatments that are available. The viability of these depend on material selection. Due to high wear and loads described previously, a case hardening process of the chosen steel is recommended. Table 18 highlights the case hardening processes studied in chapter 2.

Table 18: Characteristics of different case hardening processes.

Process	Hardness (HRC)	Process temperature range (°C)	Case Depth	Process control	Batch process
Carburizing	50-65	815-1095	Medium	High	Yes
Nitriding	50-70	500-550	Low	High	Yes
Carbonitriding	50-65	560-870	Low/medium	High	Yes
Flame Hardening	50-60	>austenizing temperature	High	Low	No
Induction Hardening	50-60	>austenizing temperature	High	Medium	No

Due to the expected complex geometry of the finished punch head and sliding surfaces, low temperature processes with shallow and controllable case depths was considered optimal. From the table it is observed that case hardening through nitriding proves beneficial with high capability for hardness, high process control and the possibility for batch processing. Additionally, the process satisfies the criterion for low temperatures and shallow case depth.

6.8.1 Punch head

Höck et. al. discovered through their efforts that, if done correctly, a combination of nitriding and the application of hard coatings proved beneficial in terms of tool properties [40]. Different hard coating processes were discussed in chapter 2 and are summarised in table 19 below.

Table 19: Characteristics of different coating processes.

Process	Process Temperature	Adhesion	Batch Process	LOS Technique	Cost
PVD	200-550°C	Moderate	Yes	Yes	High
CVD	800-1000°C	High	Yes	No	High
Electroplating	100°C	Low	No	No	Low
Thermal Spraying	Melting point of coating material	Moderate	Yes	Yes	Low

As a result of low process temperature, good adhesion and batch processing be-ing desirable parameters, the PVD technique was considered the most viable option. The line of sight technique will be able to coat the geometry using rotation of the substrate in the chamber. CVD processing was the runner-up to PVD with excellent adhesive properties, but was ultimately not recommended as a result of the process temperature interfering with the nitride layer.

Various specific coatings for the punch head was discussed in chapter 2. Diamond-like carbon coatings were deemed non-viable as a result of brittleness and poor adhesion to the substrate. Furthermore, chromium-nitride was discarded as a result of its reported low hardness and poor abrasive wear resistance.

Thus, titanium-nitride, titanium aluminium-nitride and aluminium chromium-nitride become subject for further evaluation. All the coatings may be applied through the selected PVD technique. Literature states that AlCrN exhibit greater tribological properties than TiN and TiAlN, however, testing is required to make a final decision at this stage.

6.8.2 Sliding surfaces

To aid the tribological interaction between the sliding surfaces generating radial forces in the punch, several solid lubricants were discussed in chapter 2. Having established that case hardening through nitriding is the desired base treatment of the punch components, an evaluation of the different solid lubricants was done. Depending on the environment, the different lubricants may prove beneficial.

In humid environments, molybdenum disulfide and tungsten disulfide deteriorate at a fast rate due to oxidation and increased friction between its layers. Similarly, graphite deteriorate in dry environments due to its reliance on water molecules acting as roller bearings in its lamellar structure. Teer Coatings Ltd. states that their trademarked $MoST$ has improved the properties of MoS_2 substantially. However, this is not stated or supported in literature and requires testing to verify. Despite the flaws of the discussed coatings highlighted by literature, performance might be adequate for this application.

Graphene is, according to literature, a superior coating when compared to graphite, MoS_2 and WS_2. It is stated that the coating exhibits extreme mechanical strength, liquid and gas impermeability and low COF.

This page is intentionally left blank.

7   Conclusions and Recommendations

Figure 7 highlights the efficiency of radial force output compared to axial force input. Furthermore, figure 56 displays the efficiency score of the different angles through varying COF. As a result of friction being hard to control due to environmental effects and tribological phenomena, it is recommended to choose a plane angle below 40° for the axial to radial force conversion.

As discussed in chapter 6, the number of circumferentially distributed punches depend on punch geometry, casing material and thickness. The potential standoff creation due to insufficient shear forces is considered an important factor. For the application in question, small standoff characteristics and large tears for optimal flow is desired. Additionally, the punch head geometry may wear down after a large number of perforations. This in turn may increase the shear area and render the shear force insufficient, creating standoff geometry. As a result, 6 is the maximum number of punches recommended.

Initially, different promising geometries were researched, calculated and tested to learn more about the mechanical interaction of punching. As a result of this process, it was observed that a standard press punch delivered a predictable result with few sources of error. However, due to the desired swirl flow optimised hole characteristic, it was decided to pursue more complex geometries.

Four punch geometries were designed and produced. These were subsequently punched through the casing and compared with their respective calculations. From these tests, two geometries showed promising hole characteristics. However, the test results from these geometries deviated from their pure shear based calculations.

The deviation between the calculations and test results indicated that for more complex punching geometries, finite element analysis could prove beneficial to more accurately predict the end result. These test punches and their results were used to tweak the settings for the FEA model.

Material model and simulation

Through tensile testing of specimina from the L80 casing, a material model was generated. The material properties were found to be within the required specifications for the L80 material quality. Furthermore, the material characteristics were used to optimise the simulation model in combination with test results from the TB-punches.

Through tweaking and multiple iterations, the simulation model yielded promising results. Both the deformed shape of the casing and the radial shear force from the punch coincided with testing with small deviations. Through evaluating the results of the TB-punches against their geometry, important design elements were identified. A prototype geometry with a shearing vertex combined with a flap-lifting flank was designed. Through FEA, the geometry produced promising casing deformation and acceptable radial force values. Based on the confidence gained through FEA, the prototype was produced manually.

The prototype was initially tested till casing fracture only. The test result yielded a radial shear force coinciding with FEA, with small deviations. The deviations in the test were deemed to be due to plastic deformation of the punch giving a larger shear area and thus, a larger force. Following the verification of FEA in the initial test, the prototype was tested in full hydraulic press extension. The casing obtained a plastic deformation visually comparable to that of FEA. However, multiple failure modes were observed on the prototype. Brittle fracture failure, plastic deformation of shearing vertices and the flank was observed. The constructed FEA model was considered accurate for design evaluation of punch head geometry. Figure 107 below shows the overall correlation between FEA, test results and pure shear calculations.
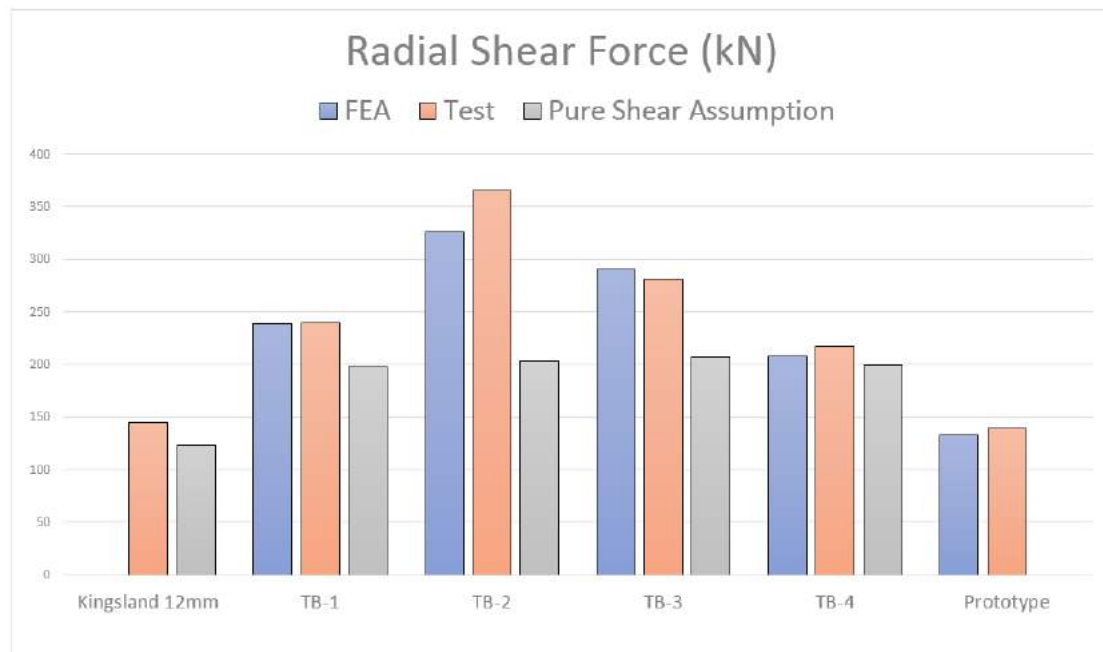
Figure 107: Comparison of results from FEA, testing and pure shear calculations.

Material, treatment and coating

From the discussion in chapter 6 it is stated that AISI 4145 and Uddeholm Unimax are both good material candidates. Due to the price difference it has been concluded to use AISI 4145 for prototype production and follow up with Unimax production once testing has yielded a successful FAT.

For Uddeholm Unimax, hardening is required to achieve optimal material properties. According to the material data sheet from Uddeholm, this process should be completed using a vacuum furnace [2].

Despite AISI 4145 being a material with good properties, it was desirable to further enhance these to lower the effects of wear and high loads. A study into the field of hardening was done. Ultimately, based on literature, a recommendation is made on case hardening the AISI 4145 parts through nitriding. This process will provide a surface layer with high hardness and strength, while maintaining the soft and ductile core to account for large deflections. Furthermore, the process temperatures are

fairly low, reducing the risk of interfering with the global properties of the component.

Moreover, due to tribological interactions, a study into surface coatings was conducted. The effort resulted in recommending the PVD technique due to low process temperatures and good adhesion to the substrate. The selection of a coating is yet to be made. However, three promising candidates in TiN, TiAlN and AlCrN are recommended for further testing.

To further aid the components in tribological interactions, research into the field of solid lubricants was completed. A final decision was not made. However, testing of PVD-applied graphite, MoS_2 and WS_2 is recommended. Due to poor availability and subsequent high costs, graphene was considered non-viable for this application despite indications of superiority in literature.

Economical Perspective

- The CPS tool offers increased efficiency when running a PWC operation as part of a P&A campaign. This is achieved through perforating on wireline prior to commencing the washing and cementation process on coiled tubing. Additionally, the tool provides standoff geometry resulting in increased cement integrity as well as guaranteeing not damaging the outer casing.

- Due to the depletion of existing oil fields, there is a rising demand for slot recovery operations. Compared to permanent P&A operations, slot recovery offers increased profitability for operator companies which in turn makes investing in new technology more attractive.

- The inevitability of permanent P&A operations secure future contracts for the tool.

8   Further work

During late spring a final prototype has been developed and produced for the CPS project, with punching geometry based on the simulation model described in this thesis. Preliminary test results coincide with results from FEA. Further simulation efforts should be done through eliminating the rigid body assumption of the punch head and comparing the results to real world testing. Through these efforts, the final geometry and material of the punch head may be identified.

Further into the summer, more testing on this tool is needed to qualify it for further use. This testing includes FAT, repetitive punching and restriction passing. Additionally, it is of interest to see how the tool reacts to punching different segments of a casing while monitoring the topside current readout.

Furthermore, supplementary research is needed on both surface coating and lubrication. It may exist coatings not mentioned in this thesis that prove better for this application. Additionally, information surrounding the discussed coatings may arise or be presented by experts in the field, changing the recommendations presented.

This page is intentionally left blank.

References

[1] A. S. C. 46.   1/4 in. titanium nitride coated high speed steel drill bit set 7 pc. s.a. URL `https://sites.google.com/site/astorescenter46/1-4-in-titanium-nitride-coated-high-speed-steel-drill-bit`.

[2] U. AB. Uddeholm unimax. 2017. URL `https://www.uddeholm.com/app/uploads/sites/45/2018/01/Uddeholm_Unimax_eng_p_1710_e7.pdf`.

[3] Aeropaca.   Electromagnetic   furnace   stirring   altek   products.   s.a.   URL   `https://www.aeropaca.org/editv2.php#RWxlY3Ryb21hZ25ldGljIEZ1cm5hY2UgU3RpcnJpbmcgQUxxURUsgUHJvZHVjdHNbfHxdaHR0cDovL3d`

[4] E. Allobody, R. Feng, and B. Young. *Finite Element Analysis and Design of Metal Structures*, volume 1. Elsevier Science & Technology, 2013.

[5] C. A. ans Services. L80 chemical composition. s.a. URL `https://www.contalloy.com/products/grade/l80`.

[6] P. Arms.   Cryptic coatings 5.56 nato ar-15 bolt carrier group - mystic silver. s.a. URL `https://www.primaryarms.com/cryptic-coatings-5.56-nato-ar-15-bolt-carrier-group-with-mystic-silver-finish`.

[7] E. P. AS. Who are we? s.a. URL `http://www.eplug.no/about-us`.

[8] C. Baumann, A. Fayard, B. Grove, J. Harvey, W. Yang, A. Govil, A. Martin, R. F. M. Garcìa, A. R. Rodriguez, J. Munro, C. V. Terrazas, and L. Zhan. Perforating innovations—shooting holes in performance models. *Oilfield Review - Autumn*, pages 14–31, 2014.

[9] D. Berman, A. Erdemir, and A. Sumant. Graphene: a new emerging lubricant. *materialstoday*, 17(1):31–42, 2014.

[10] S. Bhavikatti. *Finite Element Analysis*, volume 1. New Age International Ltd., 2004.

[11] B. Bhushan. *Introduction to Tribology*, volume 2nd edition. John Wiley Sons, Inc., 2013.

[12] P. Bob McGinty, PhD. Stress state schematics. s.a. URL `https://www.fracturemechanics.org/hole.html`.

[13] F. C Campbell. Elements of metallurgy and engineering alloys. January 2008.

[14] A. Chandiran, N. Anandan, and S. Sakthivel. Comparative study on tool life and wear resistance of titanium nitride (tin) and aluminium chromium nitride (alcrn) coated carbide inserts. *Tribology - Materials, Surfaces and Interfaces*, 6(4): 160–167, 2013.

[15] J. Christensen and C. Bastien. *Nonlinear Optimization of Vehicle Safety Structures : Modeling of Structures Subjected to Large Deformations*, volume 1. Elsevier Science & Technology, 2015.

[16] T. Coatings. Most coatings. 2019. URL `http://www.teercoatings.co.uk/index.php?page=39`.

[17] J. Collins. *Failure of Materials in Mechanical Design*, volume 2. John Wiley & Sons, Inc., 1993.

[18] J. Davis. *Surface Hardening of Steels : Understanding the Basics*, volume 1. ASM International, 2002.

[19] H. S. A. L. Desa, P. C. Offshore well plugging and abandonment: Challenges and technical soulutions. 2013. URL `https://www.onepetro.org/conference-paper/OTC-23906-MS`.

[20] T. G. Digges, S. J. Rosenberg, and G. W. Geil. Heat treatment and properties of iron and steel. 1966.

[21] J. Dini. An electroplaters view of pvd processing. Technical report, Lawrence Livermore National Laboratory, 1992.

[22] N. P. Directorate. Original reserves. 2019. URL 7.

[23] N. P. Directorate. Historical production. 2019. URL `https://www.norskpetroleum.no/en/facts/historical-production/`.

[24] N. P. Directorate. Production forecasts. 2019. URL `https://www.norskpetroleum.no/en/production-and-exports/production-forecasts/`.

[25] M. Free. Three key factors to understand machinability of carbon and alloy steel. 2012. URL `https://pmpaspeakingofprecision.com/tag/hardness/`.

[26] G. M. Gant, A.J. and L. Orkney. The wear and friction behaviour of engineering coatings in ambient air and dry nitrogen. *An International Journal on the Science and Technology of Friction, Lubrication and Wear*, 271(1):2164–2175, 2011.

[27] M. Gedeon. Grain size & material strength. 2010. URL `https://materion.com/-/media/files/alloy/newsletters/technical-tidbits/issue-no-15---grain-size-and-material-strength.pdf`.

[28] M. Gedeon. Solid solution hardening & strength. 2010. URL `https://materion.com/-/media/files/alloy/newsletters/technical-tidbits/issue-no-16-solid-solution-hardening--strength.pdf`.

[29] M. Gedeon. Strain hardening & strength. 2010. URL `https://materion.com/-/media/files/alloy/newsletters/technical-tidbits/issue-no-17-strain-hardening--strength.pdf`.

[30] M. Gedeon. Thermal strengthening mechanisms. 2010. URL `https://materion.com/-/media/files/alloy/newsletters/technical-tidbits/issue-no-18--thermal-strengthening-mechanisms.pdf`.

[31] J.-P. N. Gillies Gabolde. *Drilling Data Handbook*, volume 8th edition. IFP Publications, 2006.

[32] S. GmbH. Metal forming handbook / schuler gmbh. *SERBIULA (sistema Librum 2.0)*, May 2019.

[33] T. Gradt and T. Schneider. Tribological performance of mos2 coatings in various environments. *Lubricants*, 4(32), 2016.

[34] Haliburton. Dpu® actuated tubing perforator. 2015. URL `https://www.halliburton.com/content/dam/ps/public/lp/contents/Data_Sheets/web/H/DPU-Actuated-Tubing-Perforator.pdf?nav=en-US_wireline-perforating_public`.

[35] C. Handal. Abandonment of obsolete well and installation on the norwegian continental shelf. Master's thesis, University of Stavanger, 2014.

[36] A. Harish. Implicit vs. explicit fem. 2019. URL `https://www.simscale.com/blog/2019/01/implicit-vs-explicit-fem/`.

[37] F.-P. E. M. . F. F. Hernández, J. Modelling and experimental analysis of the effects of tool wear on form errors in stainless steel blanking. *Journal of Materials Processing Technology)*, 2006.

[38] S. Hosmani, P. Kuppusami, and R. Goyal. *An Introduction to Surface Alloying of Metals*, volume 1. Springer India, 2014.

[39] J. Huopana, S.-G. Sjöling, and M. Taborelli. Design of precision alignment of compact linear colliders accelerating structures. January 2007.

[40] K. Höck, G. Leonhardt, B. Bücken, H.-J. Spies, and B. Larisch. Process technological aspects of the production and properties of in situ combined plasma-nitrided and pvd hard-coated high alloy tool steels. September 1995.

[41] A. International. Surface hardening of steels: Understanding the basics. 2002.

[42] J. Jagielski, A. Khanna, J. Kucinski, D. Mishra, P. Pacolta, P. Sioshansi, E. Tobin, J. Thereska, V. Uglov, T. Vilaithong, J. Viviente, S. Yang, and A. Zalar. Effect of chromium nitride coating on the corrosion and wear resistance of stainless steel. *Applied Surface Science*, 156(1-4):47–64, 2000.

[43] J. Kaszynski. Improving the performance of transfer dies. 2015. URL `https://www.thefabricator.com/article/metalsmaterials/improving-the-performance-of-transfer-dies`.

[44] D. H. K. Khaira. Precipitation hardening. 2013. URL `https://www.slideshare.net/RakeshSingh125/f-precipitation-hardening`.

[45] S. Luo. Effect of the geometry and the surface treatment of punching tools on the tool life and wear conditions in the piercing of thick steel plate. *Journal of Materials Processing Technology*, 88(1):122 – 133, 1999. ISSN 0924-0136. doi: https://doi.org/10.1016/S0924-0136(98)00375-6. URL http://www.sciencedirect.com/science/article/pii/S0924013698003756.

[46] S. Metco. An introduction to thermal spray issue no. 4. Technical report, Sulzer Metco, 2013.

[47] J. Mo and M. Zhu. Sliding tribological behavior of alcrn coating. *Tribology International*, 41(12):1161–1168, 2008.

[48] M. Neale. *Lubrication and Reliability Handbook*, volume 1. Elsevier Science & Technology, 2000.

[49] Petrowiki. Perforating equipment. 2015. URL https://petrowiki.org/Perforating_equipment#Conveyance_systems.

[50] L. Quintino. Overview of coating technologies. *Surface Modification by Solid State Processing*, 1(1):1–24, 2014.

[51] J. Reddy. *Introduction to Nonlinear Finite Element Analysis*, volume 1. Oxford University Press, Incorporated, 2004.

[52] J. Reiss. What are dlc coatings? 2019. URL https://blog.trendperform.com/what-are-dlc-coatings.

[53] J. Shigley and C. R. Mischke. *Mechanical Engineering Design*, volume 6. McGraw-Hill, 2001.

[54] SolidWorks. Understanding nonlinear analysis. 2010. URL https://www.solidworks.com/sw/docs/Nonlinear_Analysis_2010_ENG_FINAL.pdf.

[55] N. Standard. D-010 well integrity and well operations. 2004.

[56] S. Subramonian. *Improvement of Punch and Die and Part Quality in Blanking of Miniature Parts*. PhD thesis, The Ohio State University, 2013.

[57] M. Technology. Flame hardening and induction hardening. s.a. URL `http://4mechtech.blogspot.com/2013/11/case-hardening-process-flame-hardening.html`.

[58] tribonet. Fatigue wear. 2017. URL `http://www.tribonet.org/wiki/fatigue-wear/`.

[59] Uddeholm. Tooling solutions for advanced high strength steels. s.a.

[60] A. University. Introduction to meshing. 2014. URL `https://altairuniversity.com/wp-content/uploads/2014/02/meshing.pdf`.

[61] J. D. Verhoeven. *Metallurgy for the Non-metallurgist*, volume Digital Edition. ASM International, 2007.

[62] J. Vetter, R. Knaup, I. Dwuletzki, E. Schneider, and S. Vogler. Hard coatings for lubrication reduction in metal forming. *Suirface Coatings & Technology*, 86-87 (2):739–747, 1996.

[63] P. J. Weiss. Stress-strain behaviour of concrete. s.a. URL `http://www.theconcreteportal.com/cons_rel.html`.

[64] M. Zhang. Improving the electrical contact property of single-walled carbon nanotube arrays by electrodeposition. *Nano-Micro Letters*, 5:242–246, 2013. ISSN 2150-5551. doi: 10.5101/nml.v5i4.p242-246. URL `http://dx.doi.org/10.5101/nml.v5i4.p242-246`.

Appendix

Appendices

- Appendix A, ISO 6892-1 tensile test standard.

- Appendix B, Comparison between MoS_2 and Ws_2

- Appendix C, NORSOK-D010 - Well integrity in drilling and well operations

- Appendix D, Questionnaire report

8.1 Appendix A

This page is intentionally left blank.

standard norge
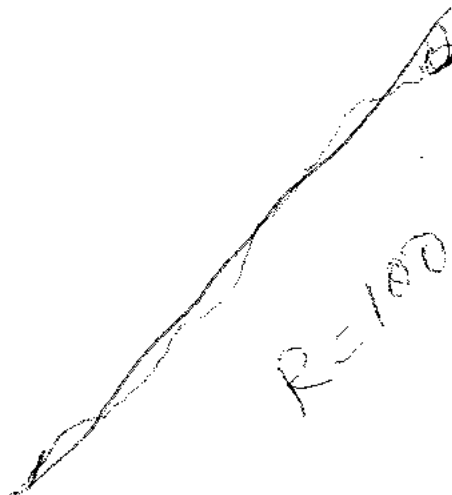
Metalliske materialer
Strekkprøving
Del 1: Prøvingsmetode i romtemperatur
(ISO 6892-1:2009)

Metallic materials
Tensile testing
Part 1: Method of test at room temperature
(ISO 6892-1:2009)

Nasjonalt forord

Den engelskspråklige versjonen av europeisk standard EN ISO 6892-1:2009 er fastsatt som Norsk Standard NS-EN ISO 6892-1:2009 i november 2009.

Denne standarden erstatter NS-EN 10002-1:2001.

National foreword

The English language version of European Standard EN ISO 6892-1:2009 has been adopted as Norwegian Standard NS-EN ISO 6892-1:2009 in November 2009.

This standard supersedes NS-EN 10002-1:2001.

EUROPEAN STANDARD

NORME EUROPÉENNE

EUROPÄISCHE NORM

EN ISO 6892-1

August 2009

ICS 77.040.10

English Version

Metallic materials - Tensile testing - Part 1: Method of test at room temperature (ISO 6892-1:2009)

Matériaux métalliques - Essai de traction - Partie 1:
Methode d'essai à température ambiante (ISO 6892-1:2009)

Metallische Werkstoffe - Zugversuch - Teil 1: Prüfverfahren
bei Raumtemperatur (ISO 6892-1:2009)

This European Standard was approved by CEN on 13 March 2009.

CEN members are bound to comply with the CEN/CENELEC Internal Regulations which stipulate the conditions for giving this European Standard the status of a national standard without any alteration. Up-to-date lists and bibliographical references concerning such national standards may be obtained on application to the CEN Management Centre or to any CEN member.

This European Standard exists in three official versions (English, French, German). A version in any other language made by translation under the responsibility of a CEN member into its own language and notified to the CEN Management Centre has the same status as the official versions.

CEN members are the national standards bodies of Austria, Belgium, Bulgaria, Cyprus, Czech Republic, Denmark, Estonia, Finland, France, Germany, Greece, Hungary, Iceland, Ireland, Italy, Latvia, Lithuania, Luxembourg, Malta, Netherlands, Norway, Poland, Portugal, Romania, Slovakia, Slovenia, Spain, Sweden, Switzerland and United Kingdom.

EUROPEAN COMMITTEE FOR STANDARDIZATION
COMITÉ EUROPÉEN DE NORMALISATION
EUROPÄISCHES KOMITEE FÜR NORMUNG

Management Centre: Avenue Marnix 17, B-1000 Brussels

Ref. No. EN ISO 6892-1:2009: E

Foreword

This document (EN ISO 6892-1:2009) has been prepared by Technical Committee ISO/TC 164 "Mechanical testing of metals" in collaboration with Technical Committee ECISS/TC 1 "Tensile testing" the secretariat of which is held by AFNOR.

This European Standard shall be given the status of a national standard, either by publication of an identical text or by endorsement, at the latest by February 2010, and conflicting national standards shall be withdrawn at the latest by February 2010.

Attention is drawn to the possibility that some of the elements of this document may be the subject of patent rights. CEN [and/or CENELEC] shall not be held responsible for identifying any or all such patent rights.

This document supersedes EN 10002-1:2001.

According to the CEN/CENELEC Internal Regulations, the national standards organizations of the following countries are bound to implement this European Standard: Austria, Belgium, Bulgaria, Cyprus, Czech Republic, Denmark, Estonia, Finland, France, Germany, Greece, Hungary, Iceland, Ireland, Italy, Latvia, Lithuania, Luxembourg, Malta, Netherlands, Norway, Poland, Portugal, Romania, Slovakia, Slovenia, Spain, Sweden, Switzerland and the United Kingdom.

Endorsement notice

The text of ISO 6892-1:2009 has been approved by CEN as a EN ISO 6892-1:2009 without any modification.

Contents

Page

iii

Foreword

ISO (the International Organization for Standardization) is a worldwide federation of national standards bodies (ISO member bodies). The work of preparing International Standards is normally carried out through ISO technical committees. Each member body interested in a subject for which a technical committee has been established has the right to be represented on that committee. International organizations, governmental and non-governmental, in liaison with ISO, also take part in the work. ISO collaborates closely with the International Electrotechnical Commission (IEC) on all matters of electrotechnical standardization.

International Standards are drafted in accordance with the rules given in the ISO/IEC Directives, Part 2.

The main task of technical committees is to prepare International Standards. Draft International Standards adopted by the technical committees are circulated to the member bodies for voting. Publication as an International Standard requires approval by at least 75 % of the member bodies casting a vote.

Attention is drawn to the possibility that some of the elements of this document may be the subject of patent rights. ISO shall not be held responsible for identifying any or all such patent rights.

ISO 6892-1 was prepared by Technical Committee ISO/TC 164, *Mechanical testing of metals*, Subcommittee SC 1, *Uniaxial testing*.

This first edition of ISO 6892-1 cancels and replaces ISO 6892:1998.

ISO 6892 consists of the following parts, under the general title *Metallic materials — Tensile testing*:

— *Part 1: Method of test at room temperature*

The following parts are under preparation:

— *Part 2: Method of test at elevated temperature*

— *Part 3: Method of test at low temperature*

The following part is planned:

— *Part 4: Method of test in liquid helium*

Introduction

During discussions concerning the speed of testing in the preparation of ISO 6892:1998, it was decided to recommend the use of strain rate control in future revisions.

In this part of ISO 6892, there are two methods of testing speeds available. The first, method A, is based on strain rates (including crosshead separation rate) and the second, method B, is based on stress rates. Method A is intended to minimize the variation of the test rates during the moment when strain rate sensitive parameters are determined and to minimize the measurement uncertainty of the test results.

Metallic materials — Tensile testing —

Part 1:
Method of test at room temperature

1 Scope

This part of ISO 6892 specifies the method for tensile testing of metallic materials and defines the mechanical properties which can be determined at room temperature.

NOTE   Annex A indicates complementary recommendations for computer controlled testing machines.

2 Normative references

The following referenced documents are indispensable for the application of this document. For dated references, only the edition cited applies. For undated references, the latest edition of the referenced document (including any amendments) applies.

ISO 377, *Steel and steel products — Location and preparation of samples and test pieces for mechanical testing*

ISO 2566-1, *Steel — Conversion of elongation values — Part 1: Carbon and low alloy steels*

ISO 2566-2, *Steel — Conversion of elongation values — Part 2: Austenitic steels*

ISO 7500-1, *Metallic materials — Verification of static uniaxial testing machines — Part 1: Tension/compression testing machines — Verification and calibration of the force-measuring system*

ISO 9513, *Metallic materials — Calibration of extensometers used in uniaxial testing*

3 Terms and definitions

For the purposes of this document, the following terms and definitions apply.

3.1
gauge length
L
length of the parallel portion of the test piece on which elongation is measured at any moment during the test

[ISO/TR 25679:2005[3]]

3.1.1
original gauge length
L_0
length between **gauge length** (3.1) marks on the piece measured at room temperature before the test

NOTE   Adapted from ISO/TR 25679:2005[3].

3.1.2
final gauge length after rupture
final gauge length after fracture
L_u
length between **gauge length** (3.1) marks on the test piece measured after rupture, at room temperature, the two pieces having been carefully fitted back together so that their axes lie in a straight line

NOTE   Adapted from ISO/TR 25679:2005[3].

3.2
parallel length
L_c
length of the parallel reduced section of the test piece

[ISO/TR 25679:2005[3]]

NOTE   The concept of parallel length is replaced by the concept of distance between grips for unmachined test pieces.

3.3
elongation
increase in the **original gauge length** (3.1.1) at any moment during the test

NOTE   Adapted from ISO/TR 25679:2005[3].

3.4
percentage elongation
elongation expressed as a percentage of the **original gauge length**, L_o (3.1.1)

[ISO/TR 25679:2005[3]]

3.4.1
percentage permanent elongation
increase in the **original gauge length** (3.1.1) of a test piece after removal of a specified stress, expressed as a percentage of the original gauge length, L_o

[ISO/TR 25679:2005[3]]

3.4.2
percentage elongation after fracture
A
permanent elongation of the gauge length after fracture, $(L_u - L_o)$, expressed as a percentage of the **original gauge length**, L_o

[ISO/TR 25679:2005[3]]

NOTE   For proportional test pieces, if the original gauge length is not equivalent to $5{,}65\sqrt{S_o}$ [1]) where S_o is the original cross-sectional area of the parallel length, the symbol A should be supplemented by a subscript indicating the coefficient of proportionality used, e.g. $A_{11{,}3}$ indicates a percentage elongation of the gauge length, L_o, of

$$A_{11{,}3} = 11{,}3\sqrt{S_o}$$

For non-proportional test pieces (see Annex B), the symbol A should be supplemented by a subscript indicating the original gauge length used, expressed in millimetres, e.g. $A_{80\,mm}$ indicates a percentage elongation of a gauge length, L_o, of 80 mm.

---

1) $5{,}65\sqrt{S_o} = 5\sqrt{(4S_o/\pi)}$.

2

3.5
extensometer gauge length
L_e
initial extensometer gauge length used for measurement of extension by means of an extensometer

NOTE 1   Adapted from ISO/TR 25679:2005[3].

NOTE 2   For measurement of yield and proof strength parameters, L_e should span as much of the parallel length of the test piece as possible. Ideally, as a minimum, L_e should be greater than $0,50L_0$ but less than approximately $0,9L_c$. This should ensure that the extensometer detects all yielding events that occur in the test piece. Further, for measurement of parameters "at" or "after reaching" maximum force, L_e should be approximately equal to L_0.

3.6
extension
increase in the **extensometer gauge length**, L_e (3.5), at any moment during the test

[ISO/TR 25679:2005[3]]

3.6.1
percentage extension
"strain"
extension expressed as a percentage of the **extensometer gauge length**, L_e (3.5)

3.6.2
percentage permanent extension
increase in the extensometer gauge length, after removal of a specified stress from the test piece, expressed as a percentage of the **extensometer gauge length**, L_e (3.5)

[ISO/TR 25679:2005[3]]

3.6.3
percentage yield point extension
A_e
in discontinuous yielding materials, the extension between the start of yielding and the start of uniform workhardening, expressed as a percentage of the **extensometer gauge length**, L_e (3.5)

NOTE   Adapted from ISO/TR 25679:2005[3].

See Figure 7.

3.6.4
percentage total extension at maximum force
A_{gt}
total extension (elastic extension plus plastic extension) at maximum force, expressed as a percentage of the **extensometer gauge length**, L_e (3.5)

See Figure 1.

3.6.5
percentage plastic extension at maximum force
A_g
plastic extension at maximum force, expressed as a percentage of the **extensometer gauge length**, L_e (3.5)

See Figure 1.

3

3.6.6

percentage total extension at fracture

A_t

total extension (elastic extension plus plastic extension) at the moment of fracture, expressed as a percentage of the **extensometer gauge length**, L_e (3.5)

See Figure 1.

3.7   Testing rate

3.7.1

strain rate

$\dot{e}_{L_e}$

increase of strain, measured with an extensometer, in **extensometer gauge length**, L_e (3.5), per time

NOTE   See 3.5.

3.7.2

estimated strain rate over the parallel length

$\dot{e}_{L_c}$

value of the increase of strain over the **parallel length**, L_c (3.2), of the test piece per time based on the **crosshead separation rate** (3.7.3) and the parallel length of the test piece

3.7.3

crosshead separation rate

v_c

displacement of the crossheads per time

3.7.4

stress rate

$\dot{R}$

increase of stress per time

NOTE   Stress rate should only be used in the elastic part of the test (method B).

3.8

percentage reduction of area

Z

maximum change in cross-sectional area which has occurred during the test, $(S_o - S_u)$, expressed as a percentage of the original cross-sectional area, S_o:

$$Z = \frac{S_o - S_u}{S_o} \times 100$$

3.9   Maximum force

NOTE   For materials which display discontinuous yielding, but where no workhardening can be established, F_m is not defined in this part of ISO 6892 [see footnote to Figure 8 c)].

3.9.1

maximum force

F_m

(materials displaying no discontinuous yielding) highest force that the test piece withstands during the test

3.9.2
maximum force
F_m
(materials displaying discontinuous yielding) highest force that the test piece withstands during the test after the beginning of workhardening

NOTE   See Figure 8 a) and b).

3.10
stress
at any moment during the test, force divided by the original cross-sectional area, S_0, of the test piece

NOTE 1   Adapted from ISO/TR 25679:2005[3].

NOTE 2   All references to stress in this part of ISO 6892 are to engineering stress.

NOTE 3   In what follows, the designations "force" and "stress" or "extension", "percentage extension" and "strain", respectively, are used on various occasions (as figure axis labels or in explanations for the determination of different properties). However, for a general description or definition of a well-defined point on a curve, the designations "force" and "stress" or "extension", "percentage extension" and "strain", respectively, are interchangeable.

3.10.1
tensile strength
R_m
stress corresponding to the **maximum force**, F_m (3.9)

[ISO/TR 25679:2005[3]]

3.10.2
yield strength
when the metallic material exhibits a yield phenomenon, stress corresponding to the point reached during the test at which plastic deformation occurs without any increase in the force

NOTE   Adapted from ISO/TR 25679:2005[3].

3.10.2.1
upper yield strength
R_{eH}
maximum value of **stress** (3.10) prior to the first decrease in force

NOTE   Adapted from ISO/TR 25679:2005[3].

See Figure 2.

3.10.2.2
lower yield strength
R_{eL}
lowest value of **stress** (3.10) during plastic yielding, ignoring any initial transient effects

[ISO/TR 25679:2005[3]]

See Figure 2.

3.10.3
proof strength, plastic extension
R_p

stress at which the plastic extension is equal to a specified percentage of the **extensometer gauge length**, L_e (3.5)

NOTE 1   Adapted from ISO/TR 25679:2005, "proof strength, non-proportional extension".

NOTE 2   A suffix is added to the subscript to indicate the prescribed percentage, e.g. $R_{p0,2}$.

See Figure 3.

3.10.4
proof strength, total extension
R_t

stress at which total extension (elastic extension plus plastic extension) is equal to a specified percentage of the **extensometer gauge length**, L_e (3.5)

NOTE 1   Adapted from ISO/TR 25679:2005[3].

NOTE 2   A suffix is added to the subscript to indicate the prescribed percentage, e.g. $R_{t0,5}$.

See Figure 4.

3.10.5
permanent set strength
R_r

stress at which, after removal of force, a specified permanent elongation or extension, expressed respectively as a percentage of **original gauge length**, L_o (3.1.1), or **extensometer gauge length**, L_e (3.5), has not been exceeded

[ISO/TR 25679:2005[3]]

See Figure 5.

NOTE   A suffix is added to the subscript to indicate the specified percentage of the original gauge length, L_o, or of the extensometer gauge length, L_e, e.g. $R_{r0,2}$.

3.11
fracture
phenomenon which is deemed to occur when total separation of the test piece occurs

NOTE   Criteria for fracture which may be used for computer controlled tests are given in Figure A.2.

4 Terms and symbols

The symbols used in this part of ISO 6892 and corresponding designations are given in Table 1.

Table 1 — Symbols and designations

Symbol	Unit	Designation
Test piece		
a_0, T [a]	mm	original thickness of a flat test piece or wall thickness of a tube
b_0	mm	original width of the parallel length of a flat test piece or average width of the longitudinal strip taken from a tube or width of flat wire
d_0	mm	original diameter of the parallel length of a circular test piece, or diameter of round wire or internal diameter of a tube
D_0	mm	original external diameter of a tube
L_0	mm	original gauge length
L'_0	mm	initial gauge length for determination of A_{wn} (see Annex I)
L_c	mm	parallel length
L_e	mm	extensometer gauge length
L_t	mm	total length of test piece
L_u	mm	final gauge length after fracture
L'_u	mm	final gauge length after fracture for determination of A_{wn} (see Annex I)
S_0	mm²	original cross-sectional area of the parallel length
S_u	mm²	minimum cross-sectional area after fracture
k	—	coefficient of proportionality (see 6.1.1)
Z	%	percentage reduction of area
Elongation		
A	%	percentage elongation after fracture (see 3.4.2)
A_{wn}	%	percentage plastic elongation without necking (see Annex I)
Extension		
A_e	%	percentage yield point extension
A_g	%	percentage plastic extension at maximum force, F_m
A_{gt}	%	percentage total extension at maximum force, F_m
A_t	%	percentage total extension at fracture
ΔL_m	mm	extension at maximum force
ΔL_f	mm	extension at fracture
Rates		
$\dot{e}_{L_e}$	s⁻¹	strain rate
$\dot{e}_{L_c}$	s⁻¹	estimated strain rate over the parallel length
$\dot{R}$	MPa s⁻¹	stress rate
v_c	mm s⁻¹	crosshead separation rate

Table 1 — Symbols and designations *(continued)*

Symbol	Unit	Designation
		Force
F_m	N	maximum force
		Yield strength — Proof strength — Tensile strength
E	MPa [b]	modulus of elasticity
m	MPa	slope of the stress-percentage extension curve at a given moment of the test
m_E	MPa	slope of the elastic part of the stress-percentage extension curve [c]
R_{eH}	MPa	upper yield strength
R_{eL}	MPa	lower yield strength
R_m	MPa	tensile strength
R_p	MPa	proof strength, plastic extension
R_r	MPa	specified permanent set strength
R_t	MPa	proof strength, total extension

[a] Symbol used in steel tube product standards.

[b] $1\ MPa = 1\ N\ mm^{-2}$.

[c] In the elastic part of the stress-percentage extension curve, the value of the slope may not necessarily represent the modulus of elasticity. This value can closely agree with the value of the modulus of elasticity if optimal conditions (high resolution, double sided, averaging extensometers, perfect alignment of the test piece, etc.) are used.

CAUTION — The factor 100 is necessary if percentage values are used.

5 Principle

The test involves straining a test piece by tensile force, generally to fracture, for the determination of one or more of the mechanical properties defined in Clause 3.

The test is carried out at room temperature between 10 °C and 35 °C, unless otherwise specified. Tests carried out under controlled conditions shall be made at a temperature of 23 °C ± 5 °C.

6 Test piece

6.1 Shape and dimensions

6.1.1 General

The shape and dimensions of the test pieces may be constrained by the shape and dimensions of the metallic product from which the test pieces are taken.

The test piece is usually obtained by machining a sample from the product or a pressed blank or casting. However, products of uniform cross-section (sections, bars, wires, etc.) and also as-cast test pieces (i.e. for cast iron and non-ferrous alloys) may be tested without being machined.

The cross-section of the test pieces may be circular, square, rectangular, annular or, in special cases, some other uniform cross-section.

Preferred test pieces have a direct relationship between the original gauge length, L_o, and the original cross-sectional area, S_o, expressed by the equation $L_o = k\sqrt{S_o}$, where k is a coefficient of proportionality, and are called proportional test pieces. The internationally adopted value for k is 5,65. The original gauge length shall be not less than 15 mm. When the cross-sectional area of the test piece is too small for this requirement to be met with, $k = 5,65$, a higher value (preferably 11,3) or a non-proportional test piece may be used.

NOTE   By using an original gauge length smaller than 20 mm, the measurement uncertainty is increased.

For non-proportional test pieces, the original gauge length, L_o, is independent of the original cross-sectional area, S_o.

The dimensional tolerances of the test pieces shall be in accordance with the Annexes B to E (see 6.2).

Other test pieces such as those specified in relevant product standards or national standards may be used by agreement with the customer, e.g. ISO 3183[1] (API 5L), ISO 11960[2] (API 5CT), ASTM A370[6], ASTM E8M[7], DIN 50125[10], IACS W2[13], and JIS Z2201[14].

6.1.2   Machined test pieces

Machined test pieces shall incorporate a transition radius between the gripped ends and the parallel length if these have different dimensions. The dimensions of the transition radius are important and it is recommended that they be defined in the material specification if they are not given in the appropriate annex (see 6.2).

The gripped ends may be of any shape to suit the grips of the testing machine. The axis of the test piece shall coincide with the axis of application of the force.

The parallel length, L_c, or, in the case where the test piece has no transition radii, the free length between the grips, shall always be greater than the original gauge length, L_o.

6.1.3   Unmachined test pieces

If the test piece consists of an unmachined length of the product or of an unmachined test bar, the free length between the grips shall be sufficient for gauge marks to be at a reasonable distance from the grips (see Annexes B to E).

As-cast test pieces shall incorporate a transition radius between the gripped ends and the parallel length. The dimensions of this transition radius are important and it is recommended that they be defined in the product standard. The gripped ends may be of any shape to suit the grips of the testing machine. The parallel length, L_c, shall always be greater than the original gauge length, L_o.

6.2   Types

The main types of test pieces are defined in Annexes B to E according to the shape and type of product, as shown in Table 2. Other types of test pieces can be specified in product standards.

Table 2 — Main types of test piece according to product type

Dimensions in millimetres

Type of product		Corresponding Annex
Sheets — Plates — Flats **Thickness** a	**Wire — Bars — Sections** **Diameter or side**	
$0,1 \leqslant a < 3$	—	B
—	< 4	C
$a \geqslant 3$	$\geqslant 4$	D
Tubes		E

6.3 Preparation of test pieces

The test pieces shall be taken and prepared in accordance with the requirements of the relevant International Standards for the different materials (e.g. ISO 377).

7 Determination of original cross-sectional area

The relevant dimensions of the test piece should be measured at sufficient cross-sections perpendicular to the longitudinal axis in the central region of the parallel length of the test piece.

A minimum of three cross-sections is recommended.

The original cross-sectional area, S_0, is the average cross-sectional area and shall be calculated from the measurements of the appropriate dimensions.

The accuracy of this calculation depends on the nature and type of the test piece. Annexes B to E describe methods for the evaluation of S_0 for different types of test pieces and contain specifications for the accuracy of measurement.

8 Marking the original gauge length

Each end of the original gauge length, L_0, shall be marked by means of fine marks or scribed lines, but not by notches which could result in premature fracture.

For proportional test pieces, the calculated value of the original gauge length may be rounded to the nearest multiple of 5 mm, provided that the difference between the calculated and marked gauge length is less than 10 % of L_0. The original gauge length shall be marked to an accuracy of ± 1 %.

If the parallel length, L_c, is much greater than the original gauge length, as, for instance, with unmachined test pieces, a series of overlapping gauge lengths may be marked.

In some cases, it may be helpful to draw, on the surface of the test piece, a line parallel to the longitudinal axis, along which the gauge lengths are marked.

9 Accuracy of testing apparatus

The force-measuring system of the testing machine shall be calibrated in accordance with ISO 7500-1, class 1, or better.

For the determination of proof strength (plastic or total extension) the used extensometer shall be in accordance with ISO 9513, class 1 or better, in the relevant range. For other properties (with higher extension) an ISO 9513, class 2 extensometer in the relevant range may be used.

10 Conditions of testing

10.1 Setting the force zero point

The force-measuring system shall be set to zero after the testing loading train has been assembled, but before the test piece is actually gripped at both ends. Once the force zero point has been set, the force-measuring system may not be changed in any way during the test.

NOTE   The use of this method ensures, that on one hand the weight of the gripping system is compensated for in the force measurement and on the other hand any force resulting from the clamping operation does not affect this measurement.

10.2 Method of gripping

The test pieces shall be gripped by suitable means, such as wedges, screwed grips, parallel jaw faces, or shouldered holders.

Every endeavour should be made to ensure that test pieces are held in such a way that the force is applied as axially as possible, in order to minimize bending (more information is given in ASTM E1012[8], for example). This is of particular importance when testing brittle materials or when determining proof strength (plastic extension), proof strength (total extension) or yield strength.

In order to obtain a straight test piece and ensure the alignment of the test piece and grip arrangement, a preliminary force may be applied provided it does not exceed a value corresponding to 5 % of the specified or expected yield strength.

A correction of the extension should be carried out to take into account the effect of the preliminary force.

10.3 Testing rate based on strain rate control (method A)

10.3.1 General

Method A is intended to minimize the variation of the test rates during the moment when strain rate sensitive parameters are determined and to minimize the measurement uncertainty of the test results.

Two different types of strain rate control are described in this section. The first is the control of the strain rate itself, $\dot{e}_{L_e}$, that is based on the feedback obtained from an extensometer. The second is the control of the estimated strain rate over the parallel length, $\dot{e}_{L_c}$, which is achieved by controlling the crosshead separation rate at a velocity equal to the desired strain rate multiplied by the parallel length.

If a material shows homogeneous deformation behaviour and the force remains nominally constant, the strain rate, $\dot{e}_{L_e}$, and the estimated strain rate over the parallel length, $\dot{e}_{L_c}$, are approximately equal. Differences exist if the material exhibits discontinuous or serrated yielding (e.g. some steels and AlMg alloys in the yield point elongation range, or materials which show serrated yielding like the Portevin-Le Chatelier effect) or if

necking occurs. If the force is increasing, the estimated strain rate may be substantially below the target strain rate due to the compliance of the testing machine.

The testing rate shall conform to the following requirements.

a) In the range up to and including the determination of R_{eH}, R_p or R_t, the specified strain rate, $\dot{e}_{L_e}$ (see 3.7.1), shall be applied. In this range, to eliminate the influence of the compliance of the tensile testing machine, the use of an extensometer clamped on the test piece is necessary to have accurate control over the strain rate. (For testing machines unable to control by strain rate, a procedure using the estimated strain rate over the parallel length, $\dot{e}_{L_c}$, may be used.)

b) During discontinuous yielding, the estimated strain rate over the parallel length, $\dot{e}_{L_c}$ (see 3.7.2), should be applied. In this range, it is impossible to control the strain rate using the extensometer clamped on to the test piece because local yielding can occur outside the extensometer gauge length. The required estimated strain rate over the parallel length may be maintained in this range sufficiently accurately using a constant crosshead separation rate, v_c (see 3.7.3);

$$v_c = L_c\, \dot{e}_{L_c} \qquad\qquad . \qquad\qquad\qquad\qquad\qquad\qquad (1)$$

where

$\dot{e}_{L_c}$ is the estimated strain rate over the parallel length;

L_c is the parallel length.

c) In the range following R_p or R_t or end of yielding (see 3.7.2), $\dot{e}_{L_e}$ or $\dot{e}_{L_c}$ can be used. The use of $\dot{e}_{L_c}$ is recommended to avoid any control problems which may arise if necking occurs outside the extensometer gauge length.

The strain rates specified in 10.3.2 to 10.3.4 shall be maintained during the determination of the relevant material property (see also Figure 9).

During switching to another strain rate or to another control mode, no discontinuities in the stress-strain curve should be introduced which distort the values of R_m, A_g or A_{gt} (see Figure 10). This effect can be reduced by a suitable gradual switch between the rates.

The shape of the stress-strain curve in the workhardening range can also be influenced by the strain rate. The testing rate used should be documented (see 10.6).

10.3.2 Strain rate for the determination of the upper yield strength, R_{eH}, or proof strength properties, R_p, and R_t

The strain rate, $\dot{e}_{L_e}$, shall be kept as constant as possible up to and including the determination of R_{eH} or R_p or R_t. During the determination of these material properties the strain rate, $\dot{e}_{L_e}$, shall be in one of the two following specified ranges (see also Figure 9).

Range 1: $\dot{e}_{L_e}$ = 0,000 07 s^{-1}, with a relative tolerance of ±20 %

Range 2: $\dot{e}_{L_e}$ = 0,000 25 s^{-1}, with a relative tolerance of ±20 % (recommended unless otherwise specified)

If the testing machine is not able to control the strain rate directly, the estimated strain rate over the parallel length, $\dot{e}_{L_c}$, i.e. constant crosshead separation rate, shall be used. This rate shall be calculated using Equation (1).

The resulting strain rate on the test piece will be lower than the specified strain rate because the compliance of the testing machine is not considered. An explanation is given in Annex F.

10.3.3 Strain rate for the determination of the lower yield strength, R_{eL}, and percentage yield point extension, A_e

Following the detection of the upper yield strength (see A.4.2), the estimated strain rate over the parallel length, $\dot{e}_{L_c}$, shall be maintained in one of the following two specified ranges (see Figure 9) until discontinuous yielding has ended.

Range 2: $\dot{e}_{L_c} = 0,000\,25\ s^{-1}$, with a relative tolerance of $\pm20\ \%$ (recommended, when R_{eL} is determined)

Range 3: $\dot{e}_{L_c} = 0,002\ s^{-1}$, with a relative tolerance of $\pm20\ \%$

10.3.4 Strain rate for the determination of the tensile strength, R_m, percentage elongation after fracture, A, percentage total extension at the maximum force, A_{gt}, percentage plastic extension at maximum force, A_g, and percentage reduction area, Z

After determination of the required yield/proof strength properties, the estimated strain rate over the parallel length, $\dot{e}_{L_c}$, shall be changed to one of the following specified ranges (see Figure 9).

Range 2: $\dot{e}_{L_c} = 0,000\,25\ s^{-1}$, with a relative tolerance of $\pm20\ \%$

Range 3: $\dot{e}_{L_c} = 0,002\ s^{-1}$, with a relative tolerance of $\pm20\ \%$

Range 4: $\dot{e}_{L_c} = 0,006\,7\ s^{-1}$, with a relative tolerance of $\pm20\ \%$ ($0,4\ min^{-1}$, with a relative tolerance of $\pm20\ \%$) (recommended unless otherwise specified)

If the purpose of the tensile test is only to determine the tensile strength, then an estimated strain rate over the parallel length of the test piece according to range 3 or 4 may be applied throughout the entire test.

10.4 Testing rate based on stress rate (method B)

10.4.1 General

The testing rates shall conform to the following requirements depending on the nature of the material. Unless otherwise specified, any convenient speed of testing may be used up to a stress equivalent to half of the specified yield strength. The testing rates above this point are specified below.

10.4.2 Yield and proof strengths

10.4.2.1 Upper yield strength, R_{eH}

The rate of separation of the crossheads of the machine shall be kept as constant as possible and within the limits corresponding to the stress rates in Table 3.

NOTE   For information, typical materials having a modulus of elasticity smaller than 150 000 MPa include magnesium, aluminium alloys, brass, and titanium. Typical materials with a modulus of elasticity greater than 150 000 MPa include wrought iron, steel, tungsten, and nickel-based alloys.

Table 3 — Stress rate

Modulus of elasticity of the material E MPa	Stress rate $\dot{R}$ MPa s^{-1}	
	min.	max.
< 150 000	2	20
≥ 150 000	6	60

10.4.2.2 Lower yield strength, R_{eL}

If only the lower yield strength is being determined, the strain rate during yield of the parallel length of the test piece shall be between 0,000 25 s^{-1} and 0,002 5 s^{-1}. The strain rate within the parallel length shall be kept as constant as possible. If this rate cannot be regulated directly, it shall be fixed by regulating the stress rate just before yield begins, the controls of the machine not being further adjusted until completion of yield.

In no case shall the stress rate in the elastic range exceed the maximum rates given in Table 3.

10.4.2.3 Upper and lower yield strengths, R_{eH} and R_{eL}

If both upper and lower yield strengths are determined during the same test, the conditions for determining the lower yield strength shall be complied with (see 10.4.2.2).

10.4.2.4 Proof strength (plastic extension) and proof strength (total extension), R_p and R_t

The rate of separation of the crossheads of the machine shall be kept as constant as possible and within the limits corresponding to the stress rates in Table 3 within the elastic range.

Within the plastic range and up to the proof strength (plastic extension or total extension), the strain rate shall not exceed 0,002 5 s^{-1}.

10.4.2.5 Rate of separation

If the testing machine is not capable of measuring or controlling the strain rate, a crosshead separation rate equivalent to the stress rate given in Table 3 shall be used until completion of yield.

10.4.2.6 Tensile strength, R_m, percentage elongation after fracture, A, percentage total extension at the maximum force, A_{gt}, percentage plastic extension at maximum force, A_g, and percentage reduction area, Z

After determination of the required yield/proof strength properties, the test rate may be increased to a strain rate (or equivalent crosshead separation rate) no greater than 0,008 s^{-1}.

If only the tensile strength of the material is to be measured, a single strain rate can be used throughout the test which shall not exceed 0,008 s^{-1}.

10.5 Choice of the method and rates

Unless otherwise agreed, the choice of method (A or B) and test rates are at the discretion of the producer or the test laboratory assigned by the producer, provided that these meet the requirements of this part of ISO 6892.

10.6 Documentation of the chosen testing conditions

In order to report the test control mode and testing rates in an abridged form, the following system of abbreviation can be used:

ISO 6892 Annn, or ISO 6892 Bn

where 'A' defines the use of method A (strain rate control), and 'B' the use of method B (stress rate based). The symbols 'nnn' are a series of up to 3 characters that refer to the rates used during each phase of the test, as defined in Figure 9, and 'n' may be added to indicate the stress rate (in MPa s^{-1}) selected during elastic loading.

EXAMPLE 1   ISO 6892-1:2009 A224 defines a test based on strain rate control, using ranges 2, 2 and 4.

EXAMPLE 2   ISO 6892-1:2009 B30 defines a test based on stress rate, performed at a nominal stress rate of 30 MPa s^{-1}.

EXAMPLE 3   ISO 6892-1:2009 B defines a test based on stress rate, performed at a nominal stress rate according to Table 3.

11 Determination of the upper yield strength

R_{eH} may be determined from the force-extension curve or peak load indicator and is defined as the maximum value of stress prior to the first decrease in force. The latter is obtained by dividing this force by the original cross-sectional area of the test piece, S_o (see Figure 2).

12 Determination of the lower yield strength

R_{eL} is determined from the force-extension curve and is defined as the lowest value of stress during plastic yielding, ignoring any initial transient effects. The latter is obtained by dividing this force by the original cross-sectional area of the test piece, S_o (see Figure 2).

For productivity of testing, R_{eL} may be reported as the lowest stress within the first 0,25 % strain after R_{eH}, not taking into account any initial transient effect. After determining R_{eL} by this procedure, the test rate may be increased as per 10.3.4. Use of this shorter procedure should be recorded on the test report.

NOTE   This clause only applies to materials having yield phenomena and when A_e is not to be determined.

13 Determination of proof strength, plastic extension

13.1 R_p is determined from the force-extension curve by drawing a line parallel to the linear portion of the curve and at a distance from it equivalent to the prescribed plastic percentage extension, e.g. 0,2 %. The point at which this line intersects the curve gives the force corresponding to the desired proof strength plastic extension. The latter is obtained by dividing this force by the original cross-sectional area of the test piece, S_o (see Figure 3).

If the straight portion of the force-extension curve is not clearly defined, thereby preventing drawing the parallel line with sufficient precision, the following procedure is recommended (see Figure 6).

When the presumed proof strength has been exceeded, the force is reduced to a value equal to about 10 % of the force obtained. The force is then increased again until it exceeds the value obtained originally. To determine the desired proof strength, a line is drawn through the hysteresis loop. A line is then drawn parallel to this line, at a distance from the corrected origin of the curve, measured along the abscissa, equal to the prescribed plastic percentage extension. The intersection of this parallel line and the force-extension curve gives the force corresponding to the proof strength. The latter is obtained by dividing this force by the original cross-sectional area of the test piece, S_o (see Figure 6).

NOTE 1   Several methods can be used to define the corrected origin of the force-extension curve. One of these is to construct a line parallel to that determined by the hysteresis loop so that it is tangential to the force-extension curve. The point where this line crosses the abscissa is the corrected origin of the force-extension curve (see Figure 6).

NOTE 2   The plastic strain at the starting point of force reduction is only slightly higher than the specified plastic extension of R_p. Starting points at much higher strain values reduce the slope of the line through the hysteresis loop.

NOTE 3   If not specified in product standards or agreed by the customer, it is inappropriate to determine proof strength during and after discontinuous yielding.

13.2 The property may be obtained without plotting the force-extension curve by using automatic devices (microprocessor, etc.), see Annex A.

NOTE   Another available method is described in GB/T 228[12].

14 Determination of proof strength, total extension

14.1 R_t is determined on the force-extension curve, taking 10.2 into consideration, by drawing a line parallel to the ordinate axis (force axis) and at a distance from this equivalent to the prescribed total percentage extension. The point at which this line intersects the curve gives the force corresponding to the desired proof strength. The latter is obtained by dividing this force by the original cross-sectional area of the test piece, S_o (see Figure 4).

14.2 The property may be obtained without plotting the force-extension curve by using automatic devices (see Annex A).

15 Method of verification of permanent set strength

The test piece is subjected to a force corresponding to the specified stress for 10 s to 12 s. This force is obtained by multiplying the specified stress by the original cross-sectional area of the test piece, S_o. After removing the force, it is then confirmed that the permanent set extension or elongation is not more than the percentage specified for the original gauge length, see Figure 5.

NOTE   This is a pass/fail test, which is not normally performed as a part of the standard tensile test. The stress applied to the test piece and the permissible permanent set extension or elongation are specified either by the product specification or the requester of the test. Example: Reporting "$R_{r0,5}$ = 750 MPa Pass" indicates that a stress of 750 MPa was applied to the test piece and the resulting permanent set was less than or equal to 0,5 %.

16 Determination of the percentage yield point extension

For materials that exhibit discontinuous yielding, A_e is determined from the force-extension curve by subtracting the extension at R_{eH} from the extension at the start of uniform workhardening. The extension at the start of uniform workhardening is defined by the intersection of a horizontal line through the last local minimum point, or a regression line through the range of yielding, prior to uniform workhardening and a line corresponding to the highest slope of the curve occurring at the start of uniform workhardening (see Figure 7). It is expressed as a percentage of the extensometer gauge length, L_e.

The method used [see Figure 7 a) or b)] should be documented in the test report.

17 Determination of the percentage plastic extension at maximum force

The method consists of determining the extension at maximum force on the force-extension curve obtained with an extensometer and subtracting the elastic strain.

Calculate the percentage plastic extension at maximum force, A_g, from Equation (2):

$$A_g = \left(\frac{\Delta L_m}{L_e} - \frac{R_m}{m_E} \right) \times 100 \tag{2}$$

where

L_e is the extensometer gauge length;

m_E is the slope of the elastic part of the stress-percentage extension curve;

R_m is the tensile strength;

ΔL_m is the extension at maximum force.

NOTE   For materials which exhibit a plateau at maximum force, the percentage plastic extension at maximum force is the extension at the mid-point of the plateau, see Figure 1.

18 Determination of the percentage total extension at maximum force

The method consists of determining the extension at maximum force on the force-extension curve obtained with an extensometer.

Calculate the percentage total extension at maximum force, A_{gt}, from Equation (3):

$$A_{gt} = \frac{\Delta L_m}{L_e} \times 100 \tag{3}$$

where

L_e is the extensometer gauge length;

ΔL_m is the extension at maximum force.

NOTE   For materials which exhibit a plateau at maximum force, the percentage total extension at maximum force is the extension at the mid-point of the plateau, see Figure 1.

19 Determination of the percentage total extension at fracture

The method consists of determining the extension at fracture on the force-extension curve obtained with an extensometer.

Calculate the percentage total elongation at fracture, A_t, from Equation (4):

$$A_t = \frac{\Delta L_f}{L_e} \times 100 \tag{4}$$

where

L_e is the extensometer gauge length;

ΔL_f is the extension at fracture.

20 Determination of percentage elongation after fracture

20.1 Percentage elongation after fracture shall be determined in accordance with the definition given in 3.4.2.

For this purpose, the two broken pieces of the test piece shall be carefully fitted back together so that their axes lie in a straight line.

Special precautions shall be taken to ensure proper contact between the broken parts of the test piece when measuring the final gauge length. This is particularly important for test pieces of small cross-section and test pieces having low elongation values.

Calculate the percentage elongation after fracture, A, from Equation (5):

$$A = \frac{L_u - L_o}{L_o} \times 100 \qquad (5)$$

where

L_o is the original gauge length;

L_u is the final gauge length after fracture.

Elongation after fracture, $L_u - L_o$, shall be determined to the nearest 0,25 mm or better using a measuring device with sufficient resolution.

If the specified minimum percentage elongation is less than 5 %, it is recommended that special precautions be taken (see Annex G). The result of this determination is valid only if the distance between the fracture and the nearest gauge mark is not less than $L_o/3$. However, the measurement is valid, irrespective of the position of the fracture, if the percentage elongation after fracture is equal to or greater than the specified value.

20.2 When extension at fracture is measured using an extensometer, it is not necessary to mark the gauge lengths. The elongation is measured as the total extension at fracture, and it is therefore necessary to deduct the elastic extension in order to obtain percentage elongation after fracture. To obtain comparable values with the manual method, additional adjustments can be applied (e.g. high enough dynamic and frequency bandwidth of the extensometer, see A.3.2).

The result of this determination is valid only if fracture and localized extension (necking) occurs within the extensometer gauge length, L_e. The measurement is valid regardless of the position of the fracture cross-section if the percentage elongation after fracture is equal to or greater than the specified value.

If the product standard specifies the determination of percentage elongation after fracture for a given gauge length, the extensometer gauge length should be equal to this length.

20.3 If elongation is measured over a given fixed length, it can be converted to proportional gauge length, using conversion formulae or tables as agreed before the commencement of testing (e.g. as in ISO 2566-1 and ISO 2566-2).

NOTE   Comparisons of percentage elongation are possible only when the gauge length or extensometer gauge length, the shape and area of the cross-section are the same or when the coefficient of proportionality, k, is the same.

21 Determination of percentage reduction of area

Percentage reduction of area shall be determined in accordance with the definition given in 3.8.

If necessary, the two broken pieces of the test piece shall be carefully fitted back together so that their axes lie in a straight line.

Calculate the percentage reduction of area, Z, from Equation (6):

$$Z = \frac{S_o - S_u}{S_o} \times 100 \qquad (6)$$

where

S_o is the original cross-sectional area of the parallel length;

S_u is the minimum cross-sectional area after fracture.

Measure S_u to an accuracy of $\pm 2\,\%$ (see Figure 13).

NOTE   Measuring S_u with an accuracy of $\pm 2\,\%$ on small diameter round test pieces, or test pieces with other cross-sectional geometries, may not be possible.

22 Test report

The test report shall contain at least the following information unless otherwise agreed by the parties concerned:

a)   reference to this part of ISO 6892 extended with the test condition information specified in 10.6, e.g. ISO 6892-1:2009 A224;

b)   identification of the test piece;

c)   specified material, if known;

d)   type of test piece;

e)   location and direction of sampling of test pieces, if known;

f)   testing control mode(s) and testing rate(s) or testing rate range(s) (see 10.6) if different from the recommended methods and values given in 10.3 and 10.4;

g)   test results.

Results should be rounded to the following precisions or better, if not otherwise specified in product standards:

—   strength values, in megapascals, to the nearest whole number;

—   percentage yield point extension values, A_e, to the nearest 0,1 %;

—   all other percentage extension and elongation values to the nearest 0,5 %;

—   percentage reduction of area, Z, to the nearest 1 %.

23 Measurement uncertainty

23.1 General

Measurement uncertainty analysis is useful for identifying major sources of inconsistencies of measured results.

Product standards and material property databases based on this part of ISO 6892 and earlier editions of ISO 6892 have an inherent contribution from measurement uncertainty. It is therefore inappropriate to apply further adjustments for measurement uncertainty and thereby risk failing product which is compliant. For this

reason, the estimates of uncertainty derived by following this procedure are for information only, unless specifically instructed otherwise by the customer.

23.2 Test conditions

The test conditions and limits defined in this part of ISO 6892 shall not be adjusted to take account of uncertainties of measurement, unless specifically instructed otherwise by the customer.

23.3 Test results

The estimated measurement uncertainties shall not be combined with measured results to assess compliance to product specifications, unless specifically instructed otherwise by the customer.

For consideration of uncertainty, see Annexes J and K, which provide guidance for the determination of uncertainty related to metrological parameters and values obtained from the interlaboratory tests on a group of steels and aluminium alloys.
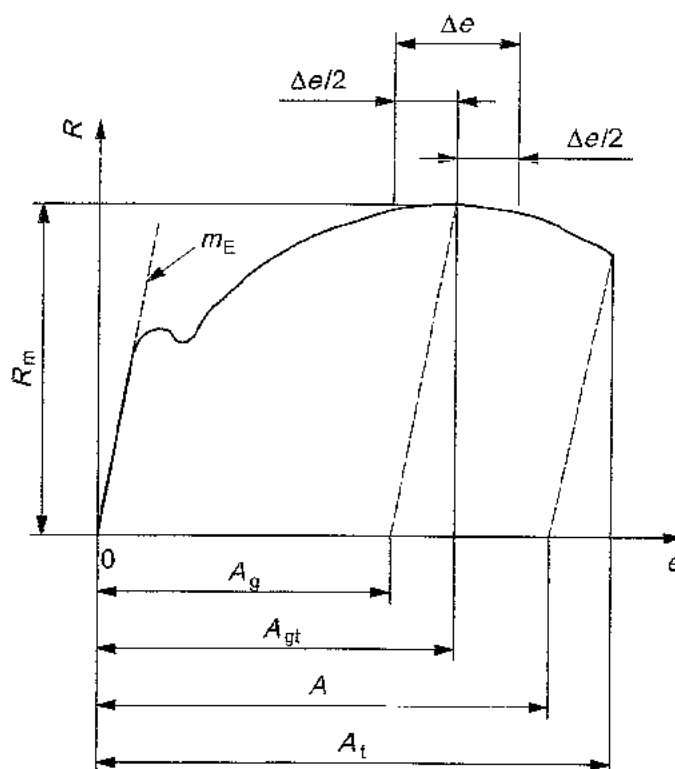
Key

A percentage elongation after fracture [determined from the extensometer signal or directly from the test piece (see 20.1)]

A_g percentage plastic extension at maximum force

A_{gt} percentage total extension at maximum force

A_t percentage total extension at maximum fracture

e percentage extension

m_E slope of the elastic part of the stress-percentage extension curve

R stress

R_m tensile strength

Δe plateau extent (for determination of A_g, see Clause 17, for determination of A_{gt}, see Clause 18)
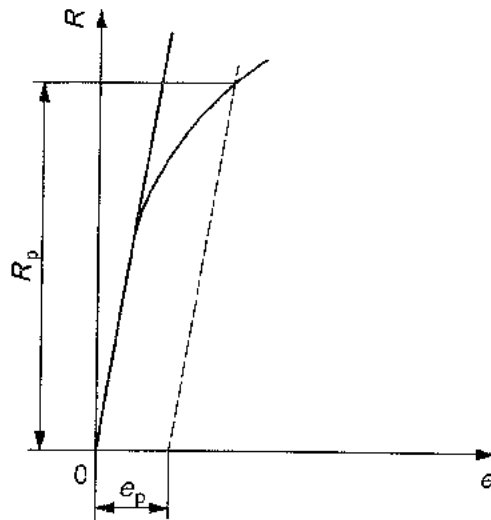
Figure 1 — Definitions of extension

20

Key
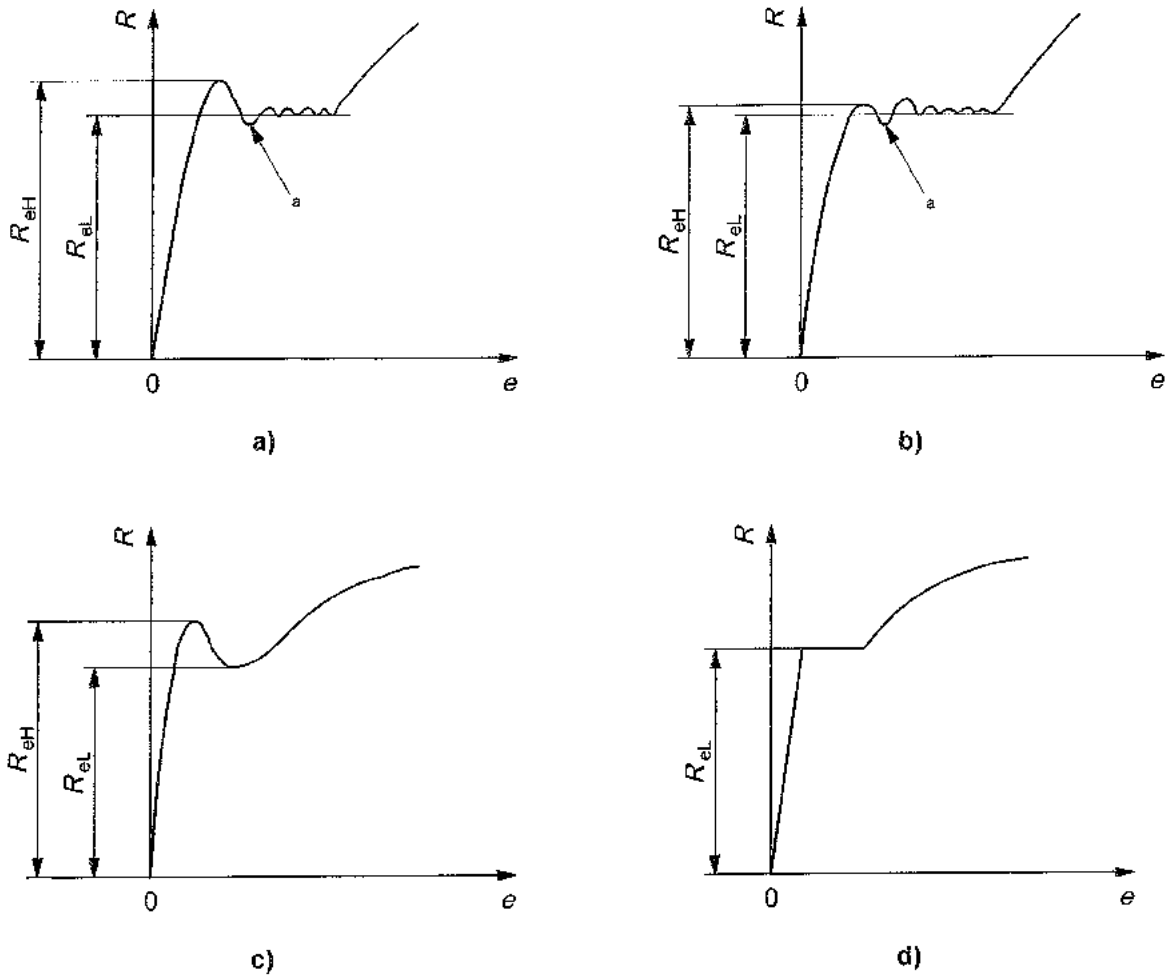
e percentage extension

R stress

R_{eH} upper yield strength

R_{eL} lower yield strength

[a]   Initial transient effect.

Figure 2 — Examples of upper and lower yield strengths for different types of curve

Key

e percentage extension

e_p specified percentage plastic extension

R stress

R_p proof strength, plastic extension

Figure 3 — Proof strength, plastic extension, R_p (see 13.1)

Key
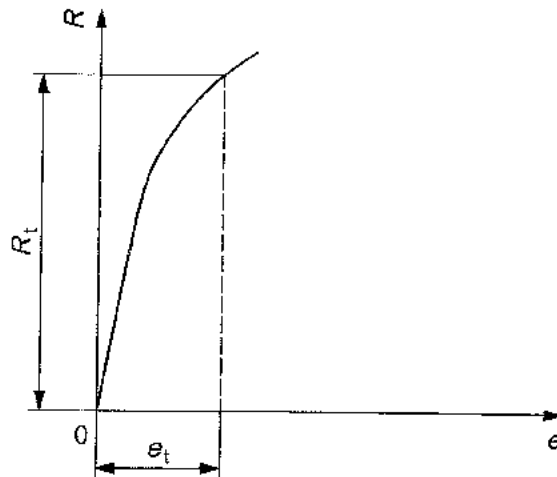
e percentage extension

e_t percentage total extension

R stress

R_t proof strength, total extension

Figure 4 — Proof strength, total extension, R_t

Key

e percentage elongation or percentage extension

e_r percentage permanent set extension or elongation

R stress

R_r specified permanent set strength

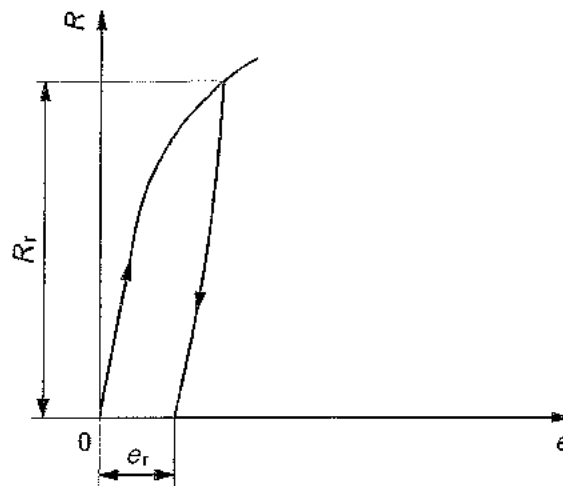**Figure 5 — Permanent set strength, R_r**
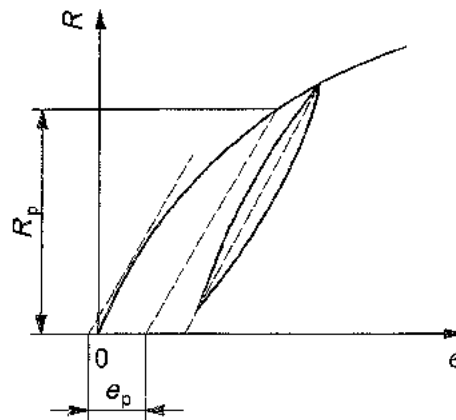
Key

e percentage extension

e_p specified percentage plastic extension

R stress

R_p proof strength, plastic extension

Figure 6 — Proof strength, plastic extension, R_p, alternative procedure (see 13.1)

a) Horizontal line method   b) Regression method
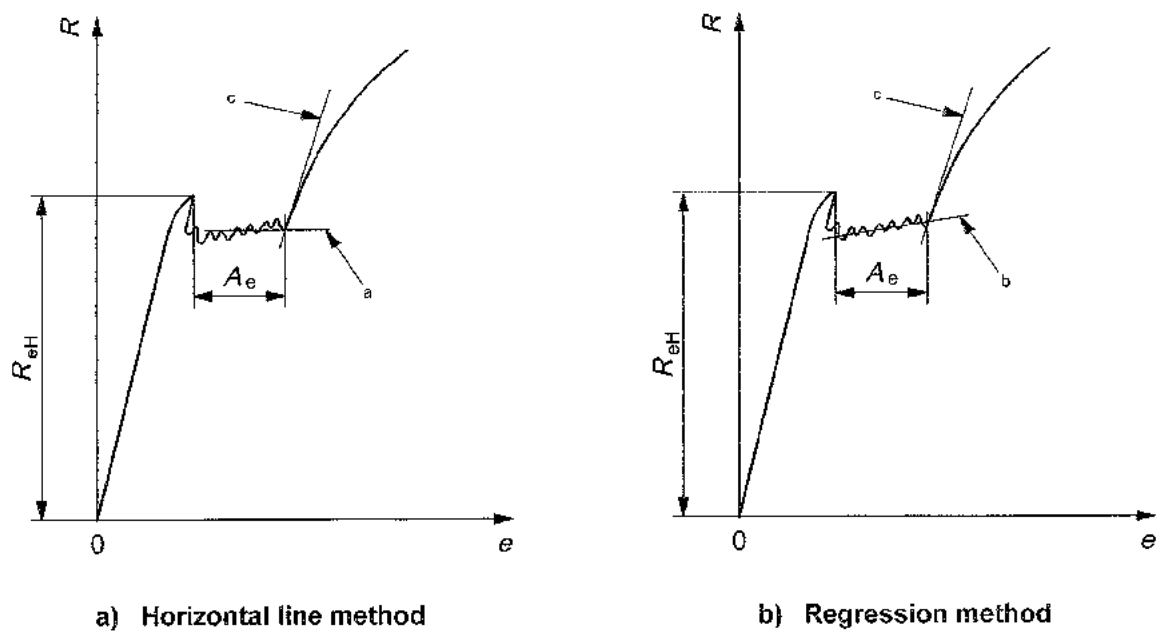
Key

A_e percentage yield point extension

e percentage extension

R stress

R_{eH} upper yield strength

a   Horizontal line through the last local minimum point, prior to uniform workhardening.

b   Regression line through the range of yielding, prior to uniform workhardening.

c   Line corresponding to the highest slope of the curve occurring at the start of uniform workhardening.

Figure 7 — Different evaluation methods for percentage yield point extension, A_e

a) $R_{eH} < R_m$

b) $R_{eH} > R_m$

c) Special case of stress-percentage extension behaviour [a]

Key
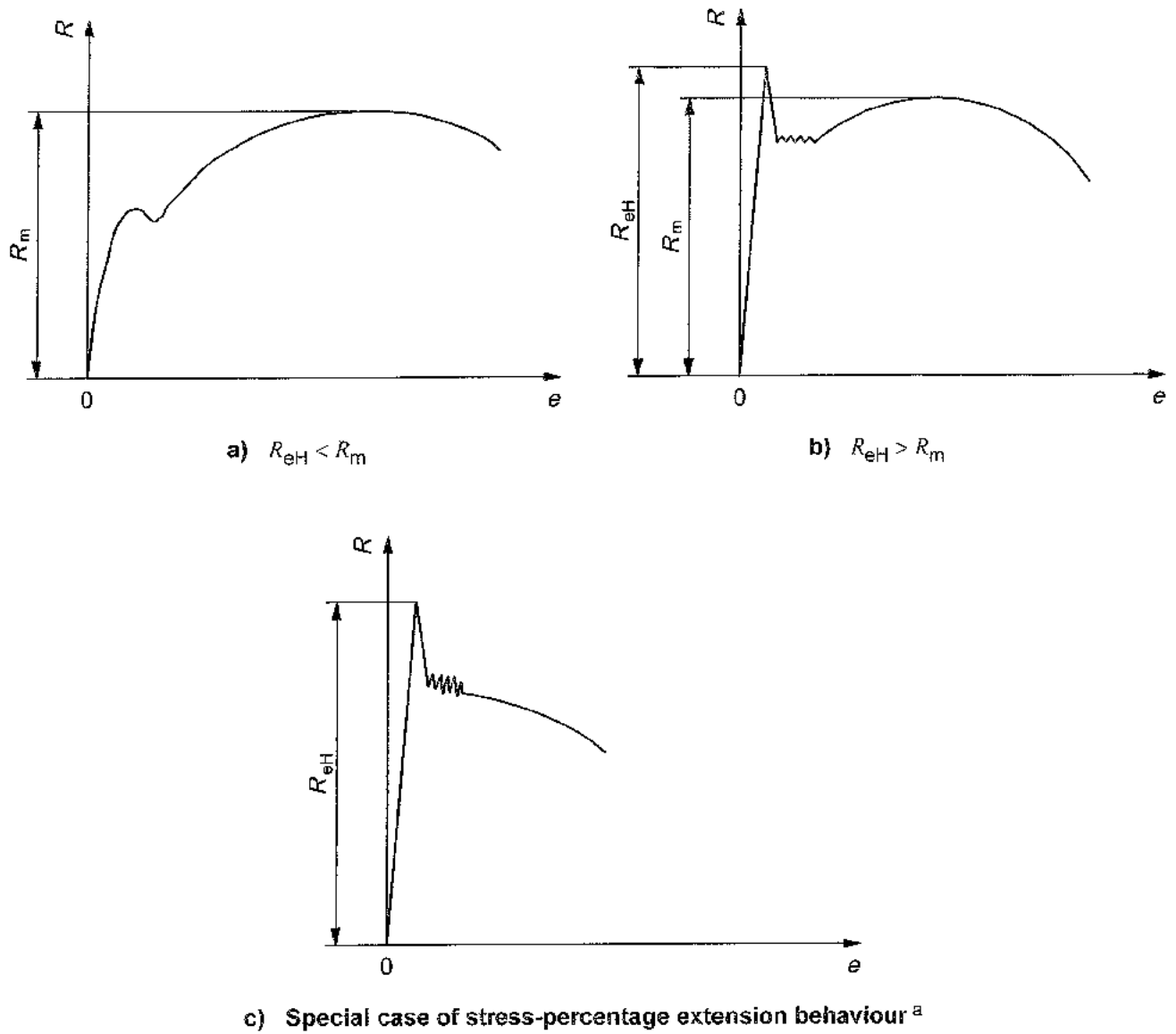
e percentage extension

R stress

R_{eH} upper yield strength

R_m tensile strength

[a]   For materials which display this behaviour, no tensile strength is defined according to this part of ISO 6892. If necessary, separate agreements can be made between the parties concerned.

Figure 8 — Different types of stress-extension curve for determination of tensile strength, R_m

a) Method A

b) Method B

Key

$\dot{e}$ strain rate

$\dot{R}$ stress rate

t time progress of the tensile test

t_c crosshead control time

t_{ec} extensometer control time or crosshead control time
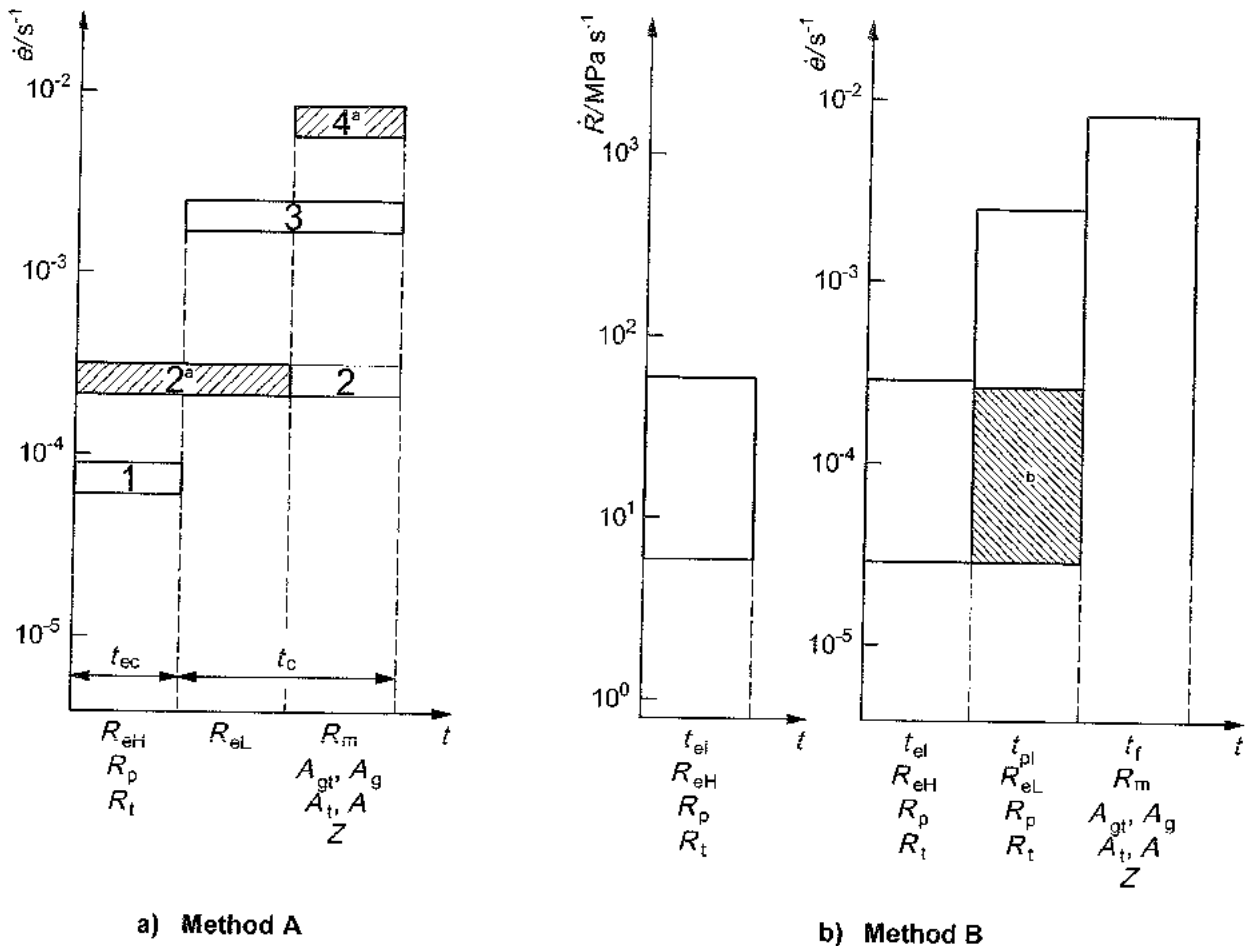
t_{el} time range (elastic behaviour) for determination of the parameters listed (see Table 1 for designations)

t_f time range (usually up to fracture) for determination of the parameters listed (see Table 1 for designations)

t_{pl} time range (plastic behaviour) for determination of the parameters listed (see Table 1 for designations)

1   range 1: $\dot{e} = 0{,}000\,07\ \text{s}^{-1}$, with a relative tolerance of $\pm 20\ \%$

2   range 2: $\dot{e} = 0{,}000\,25\ \text{s}^{-1}$, with a relative tolerance of $\pm 20\ \%$

3   range 3: $\dot{e} = 0{,}002\ \text{s}^{-1}$, with a relative tolerance of $\pm 20\ \%$

4   range 4: $\dot{e} = 0{,}006\,7\ \text{s}^{-1}$, with a relative tolerance of $\pm 20\ \%$ ($0{,}4\ \text{min}^{-1}$, with a relative tolerance of $\pm 20\ \%$)

a   Recommended.

b   Expanded range to lower rates, if testing machine is not capable of measuring or controlling the strain rate (see 10.4.2.5).

NOTE   Strain rate in the elastic range for method B is calculated from stress rate using a Young modulus of 210 000 MPa (steel).

Figure 9 — Illustration of strain rates to be used during the tensile test,
if R_{eH}, R_{eL}, R_p, R_t, R_m, A_g, A_{gt}, A, A_t and Z are determined

Key
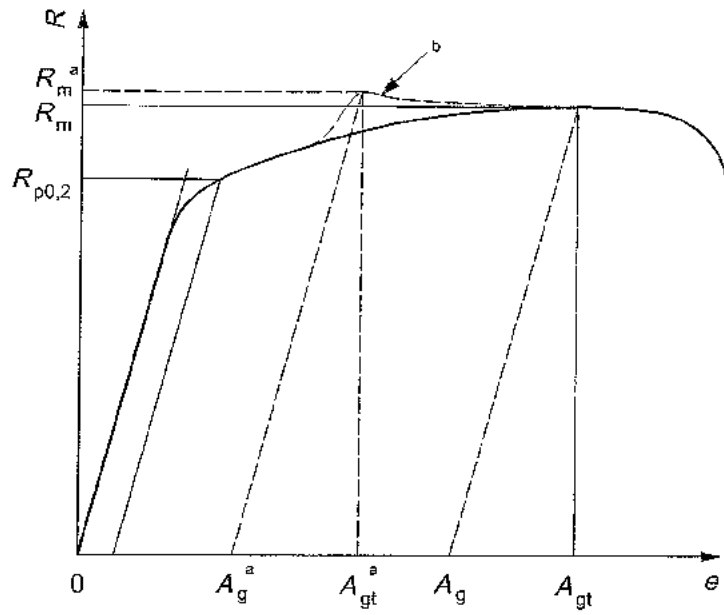
e percentage extension
R stress

[a]   False values, resulting from an abrupt strain rate increase.
[b]   Stress-strain behaviour, if strain rate is abruptly increased.

NOTE   For parameter definitions, see Table 1.

Figure 10 — Illustration of an inadmissible discontinuity in the stress-strain curve
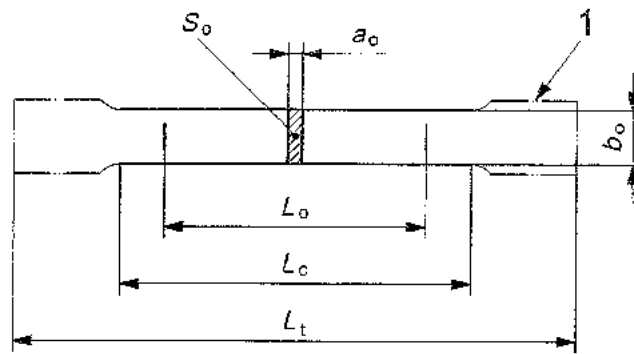
a) Before testing
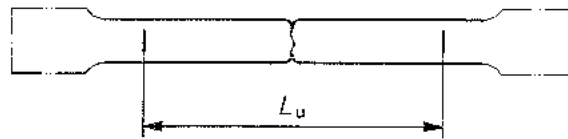
b) After testing

Key

a_0 original thickness of a flat test piece or wall thickness of a tube

b_0 original width of the parallel length of a flat test piece

L_c parallel length

L_0 original gauge length

L_t total length of test piece

L_u final gauge length after fracture

S_0 original cross-sectional area of the parallel length

1   gripped ends

NOTE   The shape of the test-piece heads is only given as a guide.

Figure 11 — Machined test pieces of rectangular cross-section (see Annexes B and D)
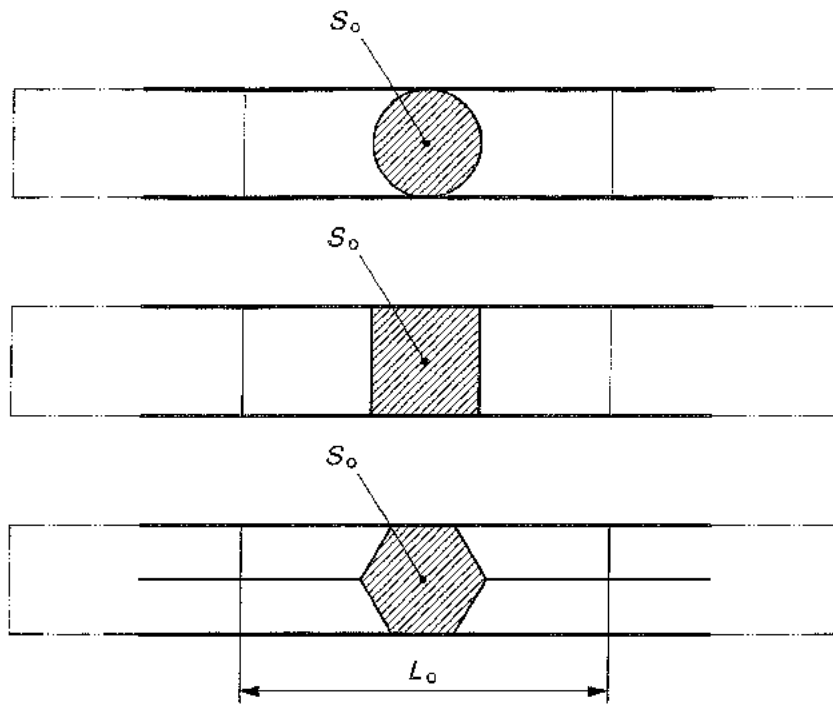
Key

L_o original gauge length

S_o original cross-sectional area

Figure 12 — Test pieces comprising an unmachined portion of the product (see Annex C)
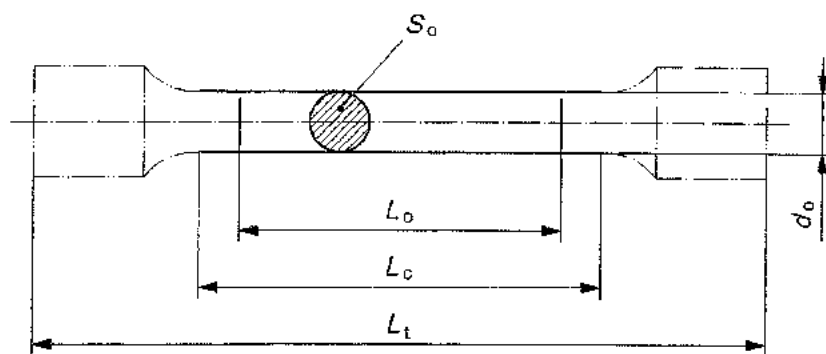
a) **Before testing**
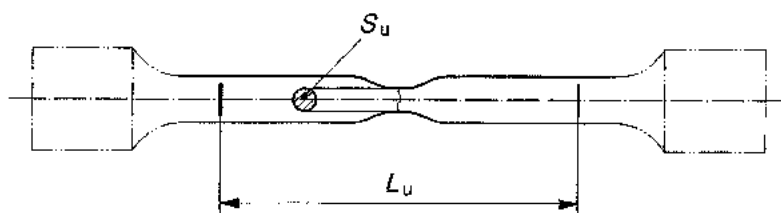
b) **After testing**

Key

d_0 original diameter of the parallel length of a circular test piece

L_c parallel length

L_0 original gauge length

L_t total length of test piece

L_u final gauge length after fracture

S_0 original cross-sectional area of the parallel length

S_u minimum cross-sectional area after fracture

NOTE   The shape of the test-piece heads is only given as a guide.

Figure 13 — Machined test pieces of round cross-section (see Annex D)

a) Before testing

b) After testing

Key

a_0 original wall thickness of a tube

D_0 original external diameter of a tube

L_0 original gauge length

L_t total length of test piece

L_u final gauge length after fracture

S_0 original cross-sectional area of the parallel length

S_u minimum cross-sectional area after fracture

1   gripped ends

Figure 14 — Test pieces comprising a length of tube (see Annex E)

a) Before testing

b) After testing

Key

a_o original wall thickness of a tube

b_o original average width of the longitudinal strip taken from a tube

L_c parallel length

L_o original gauge length

L_t total length of test piece

L_u final gauge length after fracture

S_o original cross-sectional area of the parallel length

S_u minimum cross-sectional area after fracture

1   gripped ends

NOTE   The shape of the test-piece heads is only given as a guide.

Figure 15 — Test piece cut from a tube (see Annex E)

Annex B
(normative)

Types of test pieces to be used for thin products: sheets, strips and flats between 0,1 mm and 3 mm thick

NOTE   For products of less than 0,5 mm thickness, special precautions may be necessary.

B.1 Shape of the test piece

Generally, the test piece has gripped ends which are wider than the parallel length. The parallel length, L_c, shall be connected to the ends by means of transition curves with a radius of at least 20 mm. The width of these ends should be $\geqslant 1,2b_0$, where b_0 is the original width.

By agreement, the test piece may also consist of a strip with parallel sides (parallel sided test piece). For products of width equal to or less than 20 mm, the width of the test piece may be the same as that of the product.

B.2 Dimensions of the test piece

Three different non-proportional test piece geometries are widely used (see Table B.1).

The parallel length shall not be less than $L_0 + b_0/2$.

In case of dispute, the length $L_0 + 2b_0$ should be used, unless there is insufficient material.

For parallel side test pieces less than 20 mm wide, and unless otherwise specified in the product standard, the original gauge length, L_0, shall be equal to 50 mm. For this type of test piece, the free length between the grips shall be equal to $L_0 + 3b_0$.

When measuring the dimensions of each test piece, the tolerances on shape given in Table B.2 shall apply.

For test pieces where the width is the same as that of the product, the original cross-sectional area, S_0, shall be calculated on the basis of the measured dimensions of the test piece.

The nominal width of the test piece may be used, provided that the machining tolerances and tolerances on shape given in Table B.2 have been complied with, to avoid measuring the width of the test piece at the time of the test.

Table B.1 — Dimensions of test pieces

Dimensions in millimetres

Test piece type	Width b_0	Original gauge length L_0	Parallel length L_c		Free length between the grips for parallel sided test piece
			Minimum	Recommended	
1	12,5 ± 1	50	57	75	87,5
2	20 ± 1	80	90	120	140
3	25 ± 1	50 [a]	60 [a]	—	Not defined

[a] The ratio L_0/b_0 and L_c/b_0 of a type 3 test piece in comparison to one of types 1 and 2 is very low. As a result the properties, especially the elongation after fracture (absolute value and scatter range), measured with this test piece will be different from the other test piece types.

Table B.2 — Tolerances on the width of the test piece

Dimensions and tolerances in millimetres

Nominal width of the test piece	Machining tolerance [a]	Tolerance on shape [b]
12,5	± 0,05	0,06
20	± 0,10	0,12
25	± 0,10	0,12

[a] These tolerances are applicable if the nominal value of the original cross-sectional area, S_0, is to be included in the calculation without having to measure it.

[b] Maximum deviation between the measurements of the width along the entire parallel length, L_c, of the test piece.

B.3 Preparation of test pieces

The test pieces shall be prepared so as not to affect the properties of the sample. Any areas which have been hardened by shearing or pressing shall be removed by machining.

These test pieces are predominantly prepared from sheet or strip. If possible, the as-rolled surfaces should not be removed.

NOTE   The preparation of these test pieces by punching can result in significant changes to the material properties, especially the yield/proof strength (due to workhardening). Materials which exhibit high workhardening should, generally, be prepared by milling, grinding etc.

For very thin materials, it is recommended that strips of identical widths should be cut and assembled into a bundle with intermediate layers of a paper which is resistant to the cutting oil. Each small bundle of strips should then be assembled with a thicker strip on each side, before machining to the final dimensions of the test piece.

The tolerance given in Table B.2, e.g. ± 0,05 mm for a nominal width of 12,5 mm, means that no test piece shall have a width outside the two values given below, if the nominal value of the original cross-sectional area, S_0, is to be included in the calculation without having to measure it:

12,5 mm + 0,05 mm = 12,55 mm

12,5 mm – 0,05 mm = 12,45 mm

B.4 Determination of the original cross-sectional area

S_o shall be calculated from measurements of the dimensions of the test piece.

The error in determining the original cross-sectional area shall not exceed ± 2 %. As the greatest part of this error normally results from the measurement of the thickness of the test piece, the error in measurement of the width shall not exceed ± 0,2 %.

In order to achieve test results with a reduced measurement uncertainty it is recommended that the original cross-sectional area be determined with an accuracy of ± 1 % or better. For thin materials special measurement techniques may be required.

Annex D
(normative)

Types of test pieces to be used for sheets and flats of thickness equal to or greater than 3 mm, and wire, bars and sections of diameter or thickness equal to or greater than 4 mm

D.1 Shape of the test piece

Usually, the test piece is machined and the parallel length shall be connected by means of transition radii to the gripped ends which may be of any suitable shape for the grips of the testing machine (see Figure 13). The minimum transition radius between the gripped ends and the parallel length shall be:

a) $0,75d_0$, where d_0 is the diameter of the parallel length, for the cylindrical test pieces;

b) 12 mm for other test pieces.

Sections, bars, etc., may be tested unmachined, if required.

The cross-section of the test piece may be circular, square, rectangular or, in special cases, of another shape.

For test pieces with a rectangular cross-section, it is recommended that the width to thickness ratio should not exceed 8:1.

In general, the diameter of the parallel length of machined cylindrical test pieces shall be not less than 3 mm.

D.2 Dimensions of the test piece

D.2.1 Parallel length of machined test piece

The parallel length, L_c, shall be at least equal to:

a) $L_0 + (d_0/2)$ for cylindrical test pieces;

b) $L_0 + 1,5\sqrt{S_0}$ for other test pieces.

In cases of dispute, the length $L_0 + 2d_0$ or $L_0 + 2\sqrt{S_0}$ shall be used depending on the type of test piece, unless there is insufficient material.

D.2.2 Length of unmachined test piece

The free length between the grips of the machine shall be adequate for the gauge marks to be at least a distance of $\sqrt{S_0}$ from the grips.

D.2.3 Original gauge length

D.2.3.1 Proportional test pieces

As a general rule, proportional test pieces are used where L_o is related to the original cross-sectional area, S_o, by Equation (D.1):

$$L_o = k\sqrt{S_o}$$

(D.1)

where k is equal to 5,65.

Alternatively 11,3 may be used as the k value.

Test pieces of circular cross-section should preferably have one set of dimensions given in Table D.1.

Table D.1 — Circular cross-section test pieces

Coefficient of proportionality k	Diameter d mm	Original gauge length $L_o = k\sqrt{S_o}$ mm	Minimum parallel length L_c mm
5,65	20	100	110
	14	70	77
	10	50	55
	5	25	28

D.2.3.2 Non-proportional test pieces

Non-proportional test pieces may be used if specified by the product standard.

The parallel length, L_c, should not be less than $L_o + b_o/2$. In case of dispute, the parallel length $L_c = L_o + 2b_o$ shall be used unless there is insufficient material.

Table D.2 gives details of some typical test piece dimensions.

Table D.2 — Typical flat test piece dimensions

Dimensions in millimetres

Width b_o	Original gauge length L_o	Minimum parallel length L_c	Approximately total length L_t
40	200	220	450
25	200	215	450
20	80	90	300
10	40	45	150

D.3 Preparation of test pieces

D.3.1 General

The tolerances on the transverse dimensions of machined test pieces are given in Table D.3.

An example of the application of these tolerances is given in D.3.2 and D.3.3.

D.3.2 Machining tolerances

The value given in Table D.3, e.g. ± 0,03 mm for a nominal diameter of 10 mm, means that no test piece shall have a diameter outside the two values given below, if the nominal value of the original cross-sectional area, S_o, is to be included in the calculation without having to measure it:

10 mm + 0,03 mm = 10,03 mm

10 mm − 0,03 mm = 9,97 mm

D.3.3 Tolerances on shape

The value given in Table D.3 means that, for a test piece with a nominal diameter of 10 mm which satisfies the machining conditions given above, the deviation between the smallest and largest diameters measured shall not exceed 0,04 mm.

Consequently, if the minimum diameter of this test piece is 9,99 mm, its maximum diameter shall not exceed 9,99 mm + 0,04 mm = 10,03 mm.

Table D.3 — Tolerances relating to the transverse dimensions of test pieces

Dimensions and tolerances in millimetres

Designation	Nominal transverse dimension	Machining tolerance on the nominal dimension [a]	Tolerance on shape [b]
Diameter of machined test pieces of circular cross-section and transverse dimensions of test pieces of rectangular cross-section machined on all four sides	⩾ 3 ⩽ 6	± 0,02	0,03
	> 6 ⩽ 10	± 0,03	0,04
	> 10 ⩽ 18	± 0,05	0,04
	> 18 ⩽ 30	± 0,10	0,05
Transverse dimensions of test pieces of rectangular cross-section machined on only two opposite sides	⩾ 3 ⩽ 6	± 0,02	0,03
	> 6 ⩽ 10	± 0,03	0,04
	> 10 ⩽ 18	± 0,05	0,06
	> 18 ⩽ 30	± 0,10	0,12
	> 30 ⩽ 50	± 0,15	0,15

[a] These tolerances are applicable if the nominal value of the original cross-sectional area, S_o, is to be included in the calculation without having to measure it. If these machining tolerances are not complied with, it is essential to measure every individual test piece.

[b] Maximum deviation between the measurements of a specified transverse dimension along the entire parallel length, L_c, of the test piece.

D.4 Determination of the cross-sectional area

The nominal dimensions can be used to calculate S_o for test pieces of circular cross-section and rectangular cross-section machined on all four sides that satisfy the tolerances given in Table D.3. For all other shapes of test pieces, the original cross-sectional area shall be calculated from measurements of the appropriate dimensions, with an error not exceeding $\pm$ 0,5 % on each dimension.

8.2 Appendix B

This page is intentionally left blank.

Comparison between Molybdenum Disulfide (MoS_2) & Tungsten Disulfide (WS_2)

Tungsten Disulfide (WS_2) is one of the most lubricous materials known to science. With Coefficient of Friction at 0.03, it offers excellent dry lubricity unmatched to any other substance. It can also be used in high temperature and high pressure applications. It offers temperature resistance from -450° F (-270° C) to 1200° F (650° C) in normal atmosphere and from -305° F (-188° C) to 2400° F (1316° C) in Vacuum. Load bearing property of coated film is extremely high at 300,000 psi.

Tungsten Disulfide (WS_2) can be used instead of Molybdenum Disulfide (MoS_2) and Graphite in almost all applications, and even more. Molybdenum and Tungsten are from same chemical family. Tungsten is heavier and more stable. Molybdenum Disulfide (Also known as Moly Disulfide) till now has been extremely popular due to cheaper price, easier availability and strong and innovative marketing. Tungsten Disulfide is not new chemical and has been around as long as Moly, and is used extensively by NASA, military, aerospace and automotive industry.

Till few years ago, price was Tungsten Disulfide was almost 10 times that of Molybdenum Disulfide. But since then price of Molybdenum Disulfide has doubled every six months. Now the prices of both chemicals are within comparable range. Now, it makes more economic sense to use superior dry lubricant (Tungsten Disulfide) and improve the quality and competitiveness of final product.

Tungsten Disulfide offers excellent lubrication under extreme conditions of Load, Vacuum and Temperature. The properties below show that Tungsten Disulfide offers excellent thermal stability and oxidation resistance at higher temperatures. WS_2 has thermal stability advantage of 93^oC (200^oF) over MoS_2. Coefficient of Friction of WS_2 actually reduces at higher loads.

Physical and Technical Properties

Properties	Tungsten Disulfide (WS_2) CAS No 12138-09-9	Molybdenum Disulfide (MoS_2) CAS No 1317-33-5
Colour	Silver Gray	Blue- Silver Gray
Appearance	Crystalline Solid	Crystalline Solid
Melting Point	1250° C, 1260° C (decomposes)	1185^oC decomposes
Boiling Point		450^oC
Density	7500 Kg.m^{-3}	5060 Kg.m^{-3}
Molecular Weight	248	160.08
Coefficient of Friction (COF)	0.03 Dynamic; 0.07 Static	
Thermal Stability in air	COF <0.1 till 1100^oF (594C)	COF<0.1 @600° F (316° C) increases to 0.5 @ 1100° F (594^oC)
Thermal Stability in argon	COF <0.1 till 1500° F (815° C)	COF increases rapidly starting @800° F (426° C) COF >0.1 @ 900° F (482° C)
Load bearing ability	400,000 psi for coated film COF:0.044@ 20,000 psi COF reduces to 0.024 between 200,000 to 400,000 psi	250,000 psi
Lubrication Temperature Range	Ambient: from -273° C to 650° C Vacuum(10^{-14} Torr): from -188° C to 1316° C	Ambient: from -185^oC to 350^oC Vacuum: from -185^oC to 1100^oC
Chemical Durability	Inert Substance, Non-Toxic	Inert Substance, Non-Toxic
Magnetism	Non-Magnetic	Non-Magnetic

Electrical Properties	**Has Semiconductor properties**	
Rockwell Hardness	**30 HRc**	
Coating Film Thickness	**0.5 micron**	
Corrosion Stability	**Can slow down the corrosion rate, but can not fully prevent substrate corrosion**	
Coatable Substrates	**Iron, Steel, Aluminum, Copper, other Metals, Plastics and Manmade Solids**	**Iron, Steel, Aluminum, Copper, other Metals, Plastics and Manmade Solids**
Compatibility	**Oil, Solvent, Paint, Fuel**	**Oil, Solvent, Paint, Fuel**

LOWER FRICTION

www.lowerfriction.com

M K Impex Canada

6382 Lisgar Drive
Mississauga, Ontario L5N 6X1
Canada
Phone: 416-509-4462; Fax: 905-824-1259
E-mail: sales@lowerfriction.com

8.3 Appendix C

This page is intentionally left blank.

NORSOK STANDARD

D-010

Rev. 3, August 2004

Well integrity in drilling and well operations

Foreword

The NORSOK standards are developed by the Norwegian petroleum industry to ensure adequate safety, value adding and cost effectiveness for petroleum industry developments and operations. Furthermore, NORSOK standards are as far as possible intended to replace oil company specifications and serve as references in the authorities' regulations.

The NORSOK standards are normally based on recognised international standards, adding the provisions deemed necessary to fill the broad needs of the Norwegian petroleum industry. Where relevant NORSOK standards will be used to provide the Norwegian industry input to the international standardisation process. Subject to development and publication of international standards, the relevant NORSOK standard will be withdrawn.

The NORSOK standards are developed according to the consensus principle generally applicable standards work and according to established procedures defined in NORSOK A-001.

The NORSOK standards are prepared and published with support by The Norwegian Oil Industry Association (OLF) and Federation of Norwegian Manufacturing Industries (TBL). NORSOK standards are administered and published by Standards Norway.

Introduction

This revision was initiated to make this NORSOK standard compliant with changes in legislation and adapted to evolving and new technology. In this revision, the user will find that the standard has been completely reorganised and that the content and structure is different than the previous revision. The intention has been to make it easier to find information and provide flexibility to updating or revising this NORSOK standard in the future without altering its structure. Consequently, the changes from the previous revision are not marked.

The following main changes are implemented in this revision:

- The focus of this NORSOK standard is well integrity, which is the application of technical, operational and organizational solutions to reduce the risk of uncontrolled release of formation fluids throughout the entire life cycle of the well and of course safety aspects. Recommendations for best practices are not dominant. This led to renaming this NORSOK standard to "Well integrity in drilling and well operations".
- The descriptions are mostly insensitive to type of well and type of installation.
- Clear and concise requirements (shall) and guidelines (should) have been applied to stress their importance and to differentiate the process of handling deviations from these.
- Overlapping or duplication of text or topics in other standards has been minimized.
- Well barrier related terminology with definitions has been established in lack of apparent international standard definitions.
- Pre-defined WBSs for most common situations have been included.
- A library of 50 defined WBEs with acceptance criteria has been added, which the user can apply to define a well barrier with associated standard acceptance criteria.
- Listings of situations for which well control action procedures should be in place are included.
- Underbalanced drilling and completion operations and sidetracking, plugging and abandonment activities are significantly altered.
- Production activities and pumping operations are new.

The user is encouraged to study the following "roadmap to understanding" to get a quick overview of how this NORSOK standard is structured and how to obtain the "full" overview of related requirements and guidelines:

Road Map to Understanding

| 5. Drilling activities |
| 6. Testing activities |
| 7. Completion activities |
| 8. Production activities |
| 9. Sidetracks, suspension and abandonment activities |
| 10. Wireline operations |
| 11. Coiled tubing operations |
| 12. Snubbing operations |
| 13. Under balanced drilling and completion operations |
| 14. Pumping operations |

Start

4. General principles

+

Annex A (normative)

Leak test pressures and frequency for well control equipment.

+

15. Well barrier element acceptance tables (50 tables)

+

API, ISO, NACE, NORSOK.

+

3. Definitions and abbreviations

Complete

1   Scope
This NORSOK standard focus on well integrity by defining the minimum functional and performance oriented requirements and guidelines for well design, planning and execution of well operations in Norway.

2   Normative and informative references
The following standards include provisions and guidelines which, through reference in this text, constitute provisions and guidelines of this NORSOK standard. Latest issue of the references shall be used unless otherwise agreed. Other recognized standards may be used provided it can be shown that they meet or exceed the requirements and guidelines of the standards referenced below.

2.1   Normative references

ISO 10405,	*Petroleum and natural gas industries – Care and use of casing and tubing.*
ISO 10414-1,	*Petroleum and natural gas industries – Field testing of drilling fluids – Part 1: Water-based fluids.*
ISO 10414-2,	*Petroleum and natural gas industries – Field testing of drilling fluids – Part 2: Oil-based fluids.*
ISO 10416,	*Petroleum and natural gas industries – Drilling fluids laboratory testing.*
ISO 10417,	*Petroleum and natural gas industries – Subsurface safety valve systems – Design, installation, operation and repair.*
ISO 10423,	*Petroleum and natural gas industries – Drilling and production equipment – Wellhead and Christmas tree equipment.*
ISO 10426-1,	*Petroleum and natural gas industries – Cements and materials for well cementing – Part 1: Specification.*
ISO 10432:1999,	*Petroleum and natural gas industries – Downhole equipment – Subsurface safety valve equipment.*
ISO 11960,	*Petroleum and natural gas industries – Steel pipes for use as casing or tubing for wells.*
ISO 11961,	*Petroleum and natural gas industries – Steel pipes for use as drill pipe – Specification.*
ISO 13533,	*Petroleum and natural gas industries – Drilling and production equipment – Drill-through equipment.*
ISO 13628-4,	*Petroleum and natural gas industries – Design and operation of subsea production systems – Part 4: Subsea wellhead and tree equipment.*
ISO/DIS 13628-7,	*Petroleum and natural gas industries – Design and operation of subsea production systems – Part 7: Completion/workover riser systems.*
ISO 14310,	*Petroleum and natural gas industries – Down hole equipment – Packers and bridge plugs.*
ISO 15156-1,	*Petroleum and natural gas industries – Materials for use in H_2S-containing environments in oil and gas production – Part 1: General principles for selection of cracking-resistant materials.*
API Bull 5C2,	*Performance Properties of Casing, Tubing, and Drill Pipe.*
API Bull 5C3,	*Formulas and Calculations for Casing, Tubing, Drill Pipe, and Line Pipe Properties.*
API RP 5C7,	*Coiled Tubing Operations in Oil and Gas Well Services.*
API RP 7G,	*Drill Stem Design and Operation Limits.*
API RP 14B,	*Design, Installation, Repair and Operation of Subsurface Safety Valve Systems.*
API RP 53,	*Blowout Prevention Equipment Systems for Drilling Operations.*
API Spec 6FA,	*Fire Test for Valves.*
API Spec 6FB,	*Fire Test for End Connections.*
API Spec 6FC,	*Fire Test for Valve With Automatic Backseats.*
API Spec. 7,	*Rotary Drill Stem Elements.*
ASTM D412,	*Standard test Methods for Vulcanized Rubber and Thermoplastic Elastometers – Tension 1.*
ASTM D471,	*Standard Test Method for Rubber Property – Effect of Liquids 1.*
ASTM D2240,	*Standard Test Method for Rubber Property – Durometer Hardness 1.*

ASTM G111,   *Standard Guide for Corrosion Tests in High Temperature or High Pressure*
                        Environment.
NORSOK D-001,   *Drilling facilities.*
NORSOK D-002,   *System requirements well intervention equipment.*
NORSOK D-SR-007,   *Well testing system.*
NORSOK R-003N,   *Sikker bruk av løfteutstyr.*
                        (English version will be issued later)
NORSOK S-001,   *Technical safety.*
NORSOK Z-013,   *Risk and emergency preparedness analysis.*
OLF/NR's, No.024,   *Recommendations for Training of Drilling and Well Service Personnel.*

2.2   Informative references

None.

3   Terms, definitions and abbreviations

For the purposes of this NORSOK standard the following terms, definitions and abbreviations apply.

The terminology used in this NORSOK standard for well barriers is based on:

Primary well barrier:
This is the first object that prevents flow from a source.
Example - blue items: Strippers + CT BOP+ surface test tree,+++

Secondary well barrier:
This is the second object that prevents flow from a source.
Example - red items: Lower riser package + production tree + wellhead,+++

Well barrier element:
An object that alone can not prevent flow from one side to the other side of itself.
Example: CT BOP

Common well barrier element:
This is a barrier element that is shared between primary and secondary barrier.
Examples: Body of LRP, X.mas tree and production wing valve
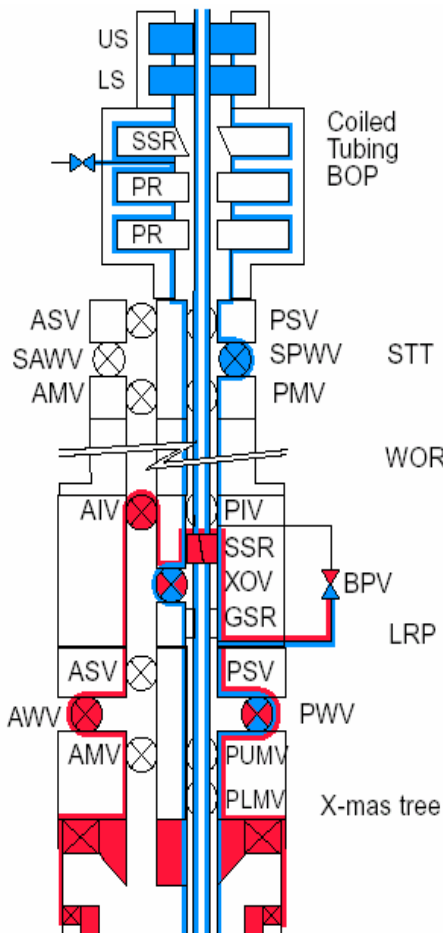
Working well barrier stage:
This is the stage which shows the well barrier elements that are used to confine the pressure in a normal working mode.
Example: Closed CT strippers + CT body + surface test tree w. closed wing valve, +++

Intermediate well barrier stage:
This is the stage(s) of a well barrier element activation sequence before the ultimate well barrier stage is reached.
Examples:
Leak in CT strippers – close CT pipe rams.

Ultimate well barrier stage:
This is the final stage of a well barrier element activation sequence which normally includes closing a shearing device.
Example: Closed CT shear ram (primary barrier) or closed master valve (secondary barrier),+++

3.1   Terms and definitions

3.1.1
A-annulus
annuli between the tubing and the production casing

3.1.2
abnormally pressured
means that the formation/reservoir pressure exceeds the hydrostatic pressure of a seawater column with reference to LAT

3.1.3
activity
preparation for and implementation of operations

3.1.4
B-annulus
annuli between the production casing and the previous casing string

3.1.5
can
verbal form used for statements of possibility and capability, whether material, physical or casual.

3.1.6
common well barrier element
barrier element that is shared between the primary and secondary well barrier

3.1.7
critical
activity or operation that potentially can cause serious injury or death to people, or significant pollution of the environment or substantial financial losses

3.1.8
deep water well
water depth exceeding 600 m LAT

3.1.9
design factor
ratio between the rated strength of the material over the estimated load

3.1.10
discharge line
line between the pump that is used for pumping and the first permanent valve on a WBE

Examples - Surface production tree, wellhead.

3.1.11
electrical cable
wire consisting of individual steel strands woven around one or more electrical conductors to provide sufficient strength to perform desired electrical work in a well

3.1.12
energised fluids
liquefied gases or liquid containing gases

3.1.13
HPHT well
high pressure and high temperature well with expected shut-in pressure exceeding 69 MPa, or a static bottomhole temperature higher than 150 ^{o}C

3.1.14
kick tolerance
maximum influx to equal MAASP

Note - MAASP is based on weakest zone in the wellbore, normally assumed to be at casing shoe.

3.1.15
leak testing
application of pressure to detect leaks in a well barrier, WBE or other objects that are designed to confine pressurised fluids (liquid or gas)

3.1.16
low head drilling

drilling operation where the dynamic bottom-hole pressure in the well bore is equal to or slightly higher than the pore pressure of the formation being drilled

3.1.17
may
verbal form used to indicate a course of action permissible within the limits of the standard

3.1.18
operation
sequence of planning and execution tasks that are carried out to complete a specific activity

3.1.19
permanent abandonment
well status, where the well or part of the well, will be plugged and abandoned permanently, and with the intention of never being used or re-entered again

3.1.20
permanent well barrier
well barrier consisting of WBEs that individually or in combination creates a seal that has a permanent/eternal characteristic

3.1.21
pipe light

tripping mode where pressure forces acting upwards on the cross sectional area of the work string is larger than the weight of the string

3.1.22
plug
"cement" plug (see Table 24) or mechanical plug

3.1.23
plugging
operation of securing a well by installing required well barriers

3.1.24
potential source of inflow
formation with permeability, but not necessarily a reservoir

3.1.25
pressure testing
application of pressure to a value that equals or exceeds the item or system WP to confirm its pressure integrity at rated WP

3.1.26
primary well barrier
first object that prevents flow from a source

3.1.27
procedure
series of steps that describes the execution of a task or piece of work

3.1.28
production operation
organizational unit that is responsible for the integrity of the well during production

3.1.29
pumping
injection or flow of a fluid from a surface reservoir and into the well

3.1.30
reservoir
permeable formation or group of formation zones originally within the same pressure regime, with a flow
potential and/or hydrocarbons present or likely to be present in the future

3.1.31
riser margin
additional fluid density to add to the hole below the mudline required to compensate for the differential
pressure between the fluid in the riser and seawater in the event of a riser disconnect

3.1.32
secondary well barrier
second object that prevents flow from a source

3.1.33
shall
verbal form used to indicate requirements strictly to be followed in order to conform to the standard and from
which no deviation is permitted, unless accepted by all involved parties

Note - The deviation process for handling of deviations and non-conformity with "shall" requirements and "should" guidelines in this
NORSOK standard shall be in accordance with responsible party's system for handling of deviations. These systems shall describe
procedures for how to deviate from requirements and guidelines listed in the regulatory regulations with guidelines and the responsible
party's steering documentation.

3.1.34
shallow gas
free gas or gas in solution that exists in permeable formation which is penetrated before the surface casing
and BOP has been installed

Note - The gas can be normally pressured or abnormally pressured.

3.1.35
should
verbal form used to indicate that among several possibilities one is recommended as particularly suitable,
without mentioning or excluding others, or that a certain course of action is preferred but not necessarily
required

Note - The deviation process for handling of deviations and non-conformity with "shall" requirements and "should" guidelines in this
NORSOK standard should be in accordance with responsible party's system for handling of deviations. It is assumed that these systems
describe procedures for how to deviate from requirements and guidelines listed in the regulations with guidelines and the responsible
party's steering documentation.

3.1.36
simultaneous activities
activities that are executed concurrently on a platform or unit, such as production activities, drilling and well
activities, maintenance and modification activities and critical activities

3.1.37
slickline
slick string of uniform diameter with sufficient strength to convey WL tools to their operating depth

3.1.38
suspension
well status, where the well operation is suspended without removing the well control equipment.

Example - Rig skidded to do short term work on another well, strike, rough weather conditions, waiting on equipment, etc.

3.1.39
surface casing
the last casing installed prior to drilling into an abnormally pressured formation or a formation containing hydrocarbons.

3.1.40
temporary abandonment
well status, where the well is abandoned and/or the well control equipment is removed, with the intention that the operation will be resumed within a specified time frame (from days up to several years).

Example - Pulling BOP for repair, re-entry at a later stage to perform sidetrack - or well test, skidding rig to do higher priority well work, assessment of well data and converting a well from an exploration to a development well, etc.

3.1.41
through tubing drilling and completion
drilling and completing operations conducted through the in situ tubing

3.1.42
trip margin
incremental increase in drilling fluid density to provide an increment of overbalance in order to compensate for effects of swabbing

3.1.43
ultimate well barrier stage
final stage of a WBE activation sequence which normally includes closing a shearing device

Note - This stage normally describes the use of a shearing device.

3.1.44
under balanced drilling
UBD

drilling operation where the dynamic bottom-hole pressure in the well bore is intentionally lower than the pore pressure of the formation being drilled

3.1.45
well barrier
envelope of one or several dependent barrier elements preventing fluids or gases from flowing unintentionally from the formation, into another formation or to surface

3.1.46
well barrier element
WBE
object that alone can not prevent flow from one side to the other side of it self

3.1.47
well control
collective expression for all measures that can be applied to prevent uncontrolled release of well bore effluents to the external environment or uncontrolled underground flow

3.1.48
well control action procedure
specified sequence of planned actions/steps to be executed when the primary well barrier fails

Note - This normally describes the activation of the secondary well barrier, e.g. shut in of well.

3.1.49
well construction team
organizational unit that has drilled and completed the well

3.1.50
well influx/inflow (kick)
unintentional inflow of formation fluid from the formation into the wellbore

3.1.51
well integrity
application of technical, operational and organisational solutions to reduce risk of uncontrolled release of
formation fluids throughout the life cycle of a well

3.1.52
well intervention
collective expression for deployment of tools and equipment in a completed well.

Example - Coiled tubing, wireline and snubbing operations.

3.2   Abbreviations

AMV	annulus master valve
ASCSSV	annulus surface controlled sub-surface valve
BHA	bottom hole assembly
BHP	bottom hole pressure
BOP	blow out preventer
BPV	back pressure valve
CT	coiled tubing
DIV	downhole isolation valve
DP	dynamically positioned
ECD	equivalent circulating density
ESD	emergency shut down
ESDV	emergency shut down valve
HPHT	high pressure high temperature
HSE	health, safety and environment
ID	internal diameter
LAT	low astronomical tide
LHD	low head drilling
LMRP	lower marine riser package
LRP	lower riser package
LWD	logging while drilling
MAASP	maximum allowable annulus surface pressure
MEDP	maximum expected design pressure
METP	maximum expected tubing pressure
MD	measured depth
MPI	magnetic particle inspection
MSDP	maximum section design pressure
MWDP	maximum well design pressure
NRV	non-return valve
OD	outer diameter
PMV	production master valve
PSD	production shut down
PWV	production wing valve
RCD	rotating control device
R/D	rig down
RIH	running in hole
ROV	remote operated vehicle
R/U	rig up
SCSSV	surface controlled subsurface safety valve
SPWV	subsea production wing valve
SSR	shear-seal ram
SSTT	subsea test tree

SSW	subsea well
STT	surface test tree
TCP	tubing conveyed perforating
TOC	top of cement
TSTP	tubing string test pressure
UB	under balanced
UBD	under balanced drilling
UBO	under balanced operation
WBE	well barrier element
WBEAC	well barrier element acceptance criteria
WBS	well barrier schematic
WHP	well head pressure
WL	wire line
WP	working pressure
XOV	cross-over valve

9 Sidetracks, suspension and abandonment

9.1 General

This section covers requirements and guidelines pertaining to well integrity during plugging of wells in connection with

- temporary suspension of well activities and operations,
- temporary or permanent abandonment of wells,
- permanent abandonment of a section of a well (side tracking, slot recovery) to construct a new wellbore with a new geological well target.

The purpose of this section is to describe the establishment of well barriers by use of WBEs and additional features required to execute this activity in a safe manner, with focus on isolation of permeable formations/reservoirs/sources of outflow, both from each other in the wellbore, and from surface.

Requirements for isolation of formations, fluids and pressures for temporary and permanent abandonment are the same. However, choice of WBEs may be different to account for abandonment time, and ability to re-enter the well, or resume operations after temporary abandonment.

9.2 Well barrier schematics

It is recommended that WBSs are developed as a practical method to demonstrate and illustrate the presence of the defined primary and secondary well barriers in the well, see 4.2. In the table below there are a number of typical scenarios listed, some of which are also attached as illustrations. The table is not comprehensive and schematics for the actual situations during an activity or operation should be made.

Item	Description	Comments	See
1.	Temporary abandonment – Non- perforated well.	Non-completed well.	9.8.1
2.	Temporary abandonment – Perforated well with BOP or production tree removed.	With well completion installed.	9.8.2
3.	Permanent abandonment - Open hole.		9.8.3
4.	Permanent abandonment – Perforated well.		9.8.4
5.	Permanent abandonment - Multibore with slotted liners or sandscreens.	Covers permanent zonal isolation of multiple reservoirs.	9.8.5
6.	Permanent abandonment - Slotted liners in multiple reservoirs.	Applies also to slot recovery/ side tracks, etc.	9.8.6
7.	Suspension - Hang-off/disconnect of mariner riser.	Hang-off drill pipe.	9.8.7

9.3 Well barrier acceptance criteria

9.3.1 Function and type of well barriers

For wells to be permanently abandoned, with several sources of inflow, the usual; one primary and one secondary well barrier, do not suffice. Hence, this subclause covers all well barriers and the functions they are intended to fulfil which may be necessary in abandonment scenarios. These well barriers may, however, not be applicable for wells where continued operations are planned, where the wellhead/ well control equipment is utilised and capable, as a secondary well barrier, to cover any source of inflow in the well. This also means that some terms used in this subclause are only applicable in the context of suspension and abandonment of wells and wellbores.

The following individual or combined well barriers shall be a result of well plugging activities:

Name	Function	Purpose
Primary well barrier.	First well barrier against flow of formation fluids to surface, or to secure a last open hole.	To isolate a potential source of inflow from surface.
Secondary well barrier, reservoir.	Back-up to the primary well barrier.	Same purpose as the primary well barrier, and applies where the potential source of inflow is also a reservoir (w/ flow potential and/ or hydrocarbons).
Well barrier between reservoirs.	To isolate reservoirs from each other.	To reduce potential for flow between reservoirs.
Open hole to surface well barrier.	To isolate an open hole from surface, which is exposed whilst plugging the well.	"Fail-safe" well barrier, where a potential source of inflow is exposed after e.g. a casing cut.
Secondary well barrier, temporary abandonment.	Second, independent well barrier in connection with drilling and well activities.	To ensure safe re-connection to a temporary abandoned well, and applies consequently only where well activities has not been concluded.

The functions of a well barrier and a plug can be combined should it fulfil more than one of the abovementioned objectives (except a secondary well barrier can never be a primary well barrier for the same reservoir).

A secondary well barrier for one reservoir formation may act as a primary well barrier for a shallower formation, if this well barrier is designed to meet the requirements of both formations.

9.3.2   Positioning of well barriers
Well barriers should be installed as close to the potential source of inflow as possible, covering all possible leak paths.

The primary and secondary well barriers shall be positioned at a depth where the estimated formation fracture pressure at the base of the plug is in excess of the potential internal pressure.

The final position of the well barrier/WBEs shall be verified.

9.3.3   Materials
The materials used in well barriers for plugging of wells shall withstand the load/ environmental conditions it may be exposed to for the time the well will be abandoned. Tests should be performed to document long term integrity of plugging materials used.

9.3.4   Leak testing and verification
When inflow testing or leak testing from above to verify the integrity of a well barrier is not possible, or when this may not give conclusive results, other means of ensuring proper installation of a well barrier shall be used. Verification through assessment of job planning and actual job performance parameters are options available.

Inflow tests shall be documented.

9.3.5   Sidetracking
The original wellbore shall be permanently abandoned prior to a side-track/ slot recovery.

9.3.6 Suspension
Suspension of operations requires the same number of well barriers as other abandonment activities. However, the need for WBE testing, and verification, can be compensated by monitoring of its performance, such as fluid level/ pressure development above well barriers. Well fluids (see Table 1) may in such cases be qualified as a WBE.

9.3.7   Temporary abandonment

It shall be possible to re-enter temporarily abandoned wells in a safe manner.

Integrity of materials used for temporary abandonment should be ensured for the planned abandonment period times two. Hence, a mechanical well barrier may be acceptable for temporary abandonment, subject to type, planned abandonment period and subsurface environment.

Degradation of casing body should be considered for longer temporary abandonment scenarios.

Temporarily abandoned subsea wellheads and templates shall be protected from external loads in areas with fishing activities, or other seabed activities etc. Hence for deep water wells, temporary seabed protection can be omitted if there is confirmation of no such activities in the area and at the depth of the abandoned seabed installations.

The pressure in tubing and annulus above the reservoir well barrier ("A" annulus) shall be monitored if a subsea completed well is planned abandoned for more than one year. An acceptable alternative if monitoring is not practicable may be to install a deep set well barrier plug.

For surface completed wells, it should be possible to monitor the pressure in the "A" annulus and in the last tubular that was installed (production tubing, casing).

9.3.8   Permanent abandonment

9.3.8.1   General

Permanently plugged wells shall be abandoned with an eternal perspective, i.e. for the purpose of evaluating the effect on the well barriers installed after any foreseeable chemical and geological process has taken place.

There shall be at least one well barrier between surface and a potential source of inflow, unless it is a reservoir (contains hydrocarbons and/ or has a flow potential) where two well barriers are required.

When plugging a reservoir, due attention to the possibilities to access this section of the well (in case of collapse, etc) and successfully install a specific WBE should be paid.

The last open hole section of a wellbore shall not be abandoned permanently without installing a permanent well barrier, regardless of pressure or flow potential. The complete borehole shall be isolated.

9.3.8.2   Permanent well barriers

Permanent well barriers shall extend across the full cross section of the well, include all annuli and seal both vertically and horizontally (see illustration). Hence, a WBE set inside a casing, as part of a permanent well barrier, shall be located in a depth interval where there is a WBE with verified quality in all annuli.

A permanent well barrier should have the following properties:

a) Impermeable
b) Long term integrity.
c) Non shrinking.
d) Ductile – (non brittle) – able to withstand mechanical loads/ impact.
e) Resistance to different chemicals/ substances (H_2S, CO_2 and hydrocarbons).
f) Wetting, to ensure bonding to steel.
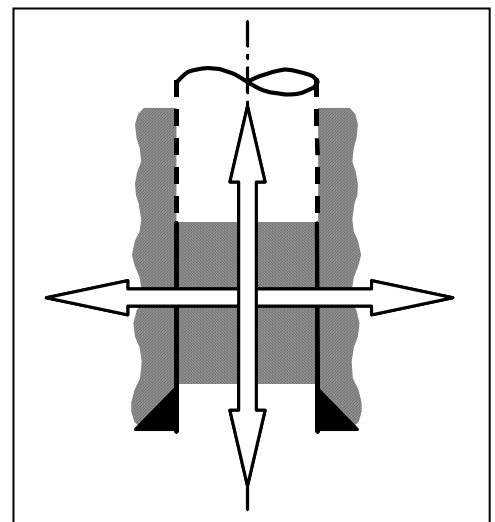
Steel tubular is not an acceptable permanent WBE unless it is supported by cement, or a plugging material with similar functional properties as listed above, (inside and outside).

Elastomer seals used as sealing components in WBEs are not acceptable for permanent well barriers.

The presence and pressure integrity of casing cement shall be verified to assess the along hole pressure integrity of this WBE. The cement in annulus will not qualify as a WBE across the well (see illustration).

Open hole cement plugs can be used as a well barrier between reservoirs. It should, as far as practicably possible, also be used as a primary well barrier, see Table 24.

Cement in the liner lap, which has not been leak tested from above (before a possible liner top packer has been set) shall not be regarded a permanent WBE.

Removal of downhole equipment is not required as long as the integrity of the well barriers is achieved.

Control cables and lines shall be removed from areas where permanent well barriers are installed, since they may create vertical leak paths through the well barrier.

When well completion tubulars are left in hole and permanent plugs are installed through and around the tubular, reliable methods and procedures to install and verify position of the plug inside the tubular and in the tubular annulus shall be established.

9.3.8.3   Special requirements

Multiple reservoir zones/ perforations located within the same pressure regime, isolated with a well barrier in between, can be regarded as one reservoir for which a primary and secondary well barrier shall be installed (see illustration).
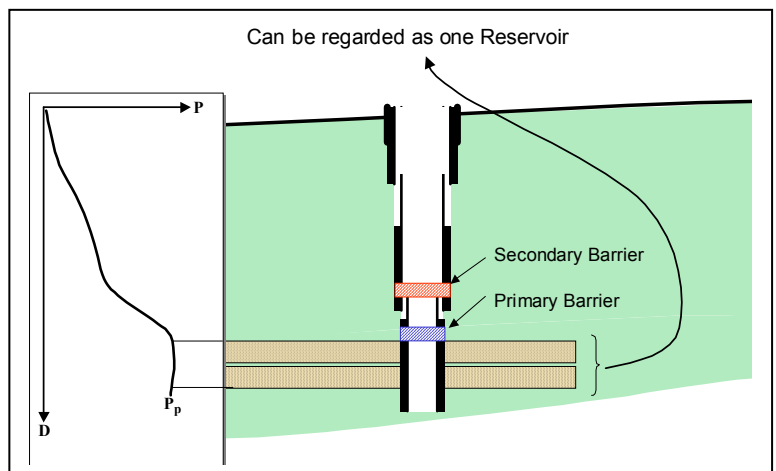
9.4   Well barrier elements acceptance criteria

9.4.1   General
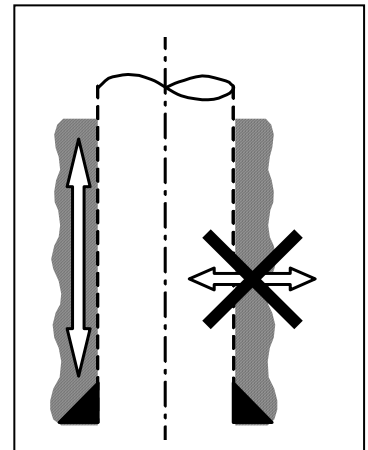
Subclause 9.8 lists the WBEs that constitute the primary and secondary barriers for situations that are illustrated.

9.4.2   Additional well barrier elements (WBEs) acceptance criteria

The following table describes features, requirements and guidelines which are additional to what is described in Clause 15.

No.	Element name	Additional features, requirements and guidelines
Table 2	Casing	Accepted as permanent WBE if cement is present inside and outside.
Table 22	Casing cement	Accepted as a permanent WBE together with casing and cement inside the casing. Should alternative materials be used for the same function a separate WBEAC shall be developed.
Table 24	Cement plug	Cased hole cement plugs used in permanent abandonment shall be set in areas with verified cement in casing annulus. Should alternative materials be used for the same function a separate WBEAC shall be developed. A cement plug installed using a pressure tested mechanical plug as a foundation should be verified by documenting the strength development using a sample slurry subjected to an ultrasonic compressive strength analysis or one that have been tested under representative temperature and/or pressure.

No.	Element name	Additional features, requirements and guidelines
Table 25	Completion string	Accepted as permanent WBE if cement is present inside and outside the tubing.
Table 43	Liner top packer	Not accepted as a permanent WBE.

9.4.3   Common well barrier elements (WBEs)

A risk analysis shall be performed and risk reducing measures applied to reduce the risk as low as reasonable practicable, see 4.2.3.3.

The following table describes risk reducing measures that can be applied when a WBE is an element in the primary and secondary well barrier:

No	Element name	Failure scenario	Probability reducing measures	Consequence reducing measures
Table 2	Casing	Leak through casing and into annulus, with possibility of fracturing formation below previous casing shoe.	None	Cement in the annulus with verified TOC above the section that is common.

9.5   Well control action procedures and drills

9.5.1   Well control action procedures

The following table describes incident scenarios for which well control action procedures should be available (if applicable) to deal with the incidents should they occur. This list is not comprehensive and additional scenarios may be applied based on the actual planned activity, see 4.2.7.

Item	Description	Comments
1.	Cutting of casing.	Trapped gas pressure in casing annulus.
2.	(SSW) Pulling casing hanger seal assembly.	Trapped gas pressure in casing annulus.
3.	Re-entry of suspended or temporary abandoned wells.	Account for trapped pressure under plugs due to possible failure of suspension plugs.

9.5.2   Well control action drills

The following well control action drills should be performed:

Item	Description	Comments
1.	Pressure build-up, or lost circulation in connection with a cutting casing operation.	To verify crew response in applying correct well control practices.
2.	Loss of well barrier whilst performing inflow test.	

9.6   Suspension, plugging and abandonment design

9.6.1   Design basis, premises and assumptions

Depths and size of permeable formations with a flow potential in any wellbore shall be known.

All elements of the well barrier shall withstand the pressure differential across the well barrier at time of installation and as long as the well barrier will be in use, see 9.3.3.

The following information should be gathered as a basis of the well barrier design and abandonment programme:

a) Well configuration (original, intermediate and present) including depths and specification of permeable formations, casing strings, primary cement behind casing status, well bores, side-tracks, etc.
b) Stratigraphic sequence of each wellbore showing reservoir(s) and information about their current and future production potential, where reservoir fluids and pressures (initial, current and in an eternal perspective) are included.
c) Logs, data and information from primary cementing operations in the well.
d) Estimated formation fracture gradient.
e) Specific well conditions such as scale build up, casing wear, collapsed casing, fill, or similar issues.

The design of abandonment well barriers consisting of cement should account for uncertainties relating to

- downhole placement techniques,
- minimum volumes required to mix a homogenous slurry,
- surface volume control,
- pump efficiency/ -parameters,
- contamination of fluids,
- shrinkage of cement.

9.6.2   Load cases

Functional and environmental loads shall be combined in the most unfavourable way.

For permanently abandoned wells, the specific gravity of well fluid accounted for in the design shall maximum be equal to a seawater gradient.

The following load cases should be applied for the abandonment design:

Item	Description	Comments
1.	Minimum depth of primary and secondary well barriers for each reservoir/potential source of inflow, taking the worst anticipated reservoir pressure for the abandonment period into account.	Not shallower than formation strength at these depths. Reservoir pressure may for permanent abandonment revert to initial/virgin level.
2.	Leak testing of casing plugs.	Criteria as given in Table 24.
3.	Burst limitations on casing string at the depths where abandonment plugs are installed.	Cannot set plug higher than what the burst rating allows (less wear factors).
4.	Collapse loads from seabed subsidence or reservoir compaction.	The effects of seabed subsidence above or in connection with the reservoir shall be included.

9.6.3   Minimum design factors

The design factors shall be as described in 5.6.4 and 7.6.4.

9.7   Other topics

9.7.1   Risks

Risk shall be assessed relating to time effects on well barriers such as long term development of reservoir pressure, possible deterioration of materials used, sagging of weight materials in well fluids, etc.

HSE risks related to removal and handling of possible scale in production tubing shall be considered in connection with plugging of development wells.

HSE risk relating to cutting of tubular goods, detecting and releasing of trapped pressure and recovery of materials with unknown status shall be assessed.

9.7.2   Removing equipment above seabed

Use of explosives to cut casing is acceptable only if measures are implemented (directed/ shaped charges and upward protection) which reduces the risk to surrounding environment to the same level as other means of cutting casing.

For permanent abandonment wells, the wellhead and the following casings shall be removed such that no parts of the well ever will protrude the seabed.

Required cutting depth below seabed should be considered in each case, and be based on prevailing local conditions such as soil, sea bed scouring, sea current erosion, etc.. The cutting depth should be 5 m below seabed.

No other obstructions related to the drilling and well activities shall be left behind on the sea floor.

9.8   Attachments – Well barrier schematics (WBS)

9.8.1   Temporary abandonment – Non-perforated well

Liner ← → Casing
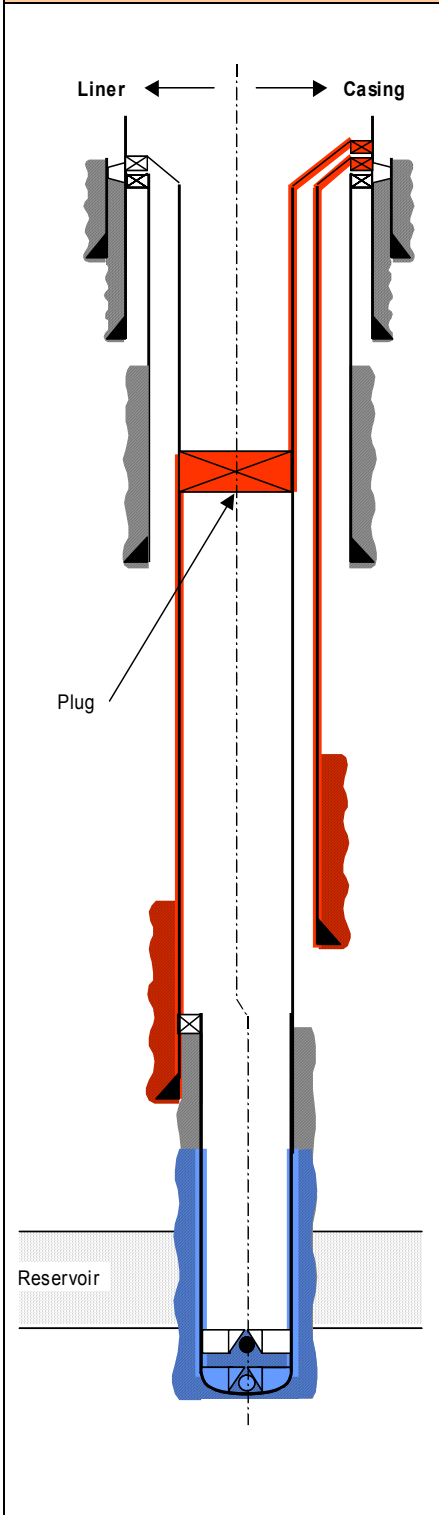
Plug

Reservoir

Well barrier elements	See Table	Comments
Primary well barrier, last open hole		
1. Cement plug	24	Shoe track.
2. Casing (liner) cement	22	
3. Casing (reservoir liner)	2	Un-perforated w/2 each float valves.
or		
1. Cement plug	24	Shoe track.
2. Casing cement	22	
3. Reservoir casing	2	Un-perforated w/2 each float valves.
Secondary well barrier, temporary abandonment		
1. Casing	2	
2. Casing cement	22	
3. Cement plug or mechanical plug	24 28	Shallow plug.
or		
1. Casing cement	22	
2. Casing	2	Intermediate
3. Wellhead	5	
4. Casing	2	Production casing.
5. Cement plug or mechanical plug	24 28	Shallow plug.

Note
None

9.8.2   Temporary abandonment – Perforated well with BOP or production tree removed
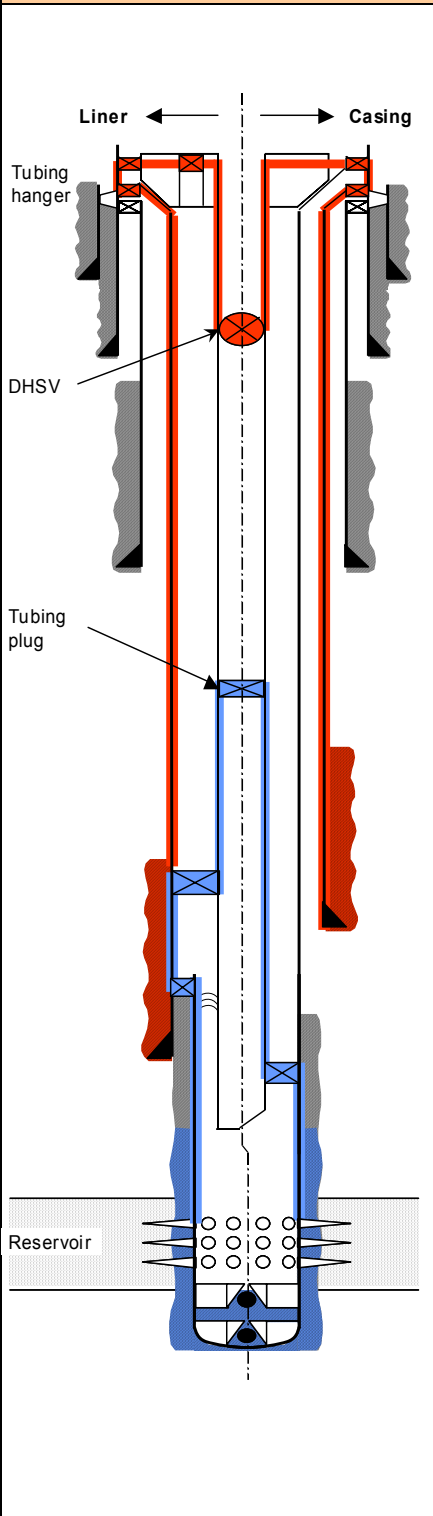
Well barrier elements	See Table	Comments
Primary well barrier		
1. Casing (liner) cement	22	
2. Casing (liner)	2	Liner above perforations.
3. Liner top packer	43	
4. Casing	2	Below production packer.
5. Production packer	7	50 m below TOC in casing annulus.
6. Completion string	25	
7. Deep set tubing plug	6	
or,		
1. Casing cement	22	
2. Casing	2	Above perforations.
3. Production packer	7	
4. Completion string	25	
5. Deep set tubing plug	6	
Secondary well barrier, reservoir		
1. Casing cement	22	Above production packer.
2. Casing	2	Common WBE, between liner top packer and production packer.
3. Wellhead	5	
4. Tubing hanger	10	
5. Tubing hanger plug	11	For SSWs.
6. Completion string	25	Down to SCSSV.
7. SCSSV	8	
or,		
1. Casing cement	22	Intermediate casing.
2. Casing	2	Intermediate casing.
3. Wellhead	5	
4. Tubing hanger	10	
5. Tubing hanger plug	11	For SSWs.
6. Completion string	25	Down to SCSSV.
7. SCSSV	8	

Note
None

9.8.3   Permanent abandonment - Open hole

Liner/Reservoir ← → Casing/No source of outflow

Reservoir

No permeable formations
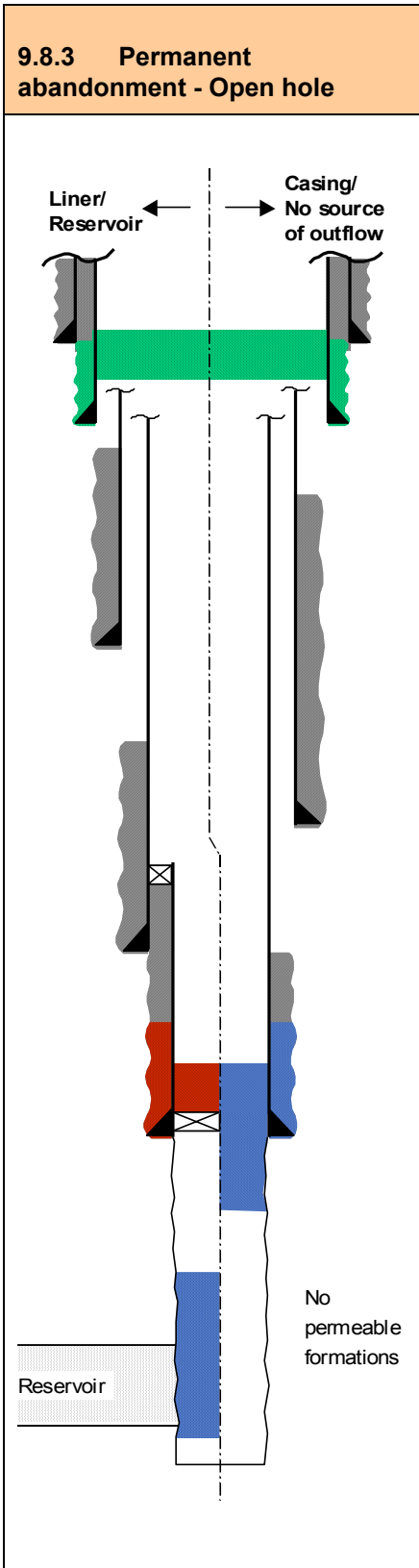
Well barrier elements	See Table	Comments
Primary well barrier		
1. Cement plug	24	Open hole.
or, ("**primary well barrier, last open hole**"):		
1. Casing cement	22	
2. Cement plug	24	Transition plug across casing shoe.
Secondary well barrier, reservoir		
1. Casing cement	22	
2. Cement plug	24	Cased hole cement plug installed on top of a mechanical plug.
Open hole to surface well barrier		
1. Cement plug	24	Cased hole cement plug.
2. Casing cement	22	Surface casing.

Notes
a. Verification of primary well barrier in the "liner case" to be carried out as detailed in Table 22.
b. The well barrier in deepest casing shoe can for both cases be designed either way, if casing/liner cement is verified and O.K.
c. The secondary well barrier shall as a minimum be positioned at a depth where the estimated formation fracture pressure exceeds the contained pressure below the well barrier.

9.8.4   Permanent abandonment - Perforated well

Tbg. left in hole

Prod. Packer
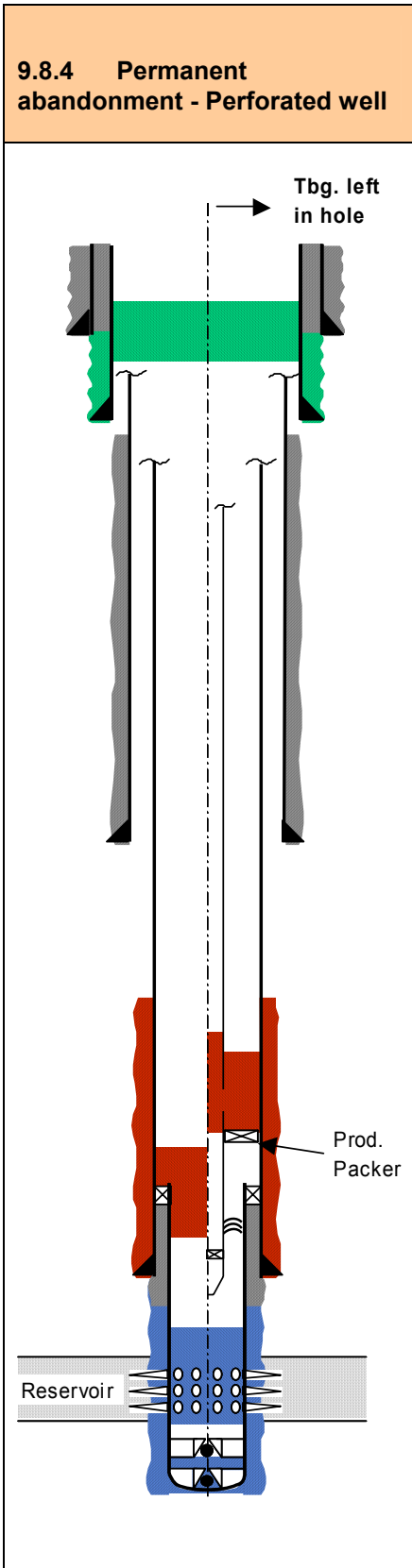
Reservoir

Well barrier elements	See Table	Comments
Primary well barrier		
1. Liner cement	22	
2. Cement plug	24	Across and above perforations.
Secondary well barrier, reservoir		
1. Casing cement	22	
2. Cement plug	24	Across liner top.
or, for tubing left in hole case:		
1. Casing cement	22	
2. Cement plug	24	Inside and outside of tubing.
Open holes to surface well barrier		
1. Cement plug	24	
2. Casing cement	22	Surface casing.

Notes
1. Cement plugs inside casing shall be set in areas with verified cement in casing annulus.
2. The secondary well barrier shall as a minimum be positioned at a depth where the estimated formation fracture pressure exceeds the contained pressure below the well barrier.

9.8.5   Permanent abandonment - Multibore with slotted liners or sand screens
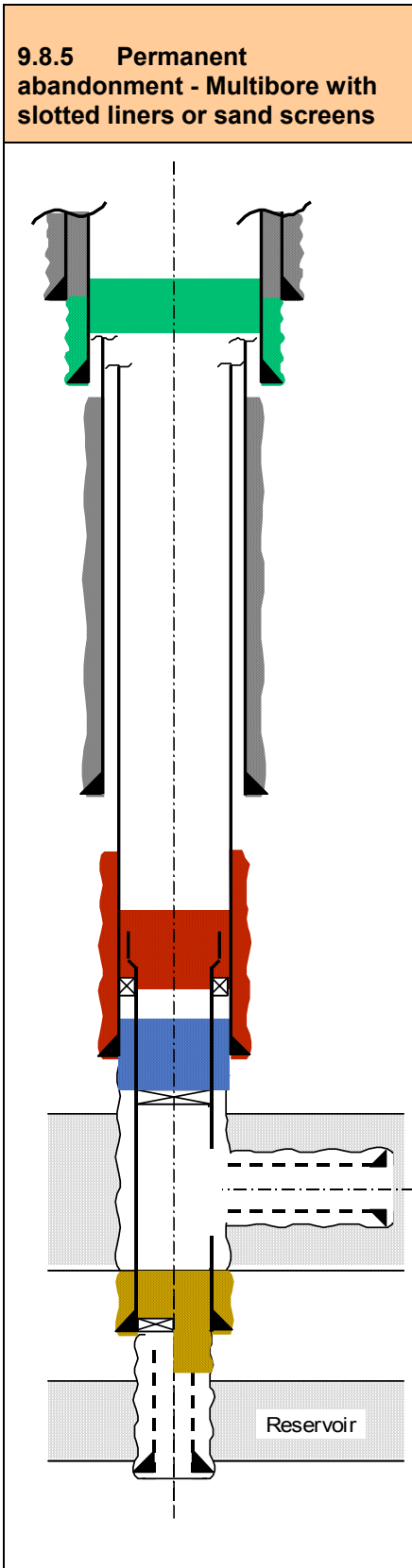
Reservoir

Well barrier elements	See Table	Comments
Barrier between reservoirs		
1. Casing cement	22	
2. Cement plug	24	Cased hole.
or,		
2. Cement plug	24	Transition plug across casing shoe.
Primary well barrier		
1. Cement plug	24	Across wellbore and casing shoe.
Secondary well barrier, reservoir		
1. Casing cement	22	
2. Cement plug	24	Casing plug across liner top.
Open Holes to surface wellbarrier		
1. Cement plug	24	Cased hole cement plug.
2. Casing cement	22	Surface casing.

Notes
1. The "well barrier between reservoirs" may act as the primary well barrier for the "deep" reservoir, and "primary well barrier" may be the secondary well barrier for "deep" reservoir, if the latter is designed to take the differential pressures for both formations.
2. Secondary well barrier shall not be set higher than the formation integrity at this depth, considering that the design criteria may be initial reservoir pressure, as applicable in each case.

9.8.6   Permanent abandonment - Slotted liners in multiple reservoirs

**Intermediate csg. cemented to previous csg shoe**

Potential Reservoir
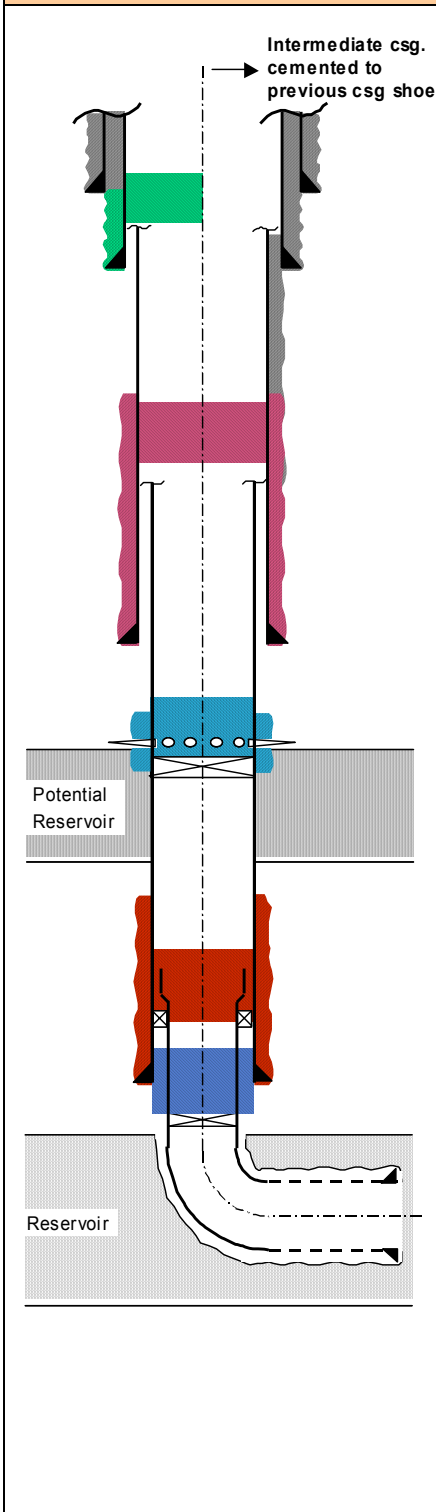
Reservoir

Well barrier elements	See Table	Comments
Primary well barrier, deep reservoir		
1. Cement plug	24	Through liner and across casing shoe/Open hole transition.
Secondary well barrier		
1. Casing cement	22	
2. Cement plug	24	Across liner top.
Primary well barrier, shallow reservoir		
1. Cement plug	22	Squeezed into perforated casing annulus above potential reservoir.
Secondary well barrier, shallow reservoir		
1. Casing cement	22	
2. Cement plug	24	
Open holes to surface well barrier		
3) Cement plug	24	Cased hole.
4) Casing cement	22	Surface casing.

Notes
1. Secondary well barrier shall not be set higher than the formation integrity at this depth, considering that the design criteria may be initial reservoir pressure, which may develop over time.
2. The case on the right hand side indicates that the intermediate casing string is cemented into surface casing, i.e. with no open annulus to surface. Hence, no open holes to surface well barrier is required.

9.8.7   Suspension - Hang-off/Disconnect of mariner riser
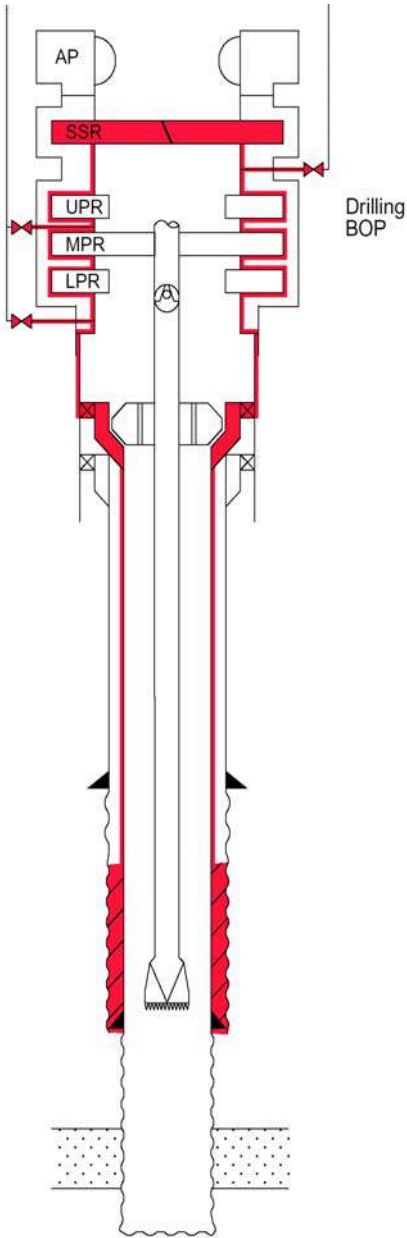
Well barrier elements	See Table	Comments
Primary well barrier		
1. Fluid column	1	Time limited barrier, see Note 1.
Secondary well barrier		
1. Casing cement	22	Last casing.
2. Casing	2	
3. Wellhead	5	
4. BOP	4	

Notes
1. Well bore fluid shall be qualified through test for the hang-off period.
2. A "storm valve" should be installed in the drillpipe hang-off assembly

8.4 Appendix D

This page is intentionally left blank.

Questionnaire report

1. What is the application for this tool?

   The purpose of this equipment is to reduce the number of wireline operations on two different job types by completing the following in a single run.

   Application no. 1
   - **Punch through the innermost casing to gain access to annulus**
   - **Minimum 4-6 circumferentially distributed holes (testing should be performed for both a 4-punch and 6-punch design so that the flow area between the punches can be evaluated)**
   - **Create both standoff and holes at all desired depths**
   - **Minimum hole size above 0,5''**
   - **Effective casing material removal ≥ 2%**
   - **Punch holes for optimized swirl/spiral annular wash flow (i.e. these should be rectangular type punches, similar to a knife, but give larger hole sizes upon exit)**

   Application no. 2

   - **Ability to selectively either:**
     - **Create standoff without perforating**
     - **Create standoff and single or multiple perforations**
   - **Effective standoff must be regardless of orientation**
   - **Minimum hole size 0,55'', where applicable. The tool should ideally give adequate feedback to be able to determine if a punch has been made or if the pipe is still integral.**

2. What Casing sizes and well layout are present during these applications?

   The tool should be developed for the following specific casing forfigurations:
   - **4,5'' 12,6ppf L80 casing installed insidce a 7'' 32ppf casing**
   - **4,5'' 12,6ppf L80 casing installed inside a 9-5/8'' 53,5ppf casing**

   Punching will be performed minimum 1m away from tubing threads and collar.

3. What available forces and resources can existing E Plug technology deliver?

   The EMT today has a torque capacity of 5600Nm, depending on environment for the tool and axial force connection this can be transformed into 1000kN of axial force as an estimate.

4. What alternatives are there to running the E Plug Combined Punch and Stand-off Tool during P&A? Are these used in light or heavy interaction?

There are two applications for this tool. The first application for just making stand-off in wells where we want to pump a through-tubing annular cement job. There is no requirement to make this standoff (centralization), it is only something that will increase the quality of the annular cement job.

- a. Section milling – *the tool is NOT an alternative to this.*
- b. Cutting and pulling - **the tool is NOT an alternative to this**.
- **c.** Perf Wash Cement with traditional guns - **the tool is an alternative to the guns used in PWC operations.**
- d. Other alternatives?
- e. Do you have any information on the typical time aspect of using these methods? - **This tool will take much longer than traditional guns.**
- **f.** What do you consider to be the advantages of the new E Plug tool? **The advantage is that the punches it makes will act to centralize the inner string, as well, there is less risk (no risk) or damaging the next casing**
    - i. Any disadvantages? **Time, possibility for having to make an extra run.**
5. General P&A
    - a. Do you have any number or guesstimate as to the number of wells that currently is undergoing P&A operations? Any yearly estimate? **This year will may do pre-P&A operations on 1-3 wells.** Total number of planned P&A operations? **That is the entire well stock, but this tool is not necessarily going to be used on all those wells. Not sure how many it could be used on, that depends on the well design.**
    - b. Any approximate or best guess on the number of runs during a typical P&A operation? If it is possible to generalize in such a way. **No, it is so well-design dependent.**
6. Could you provide a short summary on both jobs?

The first application, the plan is to do PWC operations on a dual liner section, which has mud between the two liners. CT is used for the

1. **Plug inner liner with bridge plug. (wireline)**
2. **Perforate (punch) the liner over 80 m interval (wireline)**
3. **Wash the interval using CT**
4. **Cement the interval using CT.**

The second application the tool will be used to centralize the production tubing above the production packer to enable a Through tubing annular cement job (look in NORSOK, there is an example there).

1. **Set plug in tail pipe. (wireline)**
2. **Punch tubing above production packer using the tool (wireline)**
3. **Centralize tubing using the tool(wireline)**
4. **POOH**
5. **Pump cement down production tubing, taking returns up A-annulus until a 200m long balanced cement plug is placed in tubing and A-annulus. (cement pump)**
6. **Pressure test cement.**

- a. Why does you need the punched holes optimized for swirl flow on one application but not in the other? In what cases is washing necessary?

The swirling is because we are washing out settled mud in the liner-liner annulus for a PWC job.

The first job is above the production packer where there is SW completion fluid. You don't have to wash it, just pump it out. You don't want to wash because then you need to use CT for washing and for placing the cement. On the other application, all those operations are happening on WL and with pumps.

7. For a economical point of view, what are the potential for this tool and why is this potential so important for a operating company?

Most of the new fields discovered in the world today are gas fields. This means that all the existing oil fields today are an important resource for the companies. In the effort of making these fields become more productive and stay productive for a longer time period slot recovery is of increasing interest.

To do a slot recovery the well and all its annulus must be plugged and tested. To get a good test the cement plug must seal all around the casing in the annulus. Here, in many of the old wells due to well layup these casings are always laying on low side in the horizontal section of the well. Therefore, it becomes important to do two things, one is to punch the casing to achieve contact to the annulus. The other is to lift the casing enabling cement to seal the whole circumference.

If an oil and gas company can do this in a safe and efficient manner, their oil and gas fields become much more efficient and profitable.

8. Why is a tool running on wireline so important for such applications?

A wireline tool capable of punching the inner casing and at the same time create a standoff does not exist today. By running on wireline, the rig can do it "offline", which means they don't have to use the whole operational setup on the rig. Also, wireline equipment is always present on a production rig and very quick to enable, compared to coil tubing or drill pipe.

Todays technology require either coiled tubing or drill pipe for doing such applications. Installation of coil tubing easily takes 14 days with a daily rental cost of 500 000 NOK per day. As where wireline can be enabled in one day with a daily estimate of 250 000 NOK per day of operating.